



7-2022

OTULIN's Novel Regulatory Mechanisms in Genotoxic and Inflammatory NF-kB Signaling

Mingqi Li

University of Tennessee Health Science Center

Follow this and additional works at: <https://dc.uthsc.edu/dissertations>



Part of the [Neoplasms Commons](#), and the [Therapeutics Commons](#)

Recommended Citation

Li, Mingqi (<https://orcid.org/0000-0003-4595-285X>), "OTULIN's Novel Regulatory Mechanisms in Genotoxic and Inflammatory NF-kB Signaling" (2022). *Theses and Dissertations (ETD)*. Paper 610. <http://dx.doi.org/10.21007/etd.cghs.2022.0600>.

This Dissertation is brought to you for free and open access by the College of Graduate Health Sciences at UTHSC Digital Commons. It has been accepted for inclusion in Theses and Dissertations (ETD) by an authorized administrator of UTHSC Digital Commons. For more information, please contact jwelch30@uthsc.edu.

OTULIN's Novel Regulatory Mechanisms in Genotoxic and Inflammatory NF- κ B Signaling

Abstract

Triple negative breast cancer (TNBC) is aggressive but cannot be treated with hormone therapy or molecular therapy due to the lack of a target. Chemotherapy is a systemic treatment that works by attacking rapidly growing cells, which is initially more effective for TNBC patients than those individuals with the hormone receptor-positive breast cancer. However, patients with TNBC tend to develop resistance to chemo drugs, called chemoresistance. After years of effort, the signaling pathways involved in TNBC chemoresistance are gradually revealed, including the nuclear factor-kappa B (NF- κ B) pathway. Transcription factor NF- κ B is widely involved in cancer development and progression, and its overactivation renders chemoresistance to TNBC and induces aberrant inflammation. Therefore, targeting NF- κ B becomes a feasible strategy to overcome chemoresistance. Ubiquitination is an essential post-translational modification during which ubiquitin chains are assembled on a substrate protein, leading to various cellular processes, such as endocytosis, membrane trafficking, DNA repair, signal transduction, and protein degradation. The outcome of one ubiquitinated protein is dependent on its ubiquitin linkage and the context. Our previous study has shown that the linear ubiquitin chains assembled by the linear ubiquitin chain assembly complex (LUBAC) solidly facilitate NF- κ B signaling transduction upon genotoxic stress. OTU deubiquitinase with linear linkage specificity (OTULIN) is known to cleave linear ubiquitin chains exclusively. The purpose of this dissertation is to investigate whether OTULIN can counteract LUBAC-mediated NF-

Document Type

Dissertation

Degree Name

Doctor of Philosophy (PhD)

Program

Biomedical Sciences

Research Advisor

Francesca-Fang Liao, Ph.D.

Keywords

chemoresistance; inflammation; LUBAC; NF- κ B; OTULIN; TNF-alpha

Subject Categories

Diseases | Medicine and Health Sciences | Neoplasms | Therapeutics

UNIVERSITY OF TENNESSEE HEALTH SCIENCE CENTER

DOCTORAL DISSERTATION

**OTULIN's Novel Regulatory Mechanisms in
Genotoxic and Inflammatory NF- κ B Signaling**

Author:
Mingqi Li

Advisor:
Francesca-Fang Liao, Ph.D.

*A Dissertation Presented for The Graduate Studies Council of
The University of Tennessee Health Science Center
in Partial Fulfillment of the Requirements for the Doctor of Philosophy degree from
The University of Tennessee*

in

*Biomedical Sciences: Cancer and Developmental Biology
College of Graduate Health Sciences*

July 2022

Chapter 3 © n.d. by Mingqi Li, Ling Li., et al.
All other material © 2022 by Mingqi Li.
All rights reserved.

DEDICATION

This dissertation is dedicated to
my warm family, especially to my great parents,
who have always been supporting me to go abroad for further studies.
Thanks for their unconditional love, patience, and encouragement,
which really helped me get to where I am today.

ACKNOWLEDGEMENTS

I would like to acknowledge the people who have helped me throughout my graduate studies. First, I am grateful to my advisor, Dr. Liao Francesca-Fang, for taking the time to train me and giving me the opportunity to pursue a Ph.D. degree in Biomedical Sciences. Her insightful guidance and encouragement have brought my work to an advanced level and had a big influence on me in science. It was my honor to work with a mentor with strong personal charisma, who is always optimistic, intelligent, and kind-hearted. Also, I am grateful to her for providing me additional stipend which really helped me get through the hard times. Furthermore, I am also thankful to her taking time to help me complete my dissertation on time. The experience, knowledge, and attitude learnt from her will be engraved on my mind for a lifetime.

I would also like to thank my committee members, Dr. Edwards A. Park, Dr. Kui Li, Dr. Meiyun Fan and Dr. Ramesh Narayanan, for their constructive guidance throughout my research. I was inspired to shape my project and motivated to work harder after each committee meeting or even a small talk.

To members of the past Zhaohui Wu's lab, they have taught me many experimental techniques, data analyses, and useful software. I am proud to have worked with you all before.

Additionally, I would like to thank Dr. Weikuan Gu and Harbin Medical University for giving me the opportunity to the joint Ph.D. program at UTHSC.

I appreciate my family and friends, who were always being with me.

Finally, I appreciate that this work was supported in part by NIH 1R01 AG049772, 1R01-AG058467 and 1R01 NS120327 to F. F. L; R01-CA229164 and DOD (W81XWH2110055) to R. N., UND Vice President for Research & Economic Development (VPRED) seed program (X.W.).

ABSTRACT

Triple negative breast cancer (TNBC) is aggressive and cannot be treated with hormone therapy or molecular therapy due to the lack of a target. Chemotherapy is a systemic treatment that works by attacking rapidly growing cells, which is initially more effective for TNBC patients than those individuals with the hormone receptor-positive breast cancer. However, patients with TNBC tend to develop resistance to chemo drugs, called chemoresistance. After years of effort, the signaling pathways involved in TNBC chemoresistance are gradually revealed, including the nuclear factor-kappa B (NF- κ B) pathway. Transcription factor NF- κ B is widely involved in cancer development and progression, and its overactivation renders chemoresistance to TNBC and induces aberrant inflammation. Therefore, targeting NF- κ B becomes a feasible strategy to overcome chemoresistance. Ubiquitination is an essential post-translational modification during which ubiquitin chains are assembled on a substrate protein, leading to various cellular processes, such as endocytosis, membrane trafficking, DNA repair, signal transduction, and protein degradation. The outcome of one ubiquitinated protein is dependent on its ubiquitin linkage and the context. Our previous study has shown that the linear ubiquitin chains assembled by the linear ubiquitin chain assembly complex (LUBAC) substantially facilitate NF- κ B signaling transduction upon genotoxic stress. OTU deubiquitinase with linear linkage specificity (OTULIN) is known to cleave linear ubiquitin chains exclusively. The purpose of this dissertation is to investigate whether OTULIN can counteract LUBAC-mediated NF- κ B activation upon genotoxic stress and to investigate the interplay between OTULIN and LUBAC regarding genotoxic and inflammatory responses.

In this project, three different types of cell lines (HEK293T, MDA-MB-231, and mouse embryonic fibroblast, MEF) have been used to study the mechanisms under genotoxic stress and inflammation. We generated OTULIN/LUBAC-KO clones by CRISPR-Cas9 system and found OTULIN can inhibit genotoxic NF- κ B activation by cleaving the linear ubiquitin chains of NEMO, which is a component of I κ B kinase (IKK) complex required for NF- κ B activation. Two novel modifications of OTULIN and their mechanisms were also revealed. Firstly, the linear ubiquitination of OTULIN at Lys64/66 is dependent on LUBAC under unstimulated status, which enhances the affinity of OTULIN-LUBAC interaction. Functionally, the more presence of OTULIN on LUBAC, which can be augmented by its linear ubiquitination, the stronger ability of OTULIN to inhibit NF- κ B activation because only LUBAC but not OTULIN can be directly recruited to NEMO. Secondly, OTULIN dimerizes via disulfide bonds and cleaves its linear ubiquitin chains intermolecularly in response to genotoxic stress and TNF α treatment, which leads to the dissociation of OTULIN from LUBAC and the overactivated NF- κ B signaling due to a lack of negative control from OTULIN. Consistently, OTULIN mutants deficient in LUBAC binding improved the cell viability under the treatment of chemo drug, underscoring the importance of the OTULIN-LUBAC interaction as a central mechanism for developing chemoresistance. Furthermore, three out of the six clinical TNBC patients have higher levels of OTULIN dimerization and accordingly, reduced linear ubiquitination, and higher NF- κ B activation in the tumor tissues than those

in the adjacent normal tissues, suggesting that loss-of-function OTULIN can allow NF- κ B to be activated by other factors. Bioinformatic analysis based on the published database of a large patient sample cohort indicates that OTULIN expression levels are increased in most basal-like breast cancer tissues, presumably facilitating self-dimerization/reduced linear ubiquitination.

Taken together, our findings revealed a new molecular mechanism by which TNBC patients develop chemoresistance via dysfunctional OTULIN, which is also generally applied to the NF- κ B activation during TNF α -mediated inflammatory response. Accordingly, targeting OTULIN and its interaction with LUBAC may be a viable therapeutic strategy for preventing chemoresistance and OTULIN-related diseases.

TABLE OF CONTENTS

CHAPTER 1. INTRODUCTION	1
Linear Ubiquitination.....	1
LUBAC.....	1
OTULIN.....	2
The discovery of OTULIN.....	2
The substrates of OTULIN.....	4
Key residues of OTULIN.....	4
NF- κ B Signaling.....	4
NF- κ B family and I κ B family.....	4
Canonical NF- κ B signaling pathway.....	6
Alternative NF- κ B signaling pathway.....	7
Atypical NF- κ B activation.....	7
NF- κ B in cancer.....	9
NF- κ B in chemoresistance.....	10
NF- κ B regulation mediated by OTULIN.....	10
Triple-Negative Breast Cancer.....	11
CHAPTER 2. MATERIALS AND METHODS	13
Reagents and Antibodies.....	13
Cells and Cell Culture.....	13
Target Guide Sequence Cloning with CRISPR/Cas9.....	13
Lentivirus Packaging, Virus Transduction, and Generation of Stable Clones.....	15
Site-directed Mutagenesis.....	15
Cell Viability Assay.....	15
Electrophoretic Mobility Shift Assay (EMSA).....	15
Luciferase Assay.....	17
DSS Crosslinking Assay.....	17
Immunoblotting.....	17
Co-immunoprecipitation and Immunoprecipitation.....	18
Immunoprecipitation to Detect Biotin-labeled OTULIN.....	18
Expression and Purification of GST- or His-tagged Fusion Protein.....	19
In Vitro Pulldown Assay.....	19
Mass Spectrometry (MS).....	19
Quantitative RT-PCR.....	21
Clinical Data Analysis.....	21
Statistical Analysis.....	22
CHAPTER 3. RESULTS	23
OTULIN Counteracts LUBAC in Regulating Genotoxic NF- κ B Activation.....	23
The N-terminal Domain of OTULIN Interacts with the PUB Domain of HOIP Facilitated by Linear Ubiquitination.....	25
OTULIN Is Linearly Ubiquitinated by LUBAC Under Unstressed Condition.....	30

OTULIN Linear Ubiquitination Is Required for NF- κ B Inhibition	34
Genotoxic Stress Induces OTULIN Dimerization and Self-deubiquitination Required for NF- κ B Activation	36
OTULIN Loss of Function Is Detected in Clinical TNBC Samples	47
CHAPTER 4. DISCUSSION	55
The Ubiquitin System in NF- κ B Activation	55
The Novel Mechanism of OTULIN-LUBAC Interplay	55
Intermolecular Dimerization Mediated by Disulfide Bonds.....	56
Ubiquitination of OTULIN.....	57
OTULIN's Differential Functions in NF- κ B and Wnt/ β -catenin Pathway	57
The Regulation of OTULIN Expression.....	58
Mechanistic Importance of Our Study	58
The Overall Significance of Our Study	58
OTULIN in COVID-19 patients	58
OTULIN in neurodegenerative diseases	59
CHAPTER 5. CONCLUSIONS AND FUTURE DIRECTIONS	61
Conclusions.....	61
The Roles of OTULIN in Neuroinflammation and Tau Accumulation.....	61
OTULN inhibitor promotes the mRNA levels of pro-inflammatory cytokines.....	63
Linear ubiquitination of tau by LUBAC associates with its degradation	63
OTULIN reduces tau linear ubiquitination and increases tau proteotoxicity by enhancing its protein stability	66
LIST OF REFERENCES.....	69
VITA.....	81

LIST OF TABLES

Table 2-1. SgRNA sequences for cell gene knockout.....	14
Table 2-2. Primer sequences for OTULIN mutations.	16
Table 3-1. Fold change of the protein expression.	53

LIST OF FIGURES

Figure 1-1. Model for HOIP-mediated linear ubiquitination.....	3
Figure 1-2. Domain structure of HOIL-1L, HOIP, and SHARPIN.....	3
Figure 1-3. Components of NF- κ B and I κ B.....	5
Figure 1-4. Illustration of genotoxic stress-induced NF- κ B signaling cascades.....	8
Figure 2-1. Workflow of the identification of ubiquitination (GG)-modified peptides.....	20
Figure 3-1. LUBAC is required for NF- κ B activation.	24
Figure 3-2. OTULIN inhibits genotoxic NF- κ B activation.....	26
Figure 3-3. OTULIN downregulates the linear ubiquitination of NEMO.....	29
Figure 3-4. Linear ubiquitin chains facilitate the binding of OTULIN and HOIP.	31
Figure 3-5. Identification of OTULIN linear ubiquitination dependent on HOIP.	33
Figure 3-6. Different interactions between OTULIN mutants and HOIP.	35
Figure 3-7. Effects of OTULIN loss-of-function mutants on NF- κ B activation.....	37
Figure 3-8. Effects of OTULIN loss-of-function mutants on cancer cell survival via dysregulating genotoxic NF- κ B signaling.	39
Figure 3-9. Genotoxic stress induces dissociation of OTULIN-HOIP complex.	40
Figure 3-10. Intermolecular interaction of OTULIN leads to self-deubiquitination.	41
Figure 3-11. OTULIN dimerization is a pre-requisite for OTULIN self-deubiquitination and the subsequent dissociation from LUBAC under genotoxic condition.	44
Figure 3-12. Analysis of OTULIN dimers, ubiquitination, and HOIP interaction during TNF α treatment.	48
Figure 3-13. Analysis of OTULIN dimers, ubiquitination, and HOIP interaction in breast cancer clinical samples.	51
Figure 3-14. Bioinformatic analysis.	54
Figure 5-1. Graphical abstract regarding the crucial roles of OTULIN in NF- κ B-mediated chemoresistance and inflammation.	62

Figure 5-2. LPS-induced neuroinflammation is promoted by UC495.64

Figure 5-3. LUBAC ubiquitinates tau with linear ubiquitin chains and promotes its degradation.65

Figure 5-4. OTULIN is required for tau deubiquitination and aggravates tau proteotoxicity.67

LIST OF ABBREVIATIONS

AA	Amino Acid
ABIN	A20-Binding Inhibitor of NF- κ B
AD	Alzheimer's Disease
ALS	Amyotrophic Lateral Sclerosis
ASCO	American Society of Clinical Oncology
ATM	Ataxia-Telangiectasia Mutated kinase
AnkR	Ankyrin Repeats
AU	Arbitrary Unit
Bcl-2	B-Cell Lymphoma 2
CAP	College of American Pathologists
CBP	Carboplatin
CHX	Cycloheximide
CNS	Central nervous system
CPT	Camptothecin
CPDM	Chronic Proliferative Dermatitis
CYLD	Cylindromatosis
DDA	Data Dependent Acquisition
DUB	Deubiquitinating enzyme
DVL2	Disheveled 2
Dox	Doxorubicin
DMEM	Dulbecco's Modified Eagle Medium
DSS	Disuccinimidyl Suberate
DTT	Dithiothreitol
EA	Electroacupuncture
ER	Estrogen Receptor
EMT	Epithelial-Mesenchymal Transition
EMSA	Electrophoretic Mobility Shift Assay
Etop	Etoposide
FDR	False Discovery Rate
HD	Huntington's Disease
HER-2	Human Epidermal growth factor Receptor 2
HOIL-1L	Heme-Oxidized IRP2 Ubiquitin Ligase-1L
HOIP	HOIL-1L-Interacting Protein
H ₂ O ₂	Hydrogen Peroxide
I κ B	Inhibitor of κ B
IAM	Iodoacetamide
IBR	In-Between-Ring domain
IKK	I κ B Kinase
IL	Interleukin
IP	Immunoprecipitation
IR	Ionizing Radiation
LC-MS/MS	Liquid Chromatography with tandem mass spectrometry
LDD	Linear Ubiquitin Chain Determining Domain

LPS	Lipopolysaccharide
LTM	LUBAC-Tethering Motif
LUBAC	Linear Ubiquitin Chain Assembly Complex
MEF	Mouse Embryonic Fibroblast
NDD	Neurodegenerative Disease
NEMO	NF- κ B-Essential Modulator
NEM	N-ethylmaleimide
NFT	Neurofibrillary Tangle
NF- κ B	Nuclear Factor-kappa B
NMDA	N-methy-D-aspartate
NIK	NF- κ B Inducing Kinase
NOD2	Nucleotide-Oligomerization Domain-containing protein 2
NLS	Nuclear Localization Sequence
NZF	Npl4-type Zinc Finger
MS	Mass Spectrometry
OTULIN	OTU deubiquitinase with linear linkage specificity
PTM	Post-Translational Modification
PAMP	Pathogen-Associated Molecular Pattern
PARP1	Poly (ADP-Ribose) Polymerase 1
PBS	Phosphate-Buffered Saline
PD	Parkinson's Disease
PIASy	Protein Inhibitor of Activated STATy
PIDD	p54-induced death domain protein
PR	Progesterone Receptor
PUB	PNGase/UBA or UBX domain
RBR	RING-between-RING domain
RING	Really Interesting Gene
RIP	Receptor Interacting Protein
RHD	Rel Homology Domain
Sam68	SRC associated in mitosis of 68 kDA
SHARPIN	Shank-Associated RH Domain Interactor
SILAC	Stable Isotope Labelling with Amino acids in Cell culture
TAD	Transactivation Domain
TAK1	TGF-beta Activated Kinase 1
TNBC	Triple-Negative Breast Cancer
TNF	Tumor Necrosis Factor
TNFR1	Tumor Necrosis Factor Receptor 1
TRAF6	TNF Receptor-Associated Factor 6
TGF	Transforming Growth Factor
Ub	Ubiquitin
UBA	Ubiquitin-Associated domain
UBD	Ubiquitin-specific Binding Domain
UBL	Ubiquitin-Like domain
UPS	Ubiquitin-Proteasome System
WT	Wild Type

ZF
2-ME

Zinc Finger
 β -Mercaptoethanol

CHAPTER 1. INTRODUCTION

Linear Ubiquitination

Ubiquitin, a small regulatory protein of 76 amino acids (AA) with a β -grasp fold conformation, was discovered in 1975 [1, 2]. Ubiquitination is the post-translational modification (PTM) by adding ubiquitin to a substrate protein, which regulates various cellular processes, including proteasomal degradation, membrane trafficking, endocytosis, DNA repair, and signal transduction [3]. Ubiquitination is conducted by ubiquitin-activating enzymes (E1s), ubiquitin-conjugating enzymes (E2s), and ubiquitin ligases (E3s) [4]. Briefly, the flexible C terminus of ubiquitin is initially attached to some particular lysine residues of the substrates through an isopeptide bond (thioester bond) mediated by these enzymes. Subsequently, the substrate-attached ubiquitin gets elongated at its N-terminal Met1 residue or one of its seven lysine residues. (i.e., Lys6, Lys11, Lys27, Lys29, Lys33, Lys48, or Lys63) by another ubiquitin. In addition, there even exist mixed and branched ubiquitin chains [3]. Similar to a code, different ubiquitin modifications have distinct impacts on cell fates. For instance, Lys48-linked ubiquitin (K48-Ub) chains target substrates for proteasome-mediated degradation, while M1-Ub chains serve as a scaffold for nuclear factor-kappa B (NF- κ B) activation [5].

In 2006, Kirisako et al. identified a new type of ubiquitin chain that is linked through the N-terminal Met (M) of the ubiquitin in a head-to-tail manner, called M1-Ub chains [6]. M1-Ub chains (also called linear ubiquitin chains) are involved in acquired and innate immune responses, such as the NF- κ B and interferon antiviral pathways. In order to perform their specific functions, linear ubiquitin chains must be decoded by proteins containing linear ubiquitin-specific binding domain (UBD), such as NF- κ B-essential modulator (NEMO), optineurin, A20, and A20-binding inhibitors of NF- κ B (ABINs), each of which can recognize linear ubiquitin chains on specific substrate sites. The dysregulated linear ubiquitination in patients induces cancer and neurodegenerative, inflammatory, and autoimmune diseases [7, 8].

LUBAC

Linear ubiquitin chain assembly complex (LUBAC) is the only known E3 ligase that can conjugate linear ubiquitin chains on substrates. It was initially identified as a protein complex (~600 kDa) consisting of two RING finger proteins, Heme-oxidized IRP2 ubiquitin ligase-1L (HOIL-1L) and HOIL-1L-interacting protein (HOIP) [6]. Afterwards, Shank-associated RH domain interactor (SHARPIN) was recognized as an additional component of LUBAC [9]. Absence of LUBAC attenuates canonical and atypical NF- κ B signaling pathways induced by proinflammatory cytokines (such as tumor necrosis factor α , TNF α and interleukin-1 β , IL-1 β), various pathogen-associated molecular patterns (PAMPs), T cell receptor agonists, nucleotide-oligomerization domain-containing protein 2 (NOD2)-mediated inflammasome activation, and genotoxic stress [10, 11]. However, LUBAC is not implicated in the noncanonical NF- κ B pathway

[12]. Patients with LUBAC loss-of-function mutations feature paradoxical traits of susceptibility to neonatal bacterial infections and systemic inflammation [13, 14].

Both HOIP and HOIL-1L belong to the RING-between-RING (RBR) domain E3 family, which was reported to form polyubiquitin chains via a RING/HECT-hybrid mechanism [15]. During the linear ubiquitination process, (A) an acceptor ubiquitin is conjugated to the linear ubiquitin chain determining domain (LDD) and (B) an E2 conjugated with a ubiquitin binds the RING1 domain of HOIP. (C) The donor ubiquitin is then transiently transported to the catalytic active site Cys885 of the RING2 domain via a thioester bond. (D) Finally, linear ubiquitin chains are generated by linking the donor ubiquitin to the acceptor ubiquitin (**Figure 1-1**). Multiple domains of LUBAC have been studied (**Figure 1-2**). The HOIP domain of LUBAC directs both ligase catalytic activity and linear specificity via RBR domain and LDD, respectively [16, 17]. In addition, the ubiquitin-associated 1 and 2 (UBA1, UBA2) domains of HOIP are required for the LUBAC assembly by binding with the ubiquitin-like (UBL) domains of SHARPIN and HOIL-1L, respectively. Moreover, the LUBAC-tethering motifs (LTMs) in HOIL-1L and SHARPIN interact with one another to form a globular domain [18]. LUBAC possesses several zinc finger (ZF) domains playing differential roles among SHARPIN, HOIL-1L, and HOIP. The Npl4-type zinc finger (NZF) domain in SHARPIN interacts with K63-linked ubiquitin chains [19], the NZF domain in HOIL-1L interacts with linear ubiquitin chains [20], whereas the NZF1 domain of HOIP interacts with NEMO [21]. Of note, PNGase/UBA or UBX (PUB) of HOIP is reported as an AAA-ATPase p97-interacting domain that is associated with linear-specific deubiquitinating enzymes (DUBs), such as OTU deubiquitinase with linear linkage specificity (OTULIN) and the CYLD-SPATA2 complex [22-24].

OTULIN

The discovery of OTULIN

In 2013, OTULIN was reported as a special DUB that exclusively cleaves linear ubiquitin chains. Although protein A20 and CYLD are important DUBs that negatively regulate the NF- κ B pathway, OTULIN is more critical than them in NF- κ B regulation [25, 26]. The distinctive function of OTULIN underlies its involvement in various pathophysiologic processes. OTULIN plays important roles in restricting spontaneous inflammation and maintaining immune homeostasis [27] and is required for canonical Wnt signaling mediated angiogenesis, craniofacial and neuronal development [28]. Of note, OTULIN^{W96R} and OTULIN^{D336E} allelic mutations cause reduced branchial arches and embryonic lethality in mice after E12.5 [26, 28]. Otulipenia is an early-onset autoinflammatory disease caused by loss-of-function mutations in OTULIN (e.g., G174Dfs*2, Y244C, and L272P). The patients with otulipenia suffer from neonatal-onset fever, neutrophilic dermatitis/panniculitis, and failure to thrive, but no obvious primary immunodeficiency [29].

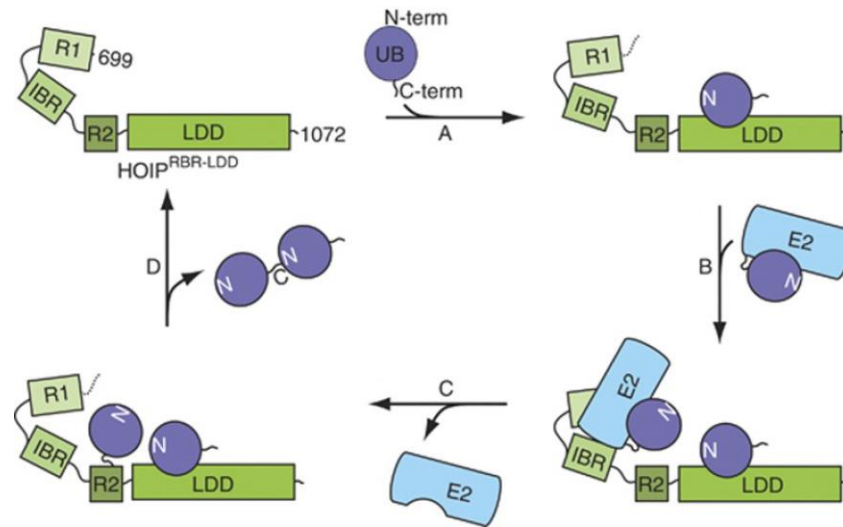


Figure 1-1. Model for HOIP-mediated linear ubiquitination.

Modified with open access permission. Smit, J.J., et al., The E3 ligase HOIP specifies linear ubiquitin chain assembly through its RING-IBR-RING domain and the unique LDD extension. EMBO J, 2012. 31(19): p. 3833-44 [16].

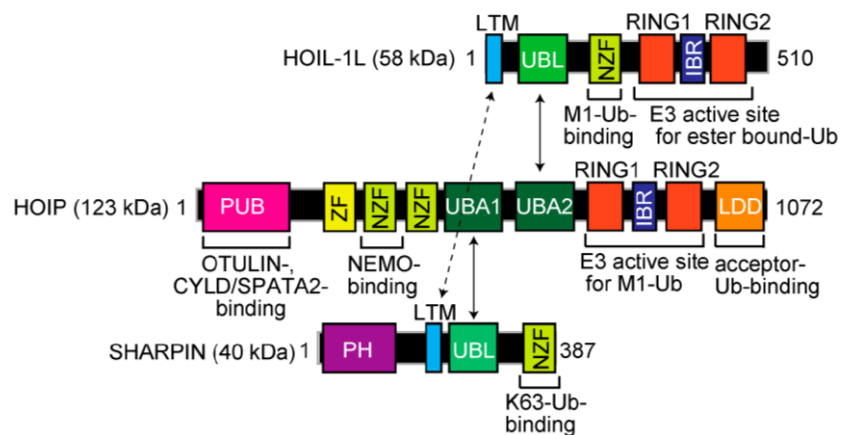


Figure 1-2. Domain structure of HOIL-1L, HOIP, and SHARPIN.

Reprinted with open access permission. Oikawa, D., et al., Linear Ubiquitin Code: Its Writer, Erasers, Decoders, Inhibitors, and Implications in Disorders. Int J Mol Sci, 2020. 21(9) [7].

The substrates of OTULIN

OTULIN removes linear ubiquitin chains from substrates, such as NEMO, RIPK1, RIPK2, ASC adaptor protein, TNFR1, MyD88, and IRF3, to block signaling propagation [26, 30-33]. OTULIN also interacts with disheveled 2 (DVL2) to cause an embryonic angiogenic phenotype in OTULIN knock-in mice [28]. Notably, adaptor proteins are required for the recruitment of OTULIN to its substrates. For example, OTULIN interacts with the PUB domain of HOIP, which is essential for the recruitment of the TNF receptor 1 complex [22].

Key residues of OTULIN

Several residues of OTULIN still play crucial roles in regulating its function. By the sequence alignment with its OTU family deubiquitinase OTUB1, cysteine 129 was found as a catalytic core of OTULIN, which is required for counteracting LUBAC function [26]. The conserved residue tyrosine 56 of OTULIN is responsible for its interaction with the PUB domain of LUBAC-HOIP subunit, which is abrogated by Tyr56 phosphorylation or mutation to phenylalanine, alanine, or glutamate [22]. Therefore, OTULIN Y56F loses its ability to block LUBAC- and TNF α -induced NF- κ B activation to a similar extent as the OTULIN C129S mutation [22, 34].

NF- κ B Signaling

Transcription factor NF- κ B was firstly identified by Ranjan Sen and David Baltimore in 1986. It was named after the B cells in which they identified it and the κ light-chain gene it affected [35]. Over three decades, plenty of work has been done to explore the functions of NF- κ B, which is significant for full understanding human pathobiology. In the complex signaling network, NF- κ B is one of the critical hubs that controls innate and adaptive immunity, inflammation, cell death and proliferation, cancer, and stress response [36-38].

NF- κ B family and I κ B family

NF- κ B is not a single protein but complexes existing as hetero- or homodimers which are composed by NF- κ B family members (**Figure 1-3A**). This family totally includes 5 members, constituting 15 NF- κ B complexes [39]. Each form of complexes may have a specific κ B site and particular cellular function [40]. The general κ B site is a palindromic DNA sequence of 5'-GGGRNWYYCC-3' (R, purine; N, any nucleotide; W, adenine or thymine; Y, pyrimidine) in enhancers or promoters [35]. NF- κ B family in mammals is composed of five Rel proteins, including p65 (RelA), RelB, c-Rel, p105/NF- κ B1 (precursor of p50), and p100/NF- κ B2 (precursor of p52). They all contain a N-terminal Rel homology domain (RHD) which consists of 300 amino acids (AAs) and has three biological functions: binding of specific DNA sequence, dimerization, and

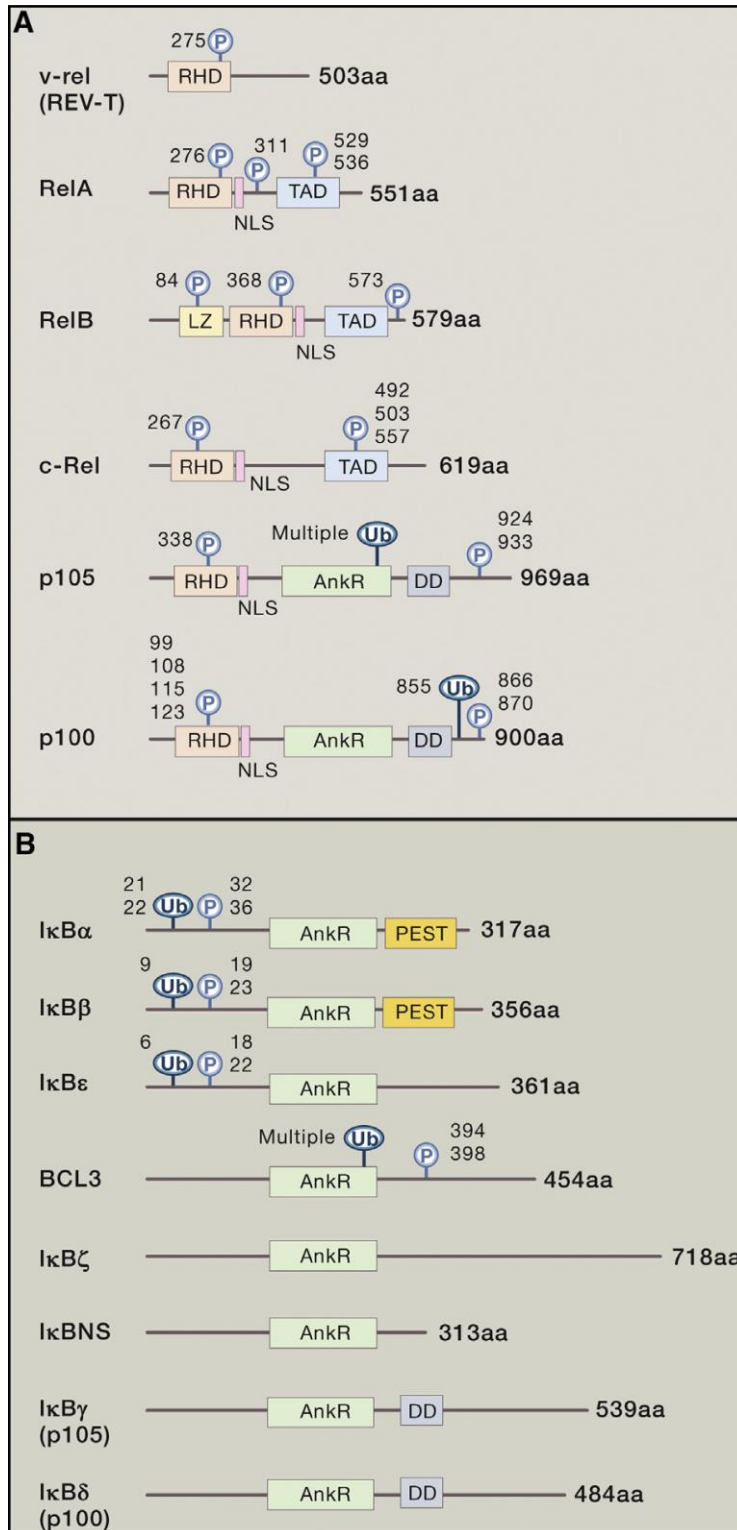


Figure 1-3. Components of NF-κB and IκB.

Modified with open access permission. Zhang, Q., M.J. Lenardo, and D. Baltimore, 30 Years of NF-kappaB: A Blossoming of Relevance to Human Pathobiology. *Cell*, 2017. 168(1-2): p. 37-57 [41].

binding of inhibitory proteins [39, 40]. NF- κ B moves into nucleus upon activation as it has a nuclear localization sequence (NLS). These five members are divided into two classes: class I proteins p50 and p52 are the products of p105 and p100, respectively, after the cleavage of C-terminal region with ankyrin repeats (AnkR) domain. p50 and p52 are regulatory protein, which need to dimerize with class II protein RelA, RelB, or c-Rel to initiate the transcription activity of target genes, because only class II proteins possess transcription transactivation domains (TADs). The most well documented paradigmatic dimers are p50:p65 and p52:RelB, which direct canonical and alternative NF- κ B activation, respectively, although the other 13 complexes still play distinct functions. In contrast to the general idea of NF- κ B, homodimers p50:p50 and p52:p52 repress, rather than activate, gene transcription as a result of TAD absence [39].

Inhibitors of κ B (I κ Bs) can bind and inhibit cytoplasmic NF- κ B in resting state [42]. I κ B family consists of eight members: I κ B α , I κ B β , I κ B ϵ , BCL-3, I κ B ζ , I κ BNS, and the C-terminal trunks of p105 (I κ B γ) and p100 (I κ B δ). All I κ B proteins possess tandem AnkRs, which can mask the NLS domain of NF- κ B to block its activation (**Figure 1-3B**). The mechanism that I κ B restricts cytoplasmic NF- κ B nuclear translocation has two functions: (1) it works as a straightforward critical brake of NF- κ B activation, and (2) it works as a switch, which can turn on the response immediately after the induction [41].

Canonical NF- κ B signaling pathway

NF- κ B can be activated in response to various stimuli, such as proinflammatory cytokines, TNF α and IL-1 for inducing macrophages and fibroblasts, antigens for B cells or T cells, PAMPs, and genotoxic stress. In terms of the response manner, NF- κ B pathways are classified into three types: canonical pathway, alternative pathway, and atypical pathway [42, 43]. This project is more related to the canonical and atypical pathways.

In canonical pathway, cells receive stimulating signals from the receptors on the cell surface, one of which is TNF receptor I (TNFR1). After binding with TNF α , TNFR1 recruits RIPK1, TRADD, TRAF2/5, and cIAP1/2, which enables cIAP1/2 to conjugate K63 ubiquitin chains on RIPK1. K63 ubiquitin chains of RIPK1 then function as scaffolds to further recruit TGF-beta activated kinase (TAK1), I κ B kinase (IKK) complexes, and LUBAC. Notably, LUBAC assembles linear ubiquitin chains to RIPK1 and NEMO, resulting in the recruitment of additional IKK complexes composed of IKK α , IKK β , and NEMO (also called IKK γ). IKK β gets activated by either TAK1 or other adjacent IKK β and then phosphorylates I κ B α at Ser32 and Ser36, leading it to K48 ubiquitination and proteasomal degradation [36]. The p50:p65 dimer is released into the nucleus, where it triggers the transcription of anti-apoptotic, inflammatory, and pro-survival genes [44]. In addition, post-translational modification of NF- κ B, such as phosphorylation, acetylation and methylation of p65, also tightly affects its transcriptional activity [45]. NF- κ B dominates the pro-survival consequence, unless

being inhibited by some genes or chemicals, such as I κ B α -SR (a nondegradable I κ B α) or cycloheximide (CHX). TNF α induces RIPK1-mediated cell death (apoptosis and necroptosis) when NF- κ B is inhibited [44].

To quickly initiate cell protective actions in response to the extracellular signal, NF- κ B proteins are pre-synthesized in most cell types, staying in latent state ready for the upcoming stimuli. Once NF- κ B gets activated, numerous genes response swiftly [36]. Of note, this induction is transient because I κ B α is also transcriptionally induced by NF- κ B and resynthesized I κ B α moves into the nucleus and removes NF- κ B from the DNA. This is a kind of negative feedback loop directed by I κ B α . In addition, other NF- κ B negative feedback genes also exist, such as A20 and miR-146a. Generally, the first round NF- κ B can last less than one hour in the nucleus even in the presence of inducer. However, if the inducer keeps stimulating the cells, the second round of NF- κ B activation will just repeat with the degradation of I κ B α and serial subsequent events. This process continues indefinitely, though weaker and weaker, until the inducer gets dissolved [46]. Hence, knockout of A20 or miR-146 abrogates the negative feedback, leading to chronic inflammation and ultimately to cancer [47, 48].

Alternative NF- κ B signaling pathway

In response to cell-differentiating or developmental stimuli, the alternative NF- κ B pathway is initiated from membrane-bound receptors, such as CD40, RANK, or Lt β R. In contrast to canonical NF- κ B signaling dependent on IKK β -mediated phosphorylation of I κ B α , the alternative pathway of NF- κ B activation relies on the NF- κ B inducing kinase (NIK)-mediated phosphorylation of IKK α homodimer. Activated IKK α then phosphorylates p100, which is processed to p52. Subsequently, p52:RelB heterodimer translocates into nucleus for its target genes' transcriptional activation [49].

Atypical NF- κ B activation

Instead of receiving stimuli from membrane-bound receptors on the cell surface, atypical NF- κ B activation by genotoxic stress involves a retrograde signaling cascade from nucleus to cytoplasm (**Figure 1-4**) [50, 51]. After the genotoxic stress caused by ionizing radiation (IR) or chemo drugs (such as doxorubicin or etoposide), NEMO firstly translocates into nucleus where it gets SUMOylated by protein inhibitor of activated STATy (PIASy) [52, 53]. SUMOylation enhances NEMO nuclear accumulation, which can also be facilitated by poly (ADP-ribose) polymerase 1 (PARP1):SRC associated in mitosis of 68 kDA (Sam68) and/or p54-induced death domain protein (PIDD):receptor interacting protein (RIP) complexes [54-56]. Ataxia-telangiectasia mutated (ATM) kinase, a pivotal kinase regulating NF- κ B activation upon DNA damage [57, 58], forms a complex with and phosphorylates nuclear accumulated NEMO, which promotes NEMO monoubiquitination [59, 60]. The complex of ATM and monoubiquitinated NEMO then exports and conveys the signal from nucleus to cytoplasm where they further recruit

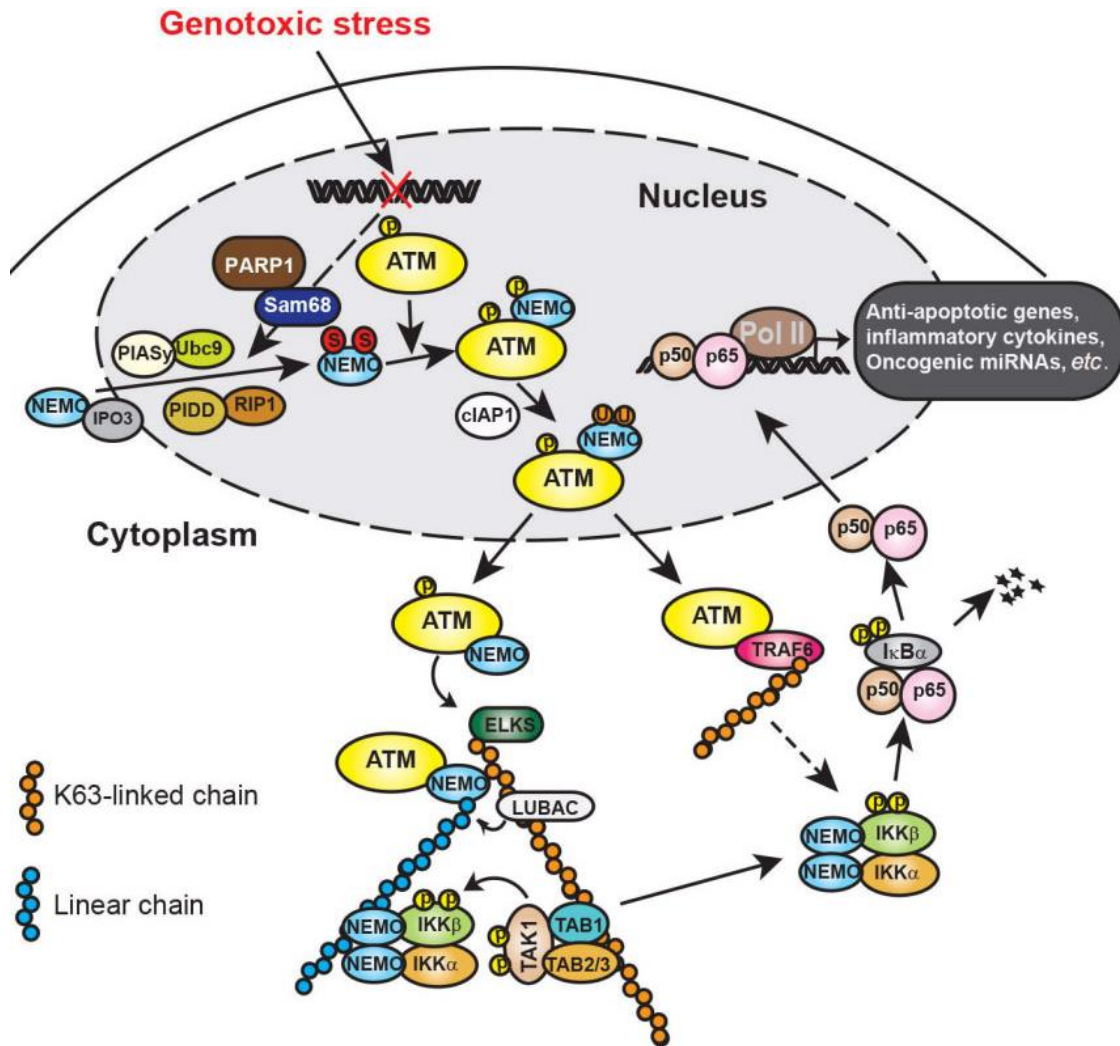


Figure 1-4. Illustration of genotoxic stress-induced NF-κB signaling cascades. Reprinted with open access permission. Wang, W., A.M. Mani, and Z.H. Wu, DNA damage-induced nuclear factor-kappa B activation and its roles in cancer progression. *J Cancer Metastasis Treat*, 2017. 3: p. 45-59 [43].

ELKS to be ubiquitinated with K63-linkage chains [52, 59, 61]. Alternatively, ATM may directly export to cytoplasm without NEMO, and promotes TNF receptor-associated factor 6 (TRAF6) K63 ubiquitination [62]. K63 ubiquitin chains of ELKS and TRAF6 herein are able to recruit NEMO, LUBAC complex, and TAK1/TAB1/TAB2 complex [11, 61, 62]. LUBAC conjugates linear ubiquitin chains on Lys285 and Lys309 of NEMO for IKK complex recruitment [11]. The scaffold of ubiquitin chains (M1 and K63 ubiquitin chains) promotes the IKK β phosphorylation by TAK1 as a major manner for NF- κ B activation in response to genotoxic stress. Subsequently, the signaling follows the canonical IKK complex-dependent fashion [43].

In addition to canonical IKK complex-dependent NF- κ B activation described above, DNA damage may also induce its activation in an alternative manner, which relies on the p52:RelB heterodimer nuclear translocation. Some studies showed the enrichment of RelB in the nuclei and p100 phosphorylation and subsequent processing to p52 in response to DNA damage, which correlates with the resistance to ionizing radiation (IR) [63-65]. However, it is still unclear how the DNA damage transmits the signal to induce alternative NF- κ B cascade. Moreover, whether ATM and NEMO are also involved in this thread remains to be determined.

NF- κ B in cancer

Cancer is caused by defective genome surveillance and signal transduction, which actually takes a long-term to accumulate [66]. Based on the major effect of NF- κ B in saving cells from apoptotic death, its activation is crucial for aggravating tumorigenesis [67]. In addition to apoptosis, NF- κ B also contributes to cancer by inflammation and mitogenic activities. These three effects work differently: the mitogenic and antiapoptotic effects drive cell proliferation and prevent cell death by affecting cells themselves which are prone to develop into cancer (intrinsic effect). The inflammatory effect provides a microenvironment suitable for cancer growing (extrinsic effect) [36]. The proinflammatory cytokines, such as TNF α and IL-1 β , modulate a variety of signaling pathways regarding inflammation and innate immunity, which is primarily regulated by NF- κ B [68]. In particular, IL-1 is recognized to play a key role in cancer by altering the tumor microenvironment and driving cancer genesis and development [69]. For example, the production of IL-1 β is associated with high risk of gastric cancer [70]. Another proinflammatory cytokine that may favor cancer is TNF α although it is named as a tumor necrosis factor. TNF α has a wide range of functions in immune homeostasis, inflammation, and host defense, and exerts distinct effects as apoptosis, necroptosis, angiogenesis, immune cell activation, differentiation, and cell migration in different context. Even though TNF α manifests pro- and antitumoral effects in a context-dependent manner, TNF α neutralization might be used to combat cancer or cancer-related complications, according to several preclinical evidence [71]. Actually, the inflammatory effect of NF- κ B is rather complex in cancer, which can be both pro-oncogenic and antioncogenic depending on the context [67].

Given its pivotal roles in cancer, it is natural to think of NF- κ B as a therapeutic target. The underlying mechanism is that activated NF- κ B promotes cell proliferation, metastasis, metabolic changes, and prevents cell death [72, 73]. Hence, basic strategy of cancer treatment is to develop NF- κ B inhibitory drugs. Thalidomide and other putative IKK inhibitors have been successfully used in myeloma [74]. However, considering the centrality of NF- κ B in innate and adaptive immunity, these drugs will also make adverse side effects potentially by suppressing immune system, such as neutrophilia, fever, or abnormal IL-1 release. Because Immune system itself is also necessary to recognize and kill tumor cells mediated by NF- κ B signaling, these NF- κ B inhibitory drugs may even worsen the cancer in some case. Thus, the development of targeting-NF- κ B drugs need to be reassessed [75].

NF- κ B in chemoresistance

IR and chemotherapeutic drugs were reported to activate NF- κ B activation underlying one clinical problem that various cancers acquire therapeutic resistance [76-79]. Genotoxic NF- κ B activation upregulates a multitude of genes that prevent apoptosis and promote proliferation in cancer cells, such as cyclin D1, Bcl-2, Bcl-xL, survivin, and XIAP [80-82]. In addition, many studies showed the high correlation between NF- κ B activity and chemoresistant feature. It was reported that DNA damage can induce the expression of proinflammatory cytokines, such as IL-6 and IL-8, which supports tumor growth, angiogenesis, cell invasion, and metastasis [83, 84]. Considering the crucial role of NF- κ B in inflammation, it is plausible that genotoxic NF- κ B activation also render cancer cells chemoresistant by modulating the transcription of proinflammatory cytokines. Furthermore, NF- κ B was reported to mediate the overexpression of oncogenic miR-181a, which can enhance cell survival and metastasis, in TNBC during doxorubicin treatment [85]. Taken together, cancer cells may acquire chemoresistance through genotoxic NF- κ B-mediated anti-apoptotic and pro-survival genes, pro-inflammatory cytokines, and oncogenic miRNAs. Therefore, it is promising to limit chemoresistance by control genotoxic NF- κ B activation.

NF- κ B regulation mediated by OTULIN

The induction of NF- κ B is complicated, which not only requires a removing of the inhibitor of κ B, but also involves many and various protein modifications, including protein-protein dimerization, phosphorylation, and ubiquitination [40, 42]. In particular, the linear ubiquitination is critical for canonical NF- κ B signaling pathway to mediate inflammatory and immune responses [86], including TNF α , IL-1, CD40, and TLR signaling pathways [9, 87-92]. Linear ubiquitination also protects cells from DNA damage-induced apoptosis during genotoxic NF- κ B activation [11]. Since ubiquitination can be counteracted by the activity of DUBs, it is plausible that the role of linear ubiquitination can be deleted by linear-linkage specific DUBs, such as CYLD and OTULIN. The role of OTULIN in attenuating linear ubiquitin-dependent signaling were

corroborated in several pathways. The overexpression of OTULIN limits linear ubiquitin chain accumulation and NF- κ B activation with the stimulation of NOD2 or TNFR1 [30], and sensitizes cells to TNF α -induced cell death [26]. In contrast, some studies showed OTULIN promoted rather than counteracted LUBAC activity by cleaving linear ubiquitin chains of LUBAC [93]. In this scenario, mice expressed with catalytically inactive OTULIN resembled the phenotype of LUBAC-deficient mice, manifesting embryonic lethality or adult auto-inflammation because of TNFR1-mediated cell death, in which the pro-survival NF- κ B signaling was diminished [94].

Triple-Negative Breast Cancer

Cancer is the second leading cause of death globally, and breast cancer has always been the most often diagnosed cancer among women for decades, constituting 24% of the total cancer cases [95, 96]. Breast cancer develops in the breast tissue, with most emergent cases occurring from the milk duct named ductal carcinoma, and other minor cases occurring from lobules named lobular carcinoma [97, 98].

Triple-negative breast cancer (TNBC) is an aggressive subtype that affects 12-18% of breast cancer patients, defined by the lack of estrogen receptor (ER), progesterone receptor (PR), and human epidermal growth factor receptor 2 (HER-2). The American Society of Clinical Oncology/College of American Pathologists (ASCO/CAP) guidelines defined TNBCs by cellular expression of ER and PR of $\leq 1\%$ and HER2 expressions of 0 to 1+, as determined by immunohistochemistry [99]. Mutations in *BRCA1*, *BRCA2*, *TP53*, *CDH1*, *PTEN*, and *STK11* are highly associated with the progression of TNBC [100-102].

Nowadays, breast cancer can be treated by surgery [103], hormonal therapy [104], chemotherapy [105], radiation [106], and immunotherapy [107]. TNBC is of particular research interest as it does not benefit from hormone or anti-HER-2 therapy and has a highly invasive nature, characteristic metastatic patterns, and poor prognosis [108-111]. Although with a generally poor breast cancer-specific outcome, most TNBCs are initially sensitive to chemotherapy [112, 113]. Doxorubicin (Dox) is one of the first line chemotherapy agent but accompanied with severe heart failure of more than 20% of patients. To avoid the fatal side effects, a lifetime dosage limit is applied [114, 115]. Unfortunately, TNBC frequently develops resistance to chemotherapy [116], which causes disease relapse, recurrence, and cancer dissemination [117]. Therefore, the chemo side effects and frequent development of resistance are major clinical limitations to use chemo drugs and treat TNBC [118]. There is an urgent need to promote drug targeting to tumor and prevent the occurrence of chemoresistance. The mechanisms of chemoresistance have been demonstrated to be complex, including epigenetics, drug inactivation, drug target alteration, drug efflux, DNA damage repair, cell death inhibition, and epithelial-mesenchymal transition (EMT) [119-121]. Remarkably, NF- κ B has been identified as a critical determinant in resistance mechanisms by supporting cancer cells survival and proliferation [122, 123]. Notably, TNF α is a proinflammatory cytokine, that is overexpressed in a variety of cancers, correlating with augmented tumor cell

proliferation, high malignancy grade, frequent metastasis and poor prognosis for the patient [95]. These data suggest TNF α could be a potential therapeutic target for cancer. In this scenario, the inhibitory effect of OTULIN on TNFR1 signaling might be another approach to limit tumor progression.

CHAPTER 2. MATERIALS AND METHODS

Reagents and Antibodies

Camptothecin (CPT), Carboplatin (CBP), etoposide (Etop), doxorubicin (Dox) and gliotoxin were purchased from Sigma-Aldrich. Human and mouse recombinant TNF α was purchased from CalBiochem and prepared in phosphate-buffered saline (PBS) containing 0.1% bovine serum albumin fraction V (Sigma-Aldrich) to a final stock concentration of 10 μ g/ml. IgGs against c-Myc (9E10), GFP (B2), I κ B- α (C-21), GST (B-14), p65 (F-6), ubiquitin (P4D1), and CYLD (H6) were purchased from Santa Cruz Biotechnology. IgGs against HA (C29F4), His (D3I10), phospho-p65 (Ser536) (93H1), phosphor-I κ B α (Ser32) (14D4), K63-Ub (D7A11), K48-Ub (D9D5), RNF31 (E6M5B), OTULIN (14127s), Biotin (7075S), cleaved caspase-3 (Asp175) (5A1E) and α -Tubulin (DM1A) were purchased from Cell Signaling Technology. Anti-HOIL-1 antibody (2E2) and anti-linear ubiquitin antibody (LUB9) were obtained from Millipore Sigma. Anti-SHARPIN antibody (ab197853) was purchased from ABCAM. N-ethylmaleimide (cat# 23030) and Iodoacetamide (cat# A39271) was purchased from Thermo Scientific.

Cells and Cell Culture

Mouse embryonic fibroblasts (MEFs), HEK293T, and MDA-MB-231 cells were grown in Dulbecco's Modified Eagle Medium (DMEM) with 10% fetal bovine serum, penicillin, and streptomycin in a 5% CO₂ humidified incubator. Wild-type, HOIL-deficient, and Sharpin^{cpdm} MEFs were kind gifts from Dr.K Iwai (Osaka University). Gene knockout cells HEK293T_HOIP-KO, HEK293T_OTULIN-KO, and MDA-MB-231_OTULIN-KO cells (≥ 2 clones, respectively) were generated by the CRISPR-Cas9 system [124].

Target Guide Sequence Cloning with CRISPR/Cas9

Different single guide RNA sequences targeting OTULIN or HOIP were acquired from Genome-scale CRISPR Knock-OUT v2 libraries supplied by Feng Zhang [124] (**Table 2-1**). Each pair of Oligos (100 μ M) were annealed in the mixture with T4 ligation buffer (B0202S; BioLabs) and ddH₂O at 37°C for 30 min followed by 95°C for 5 min and cool down to room temperature naturally. A total of 5 μ g of LentiCRISPRv2 (cat# 52961; Addgene) was digested by BsmBI in FastDigest buffer for 30 min at 37°C. The annealed oligos above were ligated with agarose gel-purified vector using QIAquick Gel Extraction Kit (cat# 28704; QIAGEN). The Lenti-sgOTULIN and Lenti-sgHOIP were subsequently generated by transformed competent DH5 α , which was selected by ampicillin.

Table 2-1. SgRNA sequences for cell gene knockout.

Name	Sequence (5' to 3')
Sg1 HOIP F	CACCGGTTGAGCTTCCCCGAAGGGC
Sg1 HOIP R	AAACGCCCTTCGGGGAAGCTCAACC
Sg2 HOIP F	CACCGGCACTGCCCATCCTGTAAAC
Sg2 HOIP R	AAACGTTTACAGGATGGGCAGTGCC
Sg1 OTULIN F	CACCGCGAGCGACCGCATGAGTCGG
Sg1 OTULIN R	AAACCCGACTCATGCGGTCGCTCGC
Sg2 OTULIN F	CACCGCGCGGACTCACTGCTCGGCC
Sg2 OTULIN R	AAACGGCCGAGCAGTGAGTCCGCGC
Sg3 OTULIN F	CACCGCAGCGTACCAGCATGAGCTC
Sg3 OTULIN R	AAACGAGCTCATGCTGGTACGCTGC

Lentivirus Packaging, Virus Transduction, and Generation of Stable Clones

HEK293T cells were seeded in 10 ml completed DMEM media in a 10 mm dish with about 70% confluence before transfection. Lentiviral sgOTULIN/sgHOIP (5 µg), Vsv-g (5 µg), pMDL-g (5 µg), and RSV-REV (5 µg) were co-transfected into HEK293T cells using 60 µl of superfect reagent (cat# 301307; QIAGEN) for 5 h incubation. The mixture was then replaced with 25 ml fresh completed DMEM media. After 60 h, cell media was collected into 50 ml centrifuge tubes and centrifuged for 15 min at 3000 rpm. The ultracentrifugation (3 h, 18000 rpm) of filtered supernatant by 0.45 µm membrane could separate the packaged virus from the media. The supernatant was discarded, and the pellet was resuspended with 100 µl DPBS. The resuspended virus was aliquoted to 10 200-µl tubes. Each tube of packaged lentivirus was mixed with 6 µg/ml polybrene and then added to HEK293T cells under about 70% confluence in 10 ml dish for virus transduction. Single stable clone screen was applied by antibiotic puromycin (2 µg/ml) selection. The knockout efficiency of each clone was determined by immunoblotting.

Site-directed Mutagenesis

OTULIN mutants (OTULIN C129S, OTULIN Y56F, OTULIN K34R, OTULIN K64/66R, OTULIN C17A, OTULIN C47A, and OTULIN C17/47A) were generated in this study (**Table 2-2**).

Cell Viability Assay

After transfected with plasmids for 6 h, cells were seeded into 96-well plates (5×10^3 /well counted by hemacytometer) in triplicates. After doxorubicin treatment for 48 h, cells were incubated with CCK8 reagent (10 µl/well; Dojindo) for 2 h followed by measuring the absorbance reading at OD₄₅₀ with a microplate reader.

Electrophoretic Mobility Shift Assay (EMSA)

Cells treated with TNF α , chemo drugs, or IR were washed with PBS three times before pellet collection. The cell pellets were stored frozen at -20°C until cell lysis. Cells was lysed with the same condition as that in immunoblotting section of methods. The conditions for EMSA were described previously [125]. Briefly, lysates (20 µg), 5X EMSA buffer (2 µl), DTT (1 µl, 0.1M), dI-dC (1 µg), and balanced H₂O to 9 µl were mixed and incubated on ice for 15 min. 5X EMSA buffer contains 375 mM NaCl, 75 mM Tris-HCl (pH 7.5), 7.5mM EDTA, 7.5mM DTT, 37.5% glycerol, 1.5% NP-40, 100 µg/ml BSA, and ddH₂O to appropriate volume. We used a double-stranded oligonucleotide probe containing the Igk intronic κB site (5'-CTCAACAGAGGGGACTTTCCGAGAGG CCAAT-3'). The Oct-1 site oligo was purchased from Promega as a control. The probe was

Table 2-2. Primer sequences for OTULIN mutations.

Name	Sequence (5' to 3')
OTULIN C129S F	CGTGGTGATAATTACTCTGCACTGAGGGCCACG
OTULIN C129S R	CGTGGCCCTCAGTGCAGAGTAATTATCACCACG
OTULIN Y56F F	CATGAGGAGGACATGTTCCGTGCTGCAGATGA
OTULIN Y56F R	TCATCTGCAGCACGGAACATGTCCTCCTCATG
OTULIN K34R F	CACGGCGCGGGACGGCGGGAGGGCGGCGGCCAGCGGGCAG
OTULIN K34R R	CTGCCCGCTGGCCGCCGCCCTCCCGCCGTCCCGCGCCGTG
OTULIN K64/66R F	CAGATGAAATAGAAAGGGAGAGAGAATTGCTTATACA
OTULIN K64/66R R	TGTATAAGCAATTCTCTCTCCCTTTCTATTTTCATCTG
OTULIN C17A F	AGGCGCGAGCGCTGCCGAGAC
OTULIN C17A R	GTCTCGGCAGCGCTCGCGCCT
OTULIN C47A F	AGATGCAGGCTCCGGCCGAGCATGAG
OTULIN C47A R	CTCATGCTCGGCCGGAGCCTGCATCT

labeled with $\gamma^{32}\text{P}$ -dATP using T4 polynucleotide kinase, and 1 μl probe was added to the above reactions for 15 min RT incubation. Following electrophoresis in a 4% native acrylamide gel, the gels were dried, DNA in gels were visualized by phosphoscreen.

Luciferase Assay

Cells for NF- κ B signaling reporter assay were co-transfected with 0.5 μg pGL4.32 (Luc2p/NF- κ B-RE/Hygro), 10 ng pGL4.74 (hRLuc/TK) (Promega), and the indicated plasmids per well of 24-well plate in triplicate. After 24 h, cells were treated with compounds as indicated in the figure and the luciferase activity was detected by a Promega GloMax 20/20 luminometer, using the Dual-luciferase Reporter Assay System (cat# E1960; Promega). Renilla luciferase activity was measured for normalization of transfection efficiency.

DSS Crosslinking Assay

HEK293T cells were treated with 2 μM of doxorubicin or DMSO for 2 hours. $\sim 1.2 \times 10^6$ cells were then washed three times and collected with 500 μl cold PBS. Crosslinker disuccinimidyl suberate (DSS) solution (cat# 21655; ThermoFisher) was added into the PBS (with cells) to a final concentration of 1 mM for incubation for 30 min at room temperature. The reaction was stopped by the quench solution with a final concentration of 10 mM Tris-HCl (pH 7.5) for 15 min at room temperature. Finally, Cells were obtained by 200 \times g centrifuge for OTULIN dimerization analysis by immunoblotting.

Immunoblotting

Cells were lysed with the RIPA buffer (cat# PI89900; Thermo Scientific) containing protease inhibitor cocktails (Roche) and phosphatase inhibitor cocktails (Roche) on ice, with randomly vigorous vortex for 30 min. After centrifuging the cell lysates at 18×10^3 g for 10 min, protein concentration of the supernatant was determined by Bradford protein assay (Bio-Rad), and the same amounts of lysates (30 μg) were mixed in 2X sample buffer (125 mM Tris-HCl, 4% SDS, 20% glycerol, 10% 2-mercaptoethanol, a pinch of bromophenol blue) and boiled for 10 min at 95°C. Alternatively, lysates were dissolved in 2X sample buffer without 2-mercaptoethanol to detect the disulfide-bond-dependent dimerization of OTULIN. Samples were loaded in appropriate concentration of polyacrylamide gels (e.g., 10%, 4-20% gradient gels, etc.) for SDS-PAGE, proteins were immunoblotted with the appropriate antibodies and subsequently visualized by chemiluminescent substrate.

Co-immunoprecipitation and Immunoprecipitation

For co-immunoprecipitation (co-IP) assays, the whole cells of 60 mm dish were collected in 1.5 ml Eppendorf tube and lysed with homemade IP lysis buffer (20 mM Tris (pH 7.0), 150 mM NaCl, 1 mM EDTA, 1 mM EGTA, 0.5% NP-40, 2 mM DTT, 0.5 mM PMSF, 20 mM β -glycerol phosphate, 1 mM sodium orthovanadate, 1 μ g/ml leupeptin, 1 μ g/ml aprotinin, 10 mM *p*-nitrophenyl phosphate, and 10 mM sodium fluoride). After the centrifuge, 5% supernatant lysates were taken as input for future use. DynabeadsTM protein A (20 μ l for each, cat# 10001D, ThermoFisher) was prepared by washing three times with IP lysis buffer and then incubated with 1 μ g primary antibody and the left cell lysates at 4°C overnight. The protein-antibody-bead conjugates were isolated by magnetic rack, followed by five washes with IP lysis buffer. Immunoprecipitated proteins were eluted with 20 μ l SDS-PAGE-loading buffer boiling for 10 min at 95°C. Regular immunoblotting was performed for the subsequent process.

To detect protein ubiquitination, cells were boiled for 30 min at 95°C in IP lysis solution containing 1% SDS to break noncovalent connections. After heating, the cell lysates were centrifuged at 18×10^3 g for 10 min at 4°C. The resultant supernatant was diluted with IP lysis buffer to 0.1% SDS and mixed with primary antibodies (1 μ g) and DynabeadsTM protein A (20 μ l) for subsequent incubation at 4 °C overnight. The loading sample preparation, SDS-PAGE in polyacrylamide gel, and protein of interest visualization were conducted in the same way as described above.

Immunoprecipitation to Detect Biotin-labeled OTULIN

HEK293T cells were grown in complete DMEM media and stimulated with TNF α (10 ng/ μ l) or etoposide (10 μ M) for the indicated amount of time. HEK293T cells were washed three times with PBS and acquired as pellets by centrifuge at 5000 \times g for 1 min, followed by vacuum to remove the extra PBS. Pellets were flicked loose and lysed with RIPA lysis buffer containing 500 μ M DCP-Bio1 and protease inhibitor cocktails on ice for 1h and given a vortex every 10 min. Cell lysates were centrifuged at 17,500 \times g for 10 min and the supernatant was transferred to new 1.5 ml Eppendorf tubes. Protein concentration was determined by Bradford protein assay. An aliquot of 30 μ g protein was separated for input. 300 μ g of each sample was preincubated with 20 μ l Dynabeads-protein A magnetic beads preequilibrated in lysis buffer (no antibody) for 2 h at 4°C, and beads were isolated by magnetic rack and discarded to exclude the nonspecific protein-beads binding. In addition, a fresh aliquot (20 μ l) of beads was preincubated with 3 μ l of anti-HA antibody for 2 h at 4°C. The antibody-crosslinked beads were collected and incubated with preprocessed lysates overnight at 4°C. The next day, supernatants were removed, and beads were washed three times with cold RIPA buffer. HA-OTULIN protein was eluted with 25 μ L SDS sample buffer by boiling at 95°C for 10 min. Total supernatants of eluted protein and SDS sample buffer-boiled Input were loaded into 4-20% gradient polyacrylamide gels and separated by SDS-PAGE. The subsequent procedures were PVDF membrane transfer, 5% milk blocking, and incubation with HRP-

conjugated anti-biotin antibody (1:1000) or anti-HA antibody (1:1000) overnight at 4°C. For the latter one, additional incubation with an HRP-conjugated secondary IgG antibody for 2 h at 24°C was needed. PVDF membrane was washed with TBST buffer for 30 min, replacing fresh buffer every 10 min. Finally, protein of interest was visualized by chemiluminescent approach.

Expression and Purification of GST- or His-tagged Fusion Protein

pGEX-5X.1-GST-PIM, pGEX-5X.1-GST-PIM-Ub4, pGEX-4T-2-GST-PUB_WT, pGEX-4T-2-GST-PUB_D117A, pGEX-4T-2-GST-PUB_E127A, pGEX-4T-2-GST-PUB_D117A/E127A, pET28a-His-PUB, pET28a-His-PIM-Ub4, and pET28a-His-Ub4 constructs were expressed in BL21 (DE3) cells. Cells with GST or His constructs were grown at 37 °C in 250 ml LB medium with 100 µg/ml ampicillin or 50 µg/ml kanamycin, respectively, to an OD₆₀₀ of 0.4-0.6. The culture was further incubated with IPTG to a final concentration of 0.1 mM for 2.5 h. Cells were collected at 5000 ×g for 15 min at room temperature. Pellet resuspending in 5 ml ice-cold PBS with proteinase inhibitor cocktails was sonicated for lysis. Triton X-100 was added to a final concentration of 1% to avoid the association of fusion protein with bacterial proteins. To remove insoluble material and cell debris, the mixture was centrifuged for 5 min at 10,000 ×g at 4°C. GST- or His-containing supernatant was added with 1 ml of 50 % slurry of glutathione-agarose beads or Ni-NTA agarose beads, respectively, and mixed for 2 h at 4°C. After centrifugation at 500 ×g for 10 sec, beads were collected and washed by PBS for elution, in which glutathione-agarose beads or Ni-NTA agarose beads were mixed with reduced glutathione or imidazole, respectively, in 500 µl 50 mM Tris elution buffer (pH 8.0).

In Vitro Pulldown Assay

Glutathione-agarose beads or Ni-NTA agarose beads and 2 µg of each purified fusion protein of interest were added into one 1.5 ml Eppendorf tube and incubated for 2 h at 4 °C in 500 µl IP buffer with proteinase inhibitor cocktails. Beads were washed three times by IP buffer to remove non-bound protein before elution in 20 µl 2X SDS loading buffer for immunoblotting.

Mass Spectrometry (MS)

In-gel digestion of a gel band (OTULIN) was performed overnight at 37°C using In-Gel Tryptic Digestion kit (cat#89871x, Thermo Sci.) according to the manufacturer's protocol including optional steps for reduction and alkylation. The generated peptide mixture (25 µl) was vacuum dried for 180 min to get rid of the volatile components of the digestion buffer. The generated peptide sample was subject to LC-MS/MS analysis (**Figure 2-1**).

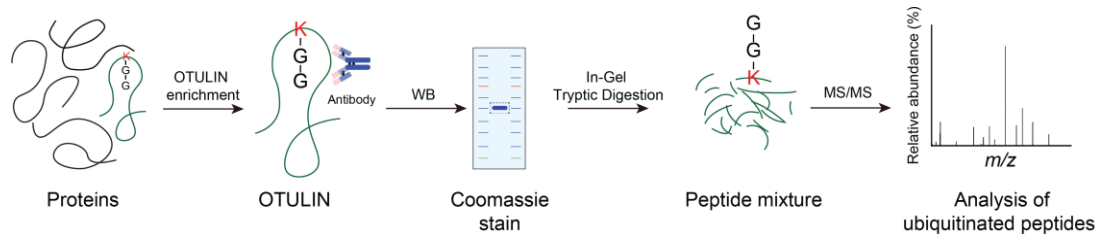


Figure 2-1. Workflow of the identification of ubiquitination (GG)-modified peptides.

For beads digestion, beads with IP OTULIN were transferred into 70 μ l of digestion buffer (DB, 100 mM ammonium bicarbonate) and incubated with 4 μ l of LysC/Trypsin mixture (cat# A41007, Thermo Scientific) dissolved at 0.1 μ g/ μ l in DB. Trypsin/Lys-C digestion was performed overnight at 37°C and 1150 rpm using Eppendorf ThermoMixer F1.5. The peptide digests were collected, and the beads were extracted with 100 μ l of 50% acetonitrile/0.5% TFA at 37°C for 10min; the extracts were combined with corresponding digests, desalted using Pierce C-18 spin tips (cat# 84850, Thermo Scientific) according to the manufacturer's protocol, and vacuum dried.

For LC-MS/MS, the dried peptide sample was re-dissolved in 30 μ l of loading buffer (3% acetonitrile, 0.1% TFA), and 5 μ l was analyzed using LC-MS/MS method with 160 min LC gradient for peptide/protein identification and mapping of specified PTM sites. Raw MS data were acquired on an Orbitrap Fusion Lumos mass spectrometer (Thermo Fisher) as previously described [126].

The analysis the acquired raw MS data was performed within a mass informatics platform Proteome Discoverer 2.2 (Thermo Fisher) as previously described [126].

Quantitative RT-PCR

Total RNA was extracted from HEK293T cells by TRIzol reagent (Invitrogen) following the manufacturer's instructions. The cDNA was synthesized from 2 μ g of total RNA using the RevertAid First Strand cDNA Synthesis kit (Thermo Scientific). qPCR was performed using SsoAdvanced Universal SYBR Green Supermix (Bio-Rad) on an Eppendorf Mastercycler realplex2. Gene specific primers were used to amplify cDNA as followed: *OTULIN* forward, 5'-GGGGCATCAGAACCGAGATTA-3' and *OTULIN* reverse, 5'-TCGCCGTATGGAGGTGAACT-3'; *GAPDH* forward, 5'-TGCACCACCAA CTGCTTAGC-3' and *GAPDH* reverse, 5'-GGCATGGACTGTGGTC ATGAG-3'; *Tnf α* forward, 5'-CCCTCACACTCAGATCATCTTCT-3' and *Tnf α* reverse, 5'-GCTACGACG TGGGCTACAG-3'; *Il-6* forward, 5'-AGTTGCCTTCTTGGGACTGA-3' and *Il-6* reverse, 5'-TCCACGATTTCCCAGAGAAC-3'; *Il-1 β* forward, 5'-AAATGCCTCGTGCT GTCTGACC-3' and *Il-1 β* reverse, 5'-CTGCTTGAGAGGTGCTGATGTACC-3'; *Gapdh* forward, 5'-GCAAATTCAACGGCACAG-3' and *Gapdh* reverse, 5'-CTCGCTCCTGGA AGATGG-3'.

Clinical Data Analysis

Immunoblotting and immunoprecipitation analysis of OTULIN were performed in breast cancer patient tumor samples and adjacent normal breast tissue samples. Specimens were collected immediately after surgery in RPMI medium containing penicillin/streptomycin or snap frozen and transported to the laboratory on ice.

Statistical Analysis

The results were presented as mean \pm SEM. Statistical analysis has been performed using Prism GraphPad 9 software. The number of independent experiments, experimental repeats, biological samples are indicated in figure legends. Multiple comparisons were made using one-way or two-way ANOVA as shown in the figure legends. $p < 0.05$ is considered significant, indicated as * $p < 0.05$, ** $p < 0.01$, *** $p < 0.001$, and **** $p < 0.0001$.

CHAPTER 3. RESULTS¹

OTULIN Counteracts LUBAC in Regulating Genotoxic NF- κ B Activation

It has been well established that NF- κ B signaling is excessively activated in response to genotoxic stress and TNF α treatment [11, 52, 87]. The LUBAC-dependent linear ubiquitination of NEMO has been reported as a crucial step of atypical and canonical NF- κ B activation, in which linear ubiquitin chains serve as signaling scaffolds to increase phosphorylation of IKK by TAK1 [11, 87]. By altering the level or activity of the LUBAC subunits (HOIP, HOIL-1L, and SHARPIN), we provided more evidence for a LUBAC-dependent mechanism underlying the canonical (TNF α treatment) and atypical (genotoxic stress) NF- κ B signaling activation. First, we found that TNF α - and chemo drugs-induced NF- κ B activation was substantially reduced in CRISPR/Cas9-cloned HOIP-KO HEK293T cells, in which the excellent knockout efficiency of HOIP (the catalytic core subunit of LUBAC) was shown by immunoblotting (**Figure 3-1A**). To exclude the off-target effect, we reconstituted wild-type (WT) HOIP or enzymatically inactive HOIP C885S in HOIP-KO HEK293T cells. HOIP WT rescued the NF- κ B activation indicated by phosphorylation of p65, phosphorylation of I κ B α , and subsequent degradation of I κ B α , which is induced by TNF α or Etop treatment. HOIP C885S failed to rescue NF- κ B activation, indicating HOIP is required for canonical and genotoxic NF- κ B activation (**Figure 3-1B**). Furthermore, gliotoxin is a highly bioactive fungal metabolite with its well-known immunosuppressive action as a functional NF- κ B inhibitor. In consistent with its new identity as a selective binder to the RBR domain of the HOIP [128], gliotoxin inhibited genotoxic NF- κ B activation by inhibiting LUBAC (**Figure 3-1C**). It was reported that the deficiency of HOIL-1 or SHARPIN dramatically reduced LUBAC E3 ligase activity [6, 9], hence we doubted whether HOIL-1 and/or SHARPIN are also required for the canonical and atypical NF- κ B activation. Using HOIL-1^{-/-} MEFs, and SHARPIN-null chronic proliferative dermatitis (cpdm) MEFs, we found that the absence of HOIL-1L and SHARPIN in MEFs also reduced the NF- κ B response to TNF α or chemo drug treatment (**Figure 3-1D, F**). In addition, NF- κ B activation increased gradually upon CPT 4 h treatment and peaked at 2 h, which was attenuated by HOIL-1 knockout at all the indicated times (**Figure 3-1E**). These data demonstrate that all the subunits of LUBAC work together for inflammatory and genotoxic NF- κ B activation.

OTULIN specifically cleaves linear ubiquitin chains which are assembled by LUBAC and has been demonstrated to inhibit inflammatory NF- κ B signaling [26, 30]. To test if OTULIN also downregulates LUBAC-mediated genotoxic NF- κ B activation, we also used CRISPR/Cas9 system to generate OTULIN-KO HEK293T and MDA-MB-231 cells. Of note, it was reported that OTULIN deficiency has cell type-specific effects

¹ Modified from final submission with permission. Li, M., et al., Reciprocal interplay between OTULIN-LUBAC determines genotoxic and inflammatory NF- κ B signal responses. Proc Natl Acad Sci U S A, in press [127].

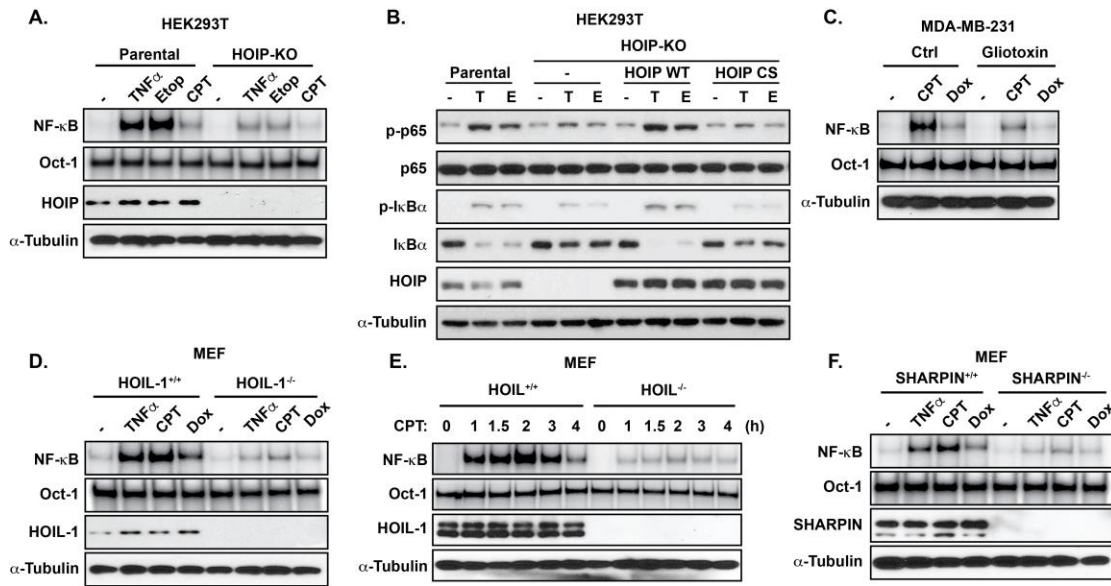


Figure 3-1. LUBAC is required for NF- κ B activation.

(A) Parental or HOIP-KO HEK293T cells were treated with TNF α (10 ng/ml, 15 min), Etop (10 μ M, 2h), or CPT (10 μ M, 2h). NF- κ B activation was analyzed by EMSA using Ig κ probe, and protein expression was determined by immunoblotting with indicated antibodies. An Oct-1-binding consensus probe and α -Tubulin were used as a control in EMSA and immunoblotting, respectively. (B) HOIP-KO HEK293T cells were reconstituted with HOIP WT or C885S mutant. Cells were treated with TNF α (10 ng/ml, 15 min) or Etop (10 μ M, 2h). Protein expression was determined by immunoblotting with antibodies as indicated. (C) MDA-MB-231 cells were pretreated with or without LUBAC inhibitor gliotoxin (1 μ M) for 24 h, and subsequently treated with CPT (10 μ M, 2h) or Dox (2 μ g/ml, 2h). NF- κ B activation was analyzed by EMSA using Ig κ probe. (D) HOIL-1^{+/+} and HOIL-1^{-/-} MEFs were treated with TNF α (10 ng/ml, 15 min), CPT (10 μ M, 2h), or Dox (2 μ g/ml, 2h). NF- κ B activation was analyzed by EMSA, and protein expression was determined by immunoblotting with indicated antibodies. (E) HOIL-1^{+/+} and HOIL-1^{-/-} MEFs were treated with CPT (10 μ M) for indicated time points, and cell lysates were analyzed by EMSA and immunoblotting to determine the NF- κ B activation and HOIL-1 knockout efficiency, respectively. (F) SHARPIN^{+/+} and SHARPIN^{-/-} MEFs were treated and analyzed as in (D).

on LUBAC degradation. Loss of OTULIN in T cells, B cells, and fibroblasts downregulates LUBAC stability, while OTULIN deficiency in myeloid cells and bone marrow-derived macrophages does not affect LUBAC abundance [27, 129]. In both HEK293T and MDA-MB-231 OTULIN-KO clones, we found a substantial upregulated ladder-shaped linear ubiquitin signal without LUBAC degradation as compared to parental cells (**Figure 3-2A, B**). Functionally, NF- κ B activation was appreciably improved by OTULIN knockout determined by EMSA upon various stimuli, including IR, Dox, CBP, Etop, CPT, and TNF α (positive control) (**Figure 3-2C through E**). In response to a time-course treatment of Dox, NF- κ B showed that much more activation in OTULIN-KO cells starting from 2 h (**Figure 3-2F**). The aberrant NF- κ B activation in OTULIN-KO cells was abolished by the reconstitution of OTULIN WT, but not the catalytic dead mutant OTULIN C129S, suggesting that OTULIN catalytic activity is required for limiting the NF- κ B activation (**Figure 3-2G**). We further showed that treatment with Etop induced much higher NF- κ B activation based on a dual-luciferase NF- κ B-dependent reporter assay in OTULIN-KO cells compared to parental cells, which was attenuated by the reconstitution of OTULIN WT (**Figure 3-2H**). OTULIN is not transcriptionally regulated by NF- κ B [130], so neither Etop nor TNF α treatment altered OTULIN transcriptional level (**Figure 3-2I, J**). Therefore, whether OTULIN can modify its function adaptively according to cellular context is still a question.

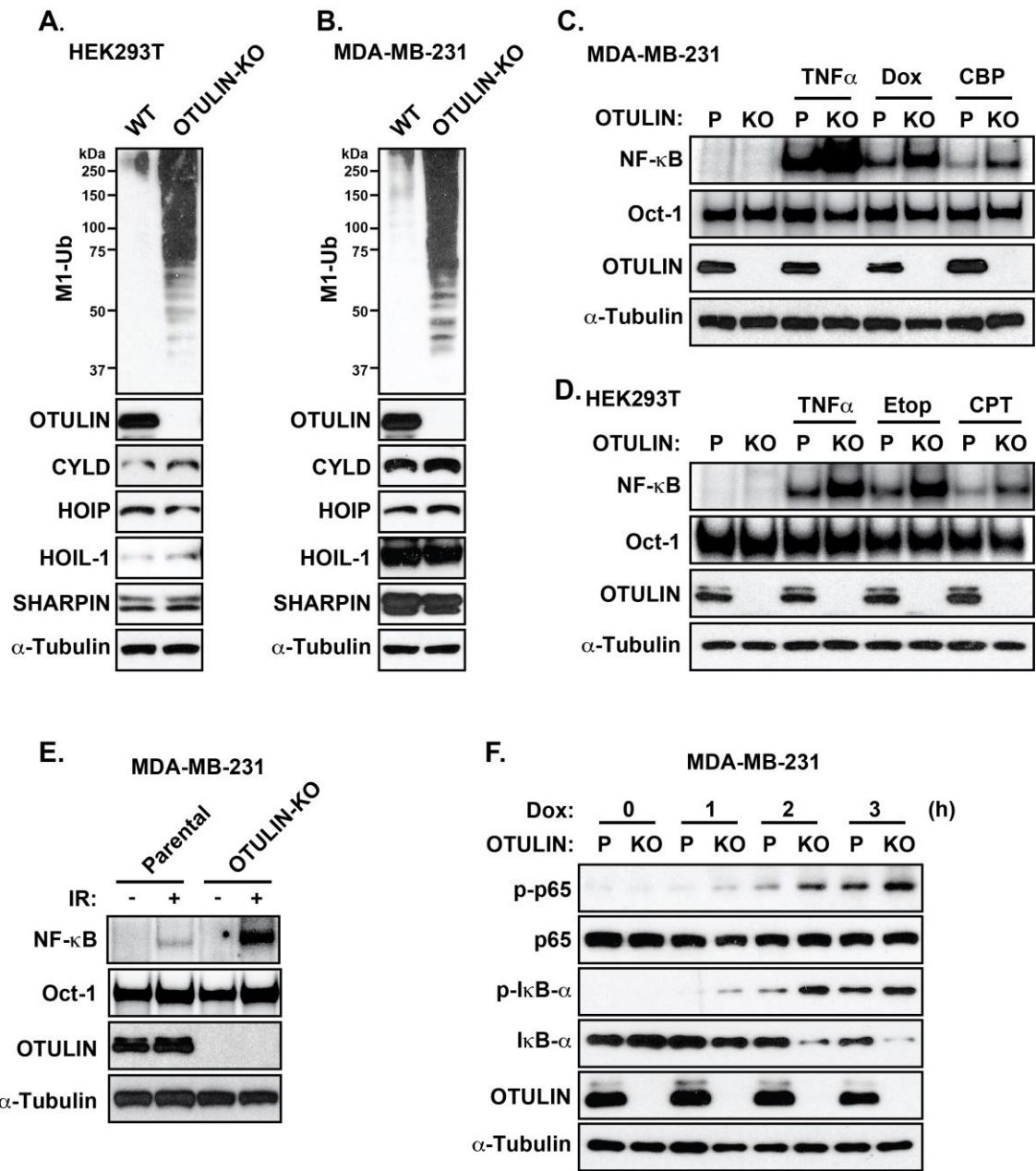
To explore how OTULIN inhibits genotoxic NF- κ B activation, we proceeded to examine the NF- κ B modulator NEMO which is known to be modified by LUBAC with linear ubiquitin chains upon genotoxic stress [11]. Consistently, the linear ubiquitination of NEMO was induced by the treatments of cytotoxic chemotherapeutic agents Etop and Dox in HEK293T cells. However, the induction of NEMO linear ubiquitination was blocked by OTULIN overexpression (**Figure 3-3A**). We further tested this result in MDA-MB-231 cells and found that OTULIN deficiency substantially promoted NEMO linear ubiquitination basal and induced levels (**Figure 3-3B**), suggesting that OTULIN can inhibit genotoxic NF- κ B through cleaving the linear ubiquitin chains of NEMO. Taken together, these data indicate that genotoxic NF- κ B signaling is counter-balanced by LUBAC and OTULIN, either molecule plays an indispensable role in regulating linear ubiquitination. This finding inspired us to investigate if there is any interplay between LUBAC-mediated linear ubiquitination and OTULIN-mediated deubiquitination events under various states, like normally unstressed, inflammatory, or genotoxic conditions.

The N-terminal Domain of OTULIN Interacts with the PUB Domain of HOIP Facilitated by Linear Ubiquitination

The PIM domain of OTULIN has been shown to interact with the PUB domain of HOIP. The presence of OTULIN on LUBAC is required for the recruitment of OTULIN to the TNFR1 complex and the counteraction of HOIP-dependent NF- κ B activation [22, 34]. It is unclear if the OTULIN-LUBAC interaction is still required for the regulation of genotoxic NF- κ B activation. To investigate the importance of OTULIN-LUBAC (through HOIP) interactions under genotoxic stress, we firstly determined the specific domains for OTULIN and HOIP interaction under normal unstressed state by using

Figure 3-2. OTULIN inhibits genotoxic NF- κ B activation.

(A, B) Immunoblotting analysis of parental and OTULIN-KO clones in HEK293T and MDA-MB-231 cells using the antibodies as indicated. (C) Parental and OTULIN-KO MDA-MB-231 cells were treated with TNF α (10 ng/ml, 15 min), Dox (2 μ g/ml, 2h), or CBP (10 μ g/ml, 2h). NF- κ B activation was analyzed by EMSA using Ig κ probe, and protein expression was determined by immunoblotting with indicated antibodies. (D) Parental and OTULIN-KO HEK293T cells were treated with TNF α (10 ng/ml, 15 min), Etop (10 μ M/ml, 2h), or CPT (10 μ M/ml, 2h). Cells were analyzed as in (C). (E) Parental and OTULIN-KO MDA-MB-231 cells were exposed to IR (10 Gy, 2h) or left untreated (-). Cells were analyzed as in (C). (F) Parental and OTULIN-KO MDA-MB-231 cells were treated with Dox (2 μ g/ml) for indicated time points and analyzed by immunoblotting. (G) OTULIN-KO HEK293T cells were reconstituted with OTULIN WT or C129S mutant. Cells were treated with TNF α (10 ng/ml, 15 min) or Etop (10 μ M, 2h). Protein expression was determined by immunoblotting with antibodies as indicated. (H) Parental, OTULIN-KO, and OTULIN-reconstituted HEK293T cells were co-transfected with κ B-Fluc/hRluc-TK reporter constructs. After 24 h, cells were treated with Etop (10 μ M, 6 h), and cell extracts were prepared to determine luciferase activity. Two-way ANOVA followed by Tukey's post-hoc test was used to determine statistical significance for multiple comparisons. *** $p < 0.001$; **** $p < 0.0001$; ns, not significant. (I) qPCR analysis of OTULIN mRNA level in HEK293T cells treated with TNF α (10 ng/ml) for 15 min or 6 h or left untreated as control group. (J) qPCR analysis of OTULIN mRNA level in HEK293T cells treated with Etop (10 μ M/ml) for 2 h or 24 h or left untreated as control group. $n = 3$ independent experiments. One-way ANOVA followed by Tukey's post-hoc test shows no statistical significance in I and J. Data were presented as Mean \pm SEM.



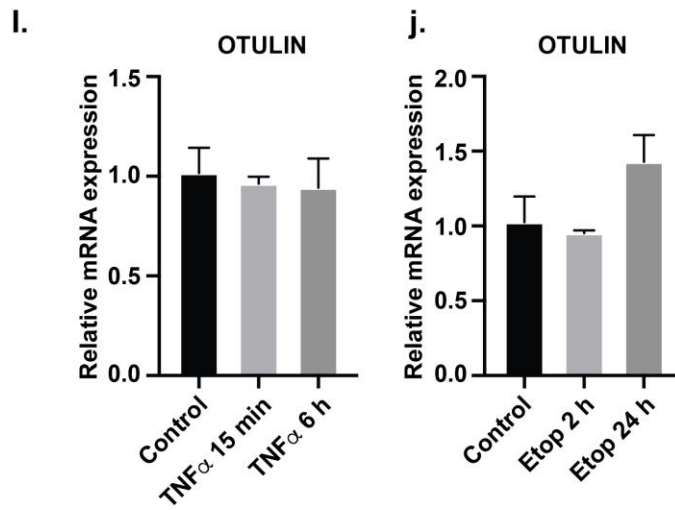
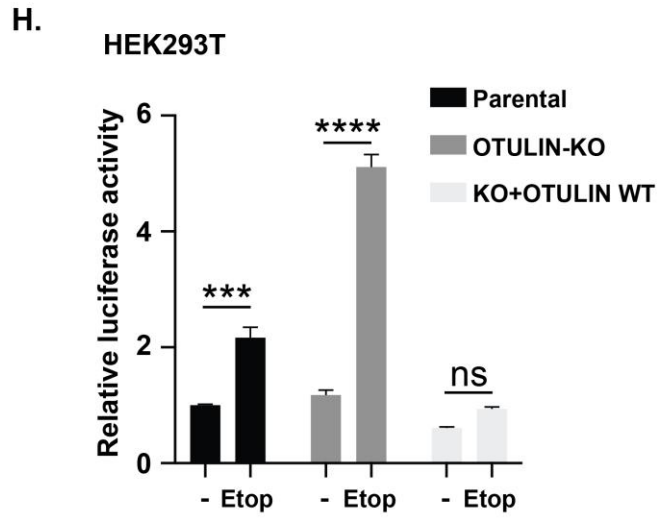
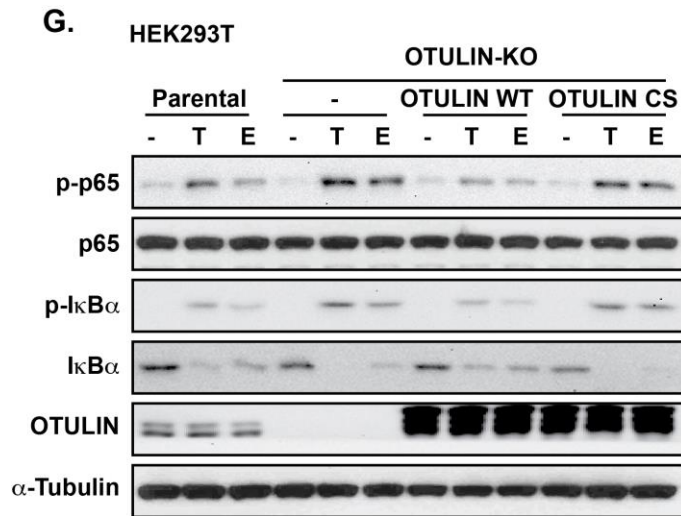


Figure 3-2. Continued.

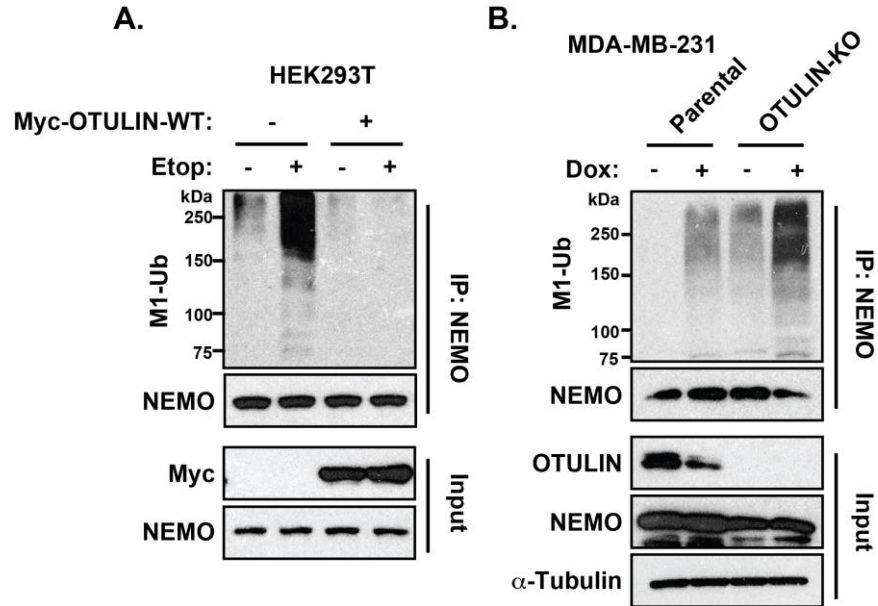


Figure 3-3. OTULIN downregulates the linear ubiquitination of NEMO. (A) Linear ubiquitination of immunoprecipitated NEMO in HEK293T cells. Following transfection with or without wild-type Myc-OTULIN, cells were treated with Etop (10 μ M, 2 h). (B) Linear ubiquitination of immunoprecipitated NEMO in parental or OTULIN-KO MDA-MB-231 cells treated with Dox (2 μ g/ml, 2 h).

domain truncation strategy. The PUB domain of the LUBAC component HOIP is highly conserved, which is also shared by PNGase [131]. PNGase-PUB electrostatically binds to ubiquitin chains and Ub-like (UBL) domain of HR23 [132]. In addition, the UBA domain of HOIP was reported to specifically interact with the UBL domain of HOIL-1L, which is pivotal for the LUBAC complex formation [6]. The NZF ubiquitin-binding domain in HOIP directs LUBAC to ubiquitinated proteins [34]. Therefore, it is plausible to postulate that HOIP might interact with ubiquitin chains of OTULIN via some of these ubiquitin-binding domains (**Figure 3-4A**), which reinforces the affinity between OTULIN and HOIP. We further asked whether OTULIN is ubiquitinated by linear ubiquitin chains, because LUBAC as an E3 ligase specific for linear ubiquitin conjugation is very likely to ubiquitinate OTULIN when they interact together. To test these hypotheses, we both investigated the specific domain for the interaction of LUBAC and OTULIN and verified the linear ubiquitination of OTULIN.

We firstly co-transfected HA-OTULIN with truncated Myc-HOIP moieties into HEK293T cells. Co-IP assay showed that the PUB-deleted HOIP completely lost the interaction with OTULIN, but not other truncated variants, indicating that the PUB domain is exclusively involved in OTULIN interaction (**Figure 3-4B**). By in vitro pulldown assay using recombinant proteins expressed with His or GST tags, we demonstrated that the N-terminus of OTULIN (1-80aa), when fused with a head-to-tail-linked tetra-ubiquitin construct (Ub4), augmented its binding further to the His-PUB, indicating that the linear ubiquitin chains of OTULIN, which was verified to be existed later, are the assistant binding partner to the HOIP-PUB (**Figure 3-4C**). This prompted us to find the specific residues of HOIP-PUB domain for linear ubiquitin chains binding. Glu73, Glu82, and Glu84 of PNGase-PUB were identified as the critical residues contributing to the electrostatic interaction with HR23-UBL and ubiquitin chains [132]. We identified two matching residues Asp117 (D) and Glu127 (E) of HOIP-PUB by sequence alignment with PNGase (**Figure 3-4D**), to be required for the interaction between HOIP-PUB and Ub4/His-N-OTULIN-Ub4 (**Figure 3-4E, F**). The interaction-deficient impact of double mutation variant (D117A and E127A) was further verified in HEK293T cells overexpressing HA-OTULIN and Myc-HOIP WT or Myc-HOIP D117A/E127A by co-IP assay (**Figure 3-4G**). Taken together, these results showed linear ubiquitin chains of OTULIN enhance its binding to HOIP through interacting with the PUB domain at Asp117 and Glu127.

OTULIN Is Linearly Ubiquitinated by LUBAC Under Unstressed Condition

LUBAC is thus far the only known E3 ligase that specifically generates linear ubiquitin chains on substrates. To confirm whether OTULIN can be ubiquitinated and to find the required residues for linear ubiquitination, we performed MS-based proteomics experiment on the enriched OTULIN protein (**Figure 2-1**). The MS data were searched against the protein database using SEQUEST. We identified a total of eight ubiquitinated OTULIN residues (K64, K66, K107, K116, K180, K198, K251, and K325). An MS/MS spectrum presents high confidence in the identification and localization of the ubiquitin modification on K64 and to a lesser extent on K66 (**Figure 3-5A**). Of note, the MS assay

Figure 3-4. Linear ubiquitin chains facilitate the binding of OTULIN and HOIP. (A) Diagram of full-length HOIP and the indicated domain-deleted mutants: HOIP-PUB deletion (52-162aa), HOIP-NZF1 deletion (350-379aa), HOIP-NZF2 deletion (399-438aa), HOIP-UBA deletion (564-615aa), or HOIP-RBR deletion (699-1072aa). (B) Co-IP analysis of the interaction between HA-OTULIN and Myc-HOIP WT, PUB-, NZF1-, NZF2-, UBA-, or RBR-deleted truncated mutant in HEK293T cells. (C) In vitro pulldown assay of His-PUB (1-185aa) by GST-N-OTULIN (1-80aa) or GST-N-OTULIN fused with linear tetra ubiquitin chains. (D) Structure-based sequence alignment of the PUB domain in HOIP and PNGase. Red labeled letters in HOIP sequence represent the corresponding conserved residues to Glu73 and Glu82 of PNGase. (E, F) In vitro pulldown assay of GST-PUB (1-185aa) WT, D117A, E127A, or D117A/E127A by His-Ub4 or His-N-OTULIN-Ub4, respectively. (G) Co-IP analysis of the interaction between HA-OTULIN and Myc-HOIP WT or Myc-HOIP D117A/E127A in HEK293T cells.

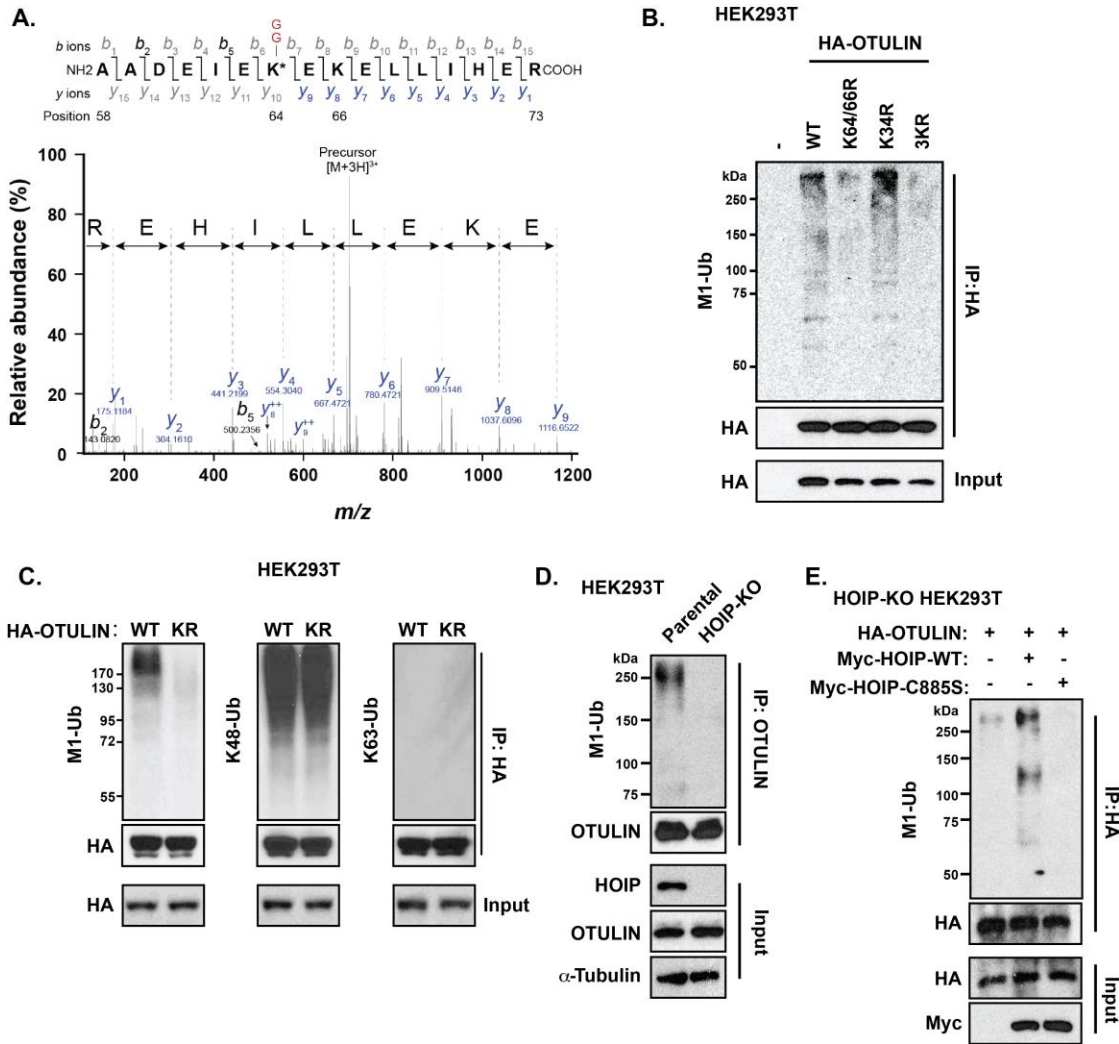


Figure 3-5. Identification of OTULIN linear ubiquitination dependent on HOIP. (A) MS/MS spectrum showing the identification of an OTULIN peptide carrying ubiquitination (GG) on lysine (K) 64. MS/MS fragmentation of the peptide (AADEIEK (-GG) EKELLIHER) is shown in the upper panel. In the bottom panel, a series of b (black) and y (blue) product ions are detected in the 3-charge MS/MS spectrum, providing high confidence in the identification and localization of the ubiquitin modification. The X-axis represents the mass to charge (m/z) ratio, and the Y-axis shows the relative intensity of different peaks. The monoisotopic precursor mass value (M+3H⁺) of the ubiquitinated peptide is shown. (B) Linear ubiquitination of immunoprecipitated HA-OTULIN WT, K64/66R, K34R, and K34/64/66R mutants in HEK293T cells. (C) Different ubiquitination levels (M1-Ub, K48-Ub, and K63-Ub) of immunoprecipitated HA-OTULIN WT or K64/66R mutants were determined in HEK293T cells. (D) Linear ubiquitination of immunoprecipitated endogenous OTULIN in parental and HOIP-KO cells. (E) Linear ubiquitination of immunoprecipitated HA-OTULIN in HOIP-KO HEK293 cells co-transfected with HA-OTULIN and Myc-HOIP WT or C885S mutant.

only revealed OTULIN's ubiquitination site, but not the ubiquitin linkage. We focused the linear investigation on the N-terminus of OTULIN (1-80aa), because this domain is well-established to be required and sufficient for the interaction with LUBAC. Linear ubiquitination was only detected in immunoprecipitated HA-OTULIN WT and K34R, but not in K64/66R mutant (**Figure 3-5B**). We further found OTULIN K48-linked ubiquitination was not affected by K64/66R mutation and K63-Ub was undetectable under normal states (**Figure 3-5C**), suggesting Lys64/66 is specific for OTULIN linear ubiquitination.

Since OTULIN binds to LUBAC in unstimulated cells, it is rational to ask whether the linear ubiquitination of OTULIN is LUBAC-dependent. RBR is known as an important group of E3 ligases required for ubiquitination [133]. For LUBAC, only the RBR domain of HOIP, but not HOIL-1L, is necessary for LUBAC to assemble linear ubiquitin chains although both HOIP and HOIL-1L belong to the RBR class of E3 ligases [6, 16]. Consequently, loss of HOIP can completely abolish LUBAC ligase activity. Therefore, we compared the linear ubiquitin level of OTULIN between parental and HOIP-KO HEK293T cells. Indeed, OTULIN could be linearly ubiquitinated in the parental cells, while the linear ubiquitin signal was abolished in HOIP-KO cells (**Figure 3-5D**). To mitigate the off-target effects, we reconstituted HOIP WT and its enzymatically inactive C885S mutant in HOIP-KO HEK293T cells. As expected, OTULIN linear ubiquitination was only rescued by HOIP WT (**Figure 3-5E**), suggesting that OTULIN is linearly ubiquitinated in a HOIP-dependent manner.

OTULIN Linear Ubiquitination Is Required for NF- κ B Inhibition

Next, we investigated the interaction between LUBAC and different OTULIN mutants and if these mutants lose their function in preventing genotoxic or inflammatory NF- κ B activation. OTULIN C129S and Y56F mutants represent two known loss-of-function mutations: the former represents a catalytically inactive variant while Tyr56 phosphorylation of OTULIN is known to cause the disruption of OTULIN-LUBAC interaction, which can be manifested by the Y56F mutation [22, 26, 34]. Three independent co-IP assays showed a complete disruption of HOIP binding to OTULIN Y56F mutant, while OTULIN K64/66R mutant lost its interaction with LUBAC by 81% compared to the interaction with OTULIN WT (**Figure 3-6A**), indicating that physical interaction between OTULIN and LUBAC requires and is stabilized by OTULIN linear ubiquitination. Interestingly, C129S mutation of OTULIN does not affect its interaction with LUBAC, although an upregulation of OTULIN linear ubiquitination was observed (**Figure 3-6B**), mightily resulting from a saturated pool of OTULIN-LUBAC complex. OTULIN Y56F mutant had no linear ubiquitination due to the absence of LUBAC interaction.

Consistent with the previous finding that both OTULIN catalytic activity and its presence on LUBAC are required for limiting inflammatory NF- κ B signaling, all three mutants lost their inhibitory roles in genotoxic and inflammatory NF- κ B signaling, indicated by linearly ubiquitinated NEMO levels, NF- κ B luciferase activity, and Igk-

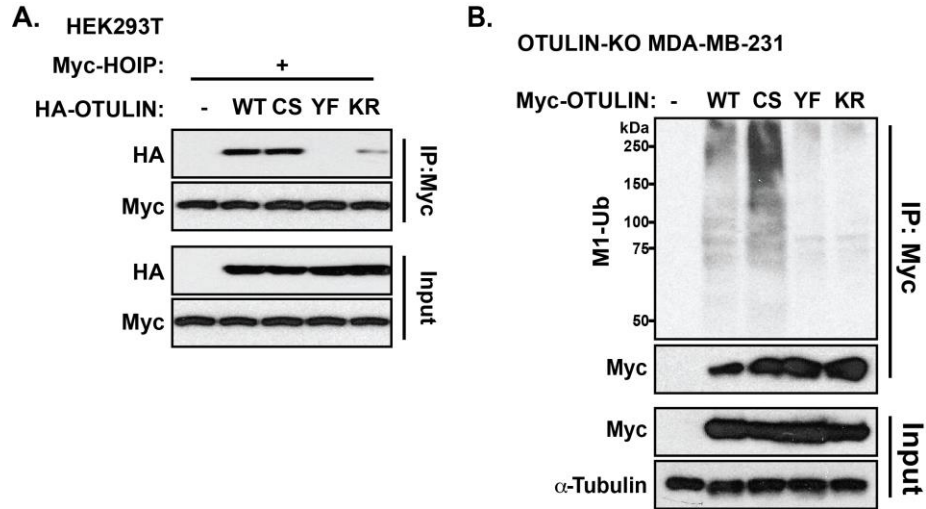


Figure 3-6. Different interactions between OTULIN mutants and HOIP. (A) Co-IP analysis of the interaction between Myc-HOIP and HA-OTULIN WT, C129S, Y56F, or K64/66R mutants in HEK293T cells. (B) Linear ubiquitination of immunoprecipitated Myc-OTULIN in OTULIN-KO MDA-MB-231 cells overexpressing OTULIN WT, C129S, Y56F, K64/66R, or not.

probed EMSA (**Figure 3-7A** through **E**). To confirm the deficit of OTULIN K64/66R mutation in restricting NF- κ B signaling, we further compared the kinetics of NF- κ B activation in response to TNF α and Etop stimuli between OTULIN WT- and K64/66R-reconstituted cells. Although OTULIN K64/66R cells had higher NF- κ B activation, OTULIN WT and K64/66R cells still peaked at the same time points (i.e., 10 min for TNF α , 2 h for Etop.) (**Figure 3-7F, G**). In addition, OTULIN-KO HEK293T cells reconstituted with OTULIN K64/66R mutant failed to inhibit NF- κ B activation compared to OTULIN WT (**Figure 3-7H**). Most of all, direct determination of cell death also demonstrated that reconstitution of Y56F or K64/66R mutant made cells tolerate to the Dox treatment via dysregulated NF- κ B signaling because the resistance was alleviated by overexpressing an I κ B α super-repressor (I κ B α -SR, undegradable) [134] or co-treated with an IKK2 inhibitor TPCA-1 (**Figure 3-8**). Collectively, these data shows that OTULIN linear ubiquitination at Lys64/66 is critical for OTULIN's counteracting role in NF- κ B activation upon TNF α treatment and genotoxic stress, which depends on the physical interaction between OTULIN and LUBAC.

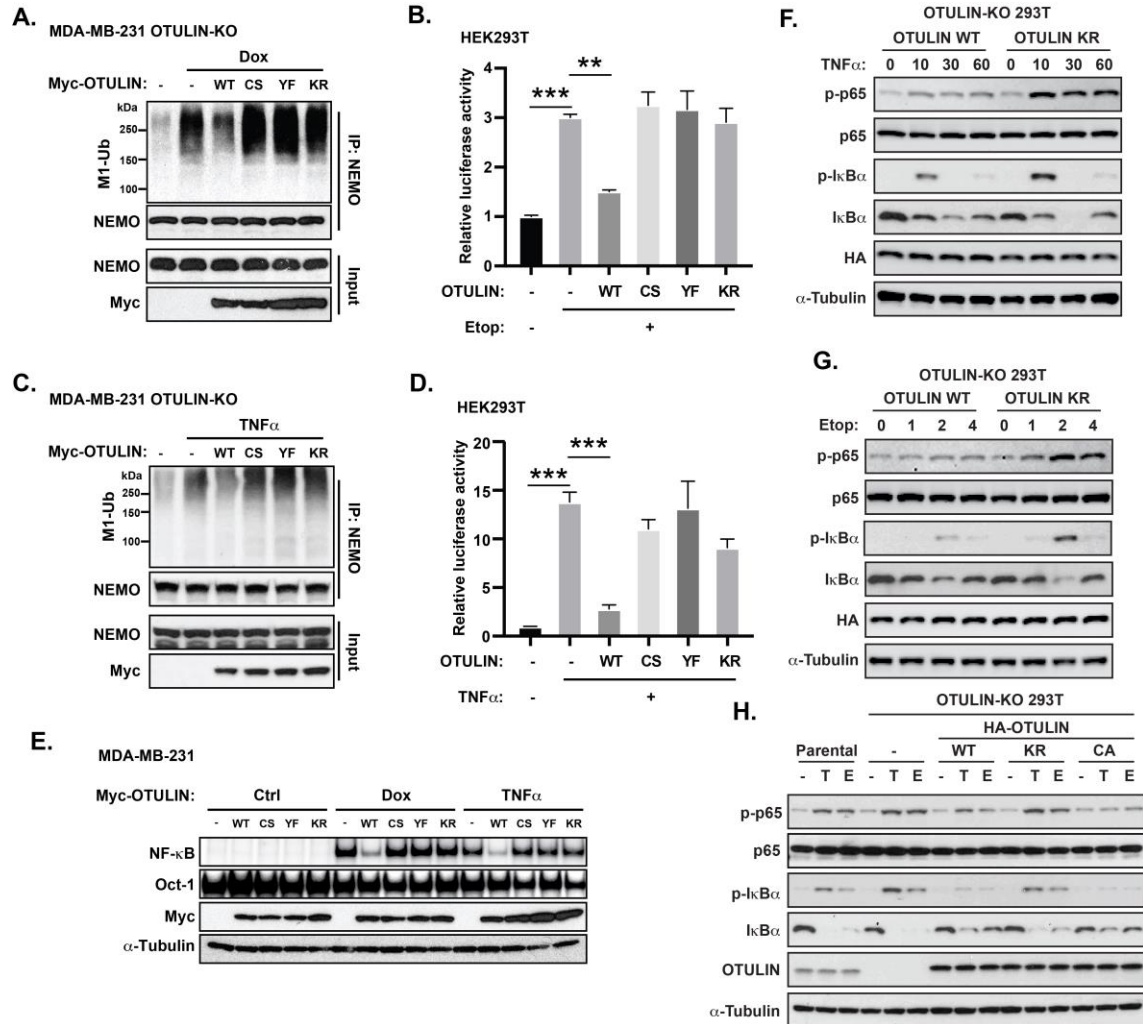
Genotoxic Stress Induces OTULIN Dimerization and Self-deubiquitination Required for NF- κ B Activation

These results led us to speculate that physical interaction between OTULIN and LUBAC might be disrupted by genotoxic stress, which underlies the overactivated NF- κ B signaling during chemotherapy. Indeed, various chemotherapeutic agents (Dox, CBP, and IR) caused a substantial loss of the physical interaction between OTULIN and HOIP (**Figure 3-9A**), which correlated with a complete loss of linear ubiquitinated OTULIN (**Figure 3-9B**). Thus far, OTULIN and cylindromatosis (CYLD) are the only two known DUBs that cleave linear ubiquitin chains *in vivo* [135]. LUBAC-SPATA2-CYLD is one of the three known different interaction profiles for the HOIP, the other two are LUBAC-OTULIN and LUBAC-p97/VCP (40-fold less affinity compared to OTULIN), suggesting that there may be at least three different cellular pools of LUBAC, dependent on cellular context or compartment [130]. Indeed, Dox did not change the pool levels of LUBAC-CYLD complex (**Figure 3-9C**). To test which DUB is responsible for OTULIN deubiquitination, the dependency of CYLD and OTULIN were tested respectively. We compared the level of linear ubiquitinated OTULIN in CYLD-null (CYLD^{-/-}) and CYLD^{+/+} cells and found no difference in OTULIN deubiquitination (**Figure 3-9D**). Interestingly, the OTULIN C129S mutant displayed higher levels of linear ubiquitin modification compared to WT group with or without Etop treatment (**Figure 3-9E**). Therefore, we reasoned that the genotoxic stress-induced deubiquitination of OTULIN may be conducted by OTULIN itself.

To further prove the module that OTULIN undergoes self-deubiquitination upon genotoxic stress, whether OTULIN can form dimer or oligomer was tested. By Co-IP analysis, it showed OTULIN expressed in two different tags as Myc and HA interacted in HEK293T cells (**Figure 3-10A**), which was not affected by any of the mutants such as OTULIN C129S, Y56F, or K64/66R (**Figure 3-10B**). Notably, it was the N-terminal

Figure 3-7. Effects of OTULIN loss-of-function mutants on NF- κ B activation.

(A) Linear ubiquitination of immunoprecipitated NEMO in OTULIN-KO MDA-MB-231 cells reconstituting with Myc-OTULIN WT, C129S, Y56F, or K64/66R mutants, under the treatment of Dox (2 μ g/ml, 2 h). (B) Dual-luciferase reporter assay of the NF- κ B activity in HEK293T cells overexpressing HA-OTULIN WT, C129S, Y56F, or K64/66R mutants, under the treatment of Etop (10 μ M, 6 h). (C) Linear ubiquitination of immunoprecipitated NEMO in OTULIN-KO MDA-MB-231 cells reconstituting with Myc-OTULIN WT, C129S, Y56F, or K64/66R mutants, under the treatment of TNF α (10 ng/ml, 15 min). (D) Dual-luciferase reporter assay of the NF- κ B activity in HEK293T cells overexpressing HA-OTULIN WT, C129S, Y56F, or K64/66R mutants, under the treatment of TNF α (10 ng/ml, 4 h). (E) Gel shift analysis of NF- κ B activation using Ig κ probe and western blot analysis of Myc tag in MDA-MB-231 cells transfected with Myc-OTULIN WT, C129S, Y56F, or K64/66R mutants, and then treated with Dox (2 μ g/ml, 2 h) or TNF α (10 ng/ml, 15 min). (F, G) OTULIN-KO HEK293T cells were reconstituted with OTULIN WT or K64/66R mutant, and then treated with TNF α (10 ng/ml) or Etop (10 μ M) for indicated time points. NF- κ B activation was analyzed by immunoblotting with indicated antibodies. (H) OTULIN-KO cells were reconstituted with OTULIN WT, K64/66R, C17/47A mutants, or not. Parental and transfected OTULIN-KO HEK293T cells were treated with (-), TNF α (10 ng/ml, 15 min), or Etop (10 μ M, 2h), followed by immunoblotting with antibodies as indicated. One-way ANOVA followed by Tukey's post-hoc test was used to determine statistical significance for multiple comparisons. **p < 0.01; ***p < 0.001; ns, not significant.



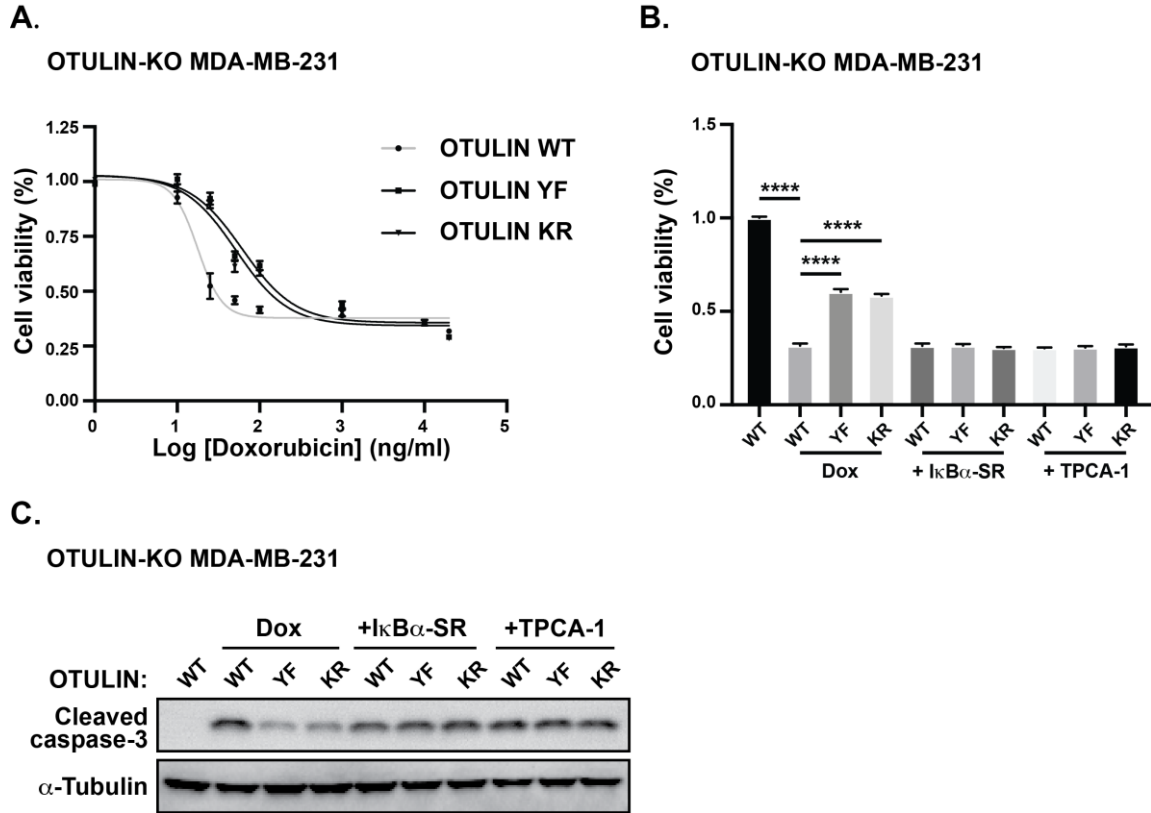


Figure 3-8. Effects of OTULIN loss-of-function mutants on cancer cell survival via dysregulating genotoxic NF- κ B signaling.

(A) Data of triplicate on the cell viability was analyzed by the CCK-8 assay in OTULIN-KO MDA-MB-231 cells treated with Dox for 48 h. Dox IC₅₀ was 17.76 ng/ml, 61.72 ng/ml, and 51.67 ng/ml in HA-OTULIN WT-, Y56F-, or K64/66R-reconstituted cells, respectively. (B) Cell viability was analyzed by CCK-8 assay in OTULIN-KO MDA-MB-231 cells reconstituted with HA-OTULIN WT, Y56F, or K64/66R. Cells were co-transfected with IκBα-SR or pretreated with TPCA-1 (1 μM), and then treated with Dox (100 ng/ml, 48 h). *n* = 5. One-way ANOVA followed by Tukey's post-hoc test was used to determine statistical significance for multiple comparisons. *****p* < 0.0001. (C) Immunoblotting analysis of cleaved caspase-3 in OTULIN-KO MDA-MB-231 cells treated as in (B).

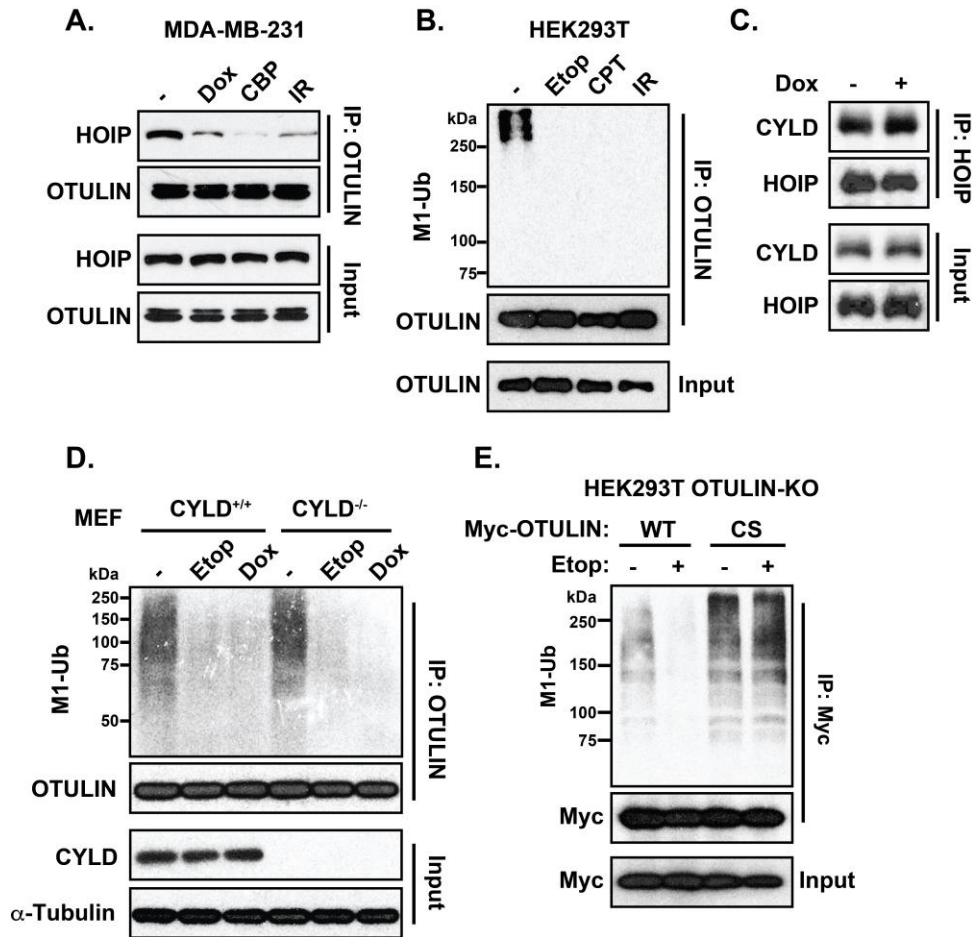
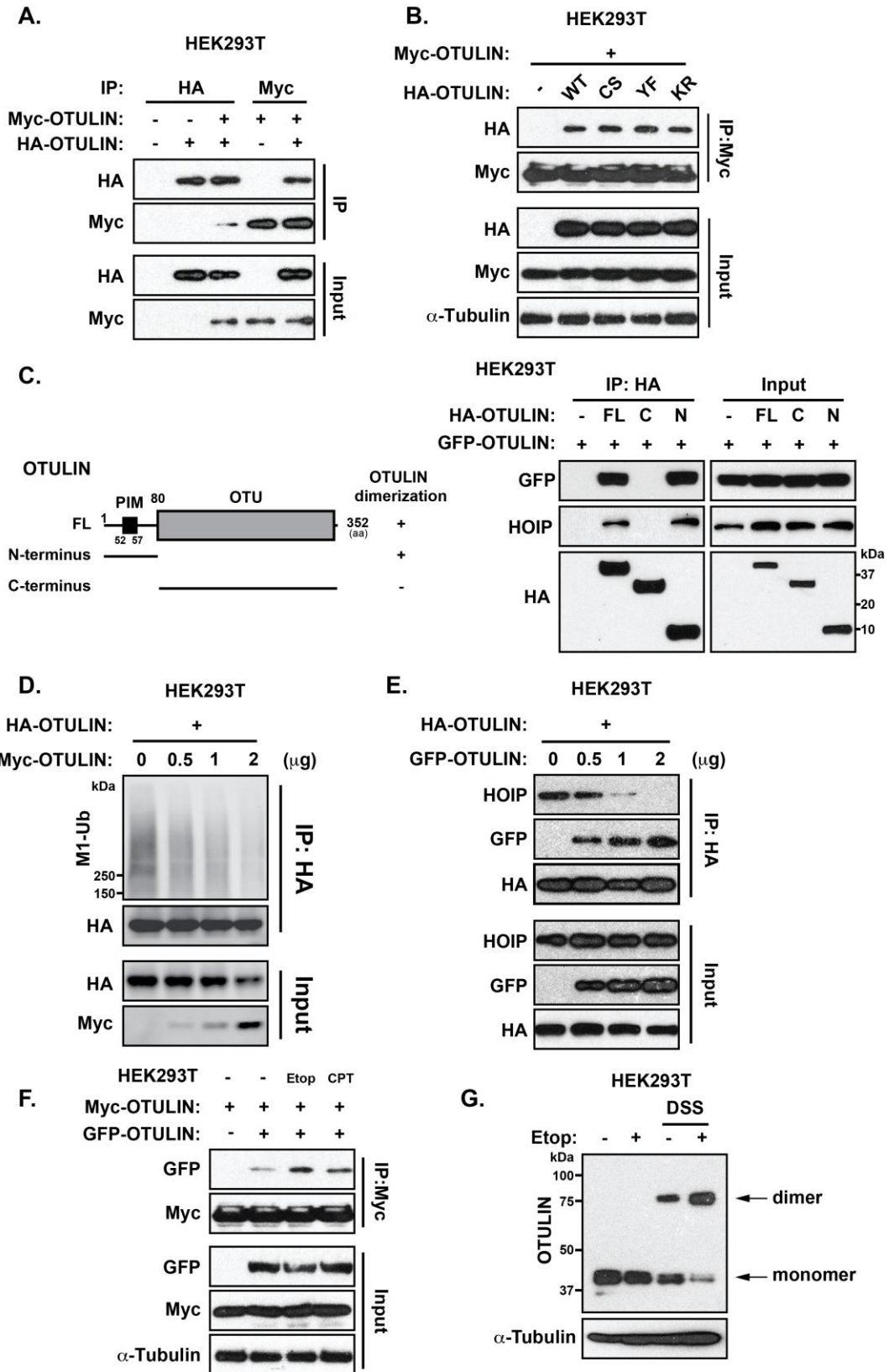


Figure 3-9. Genotoxic stress induces dissociation of OTULIN-HOIP complex. (A) Co-IP analysis of the interaction between endogenous OTULIN and HOIP in MDA-MB-231 cells treated with Dox (2 μ g/ml, 2 h), or CBP (10 μ g/ml, 2 h), or exposed to IR (10 Gy) and waiting in incubator for 2 h. (B) Linear ubiquitination of immunoprecipitated endogenous OTULIN in HEK293T cells treated with Etop (10 μ M), CPT (10 μ M), or exposed to IR (10 Gy) for 2 h. (C) Co-IP analysis of the interaction between CYLD and HOIP in MDA-MB-231 cells treated with or without Dox (2 μ g/ml, 2 h). (D) Linear ubiquitination of immunoprecipitated endogenous OTULIN in CYLD^{+/+} and CYLD^{-/-} MEFs treated with Etop (10 μ M), Dox (2 μ g/ml) for 2 h, or left untreated (-). (E) Linear ubiquitination of immunoprecipitated Myc-OTULIN in OTULIN-KO HEK293T cells reconstituted with Myc-OTULIN WT or C129S mutant, and subsequently treated with Etop (10 μ M, 2h), or left untreated (-).

Figure 3-10. Intermolecular interaction of OTULIN leads to self-deubiquitination. (A) Co-IP analysis of the interaction between Myc-OTULIN and HA-OTULIN in HEK293T cells co-transfected with Myc-OTULIN and HA-OTULIN. (B) Co-IP analysis of the interaction between Myc-OTULIN and HA-OTULIN in HEK293T cells co-transfected with Myc-OTULIN and HA-OTULIN WT, C129S, Y56F, or K64/66R mutants. (C) Mapping of OTULIN domain required for the OTULIN dimerization. Interactions among the N- or C-terminal domains of OTULIN were analyzed by co-IP assay in HEK293T cells. (D) Linear ubiquitination of immunoprecipitated HA-OTULIN in HEK293T cells co-transfected with HA-OTULIN and with increasing amount of Myc-OTULIN. (E) Co-IP analysis of the OTULIN interaction and the HOIP-OTULIN interaction in HEK293T cells co-transfected with HA-OTULIN and with increasing amount of Myc-OTULIN. (F) Co-IP analysis of the interaction between Myc-OTULIN and GFP-OTULIN in HEK293T cells treated with Etop (10 μ M, 2h), CPT (10 μ M, 2h), or left with untreated (-). (G) DSS crosslinking assay reveals the formation of OTULIN dimers by immunoblotting analysis. HEK293T cells were treated with or without Etop (10 μ M, 2h) followed by the crosslinking assay described in methods.

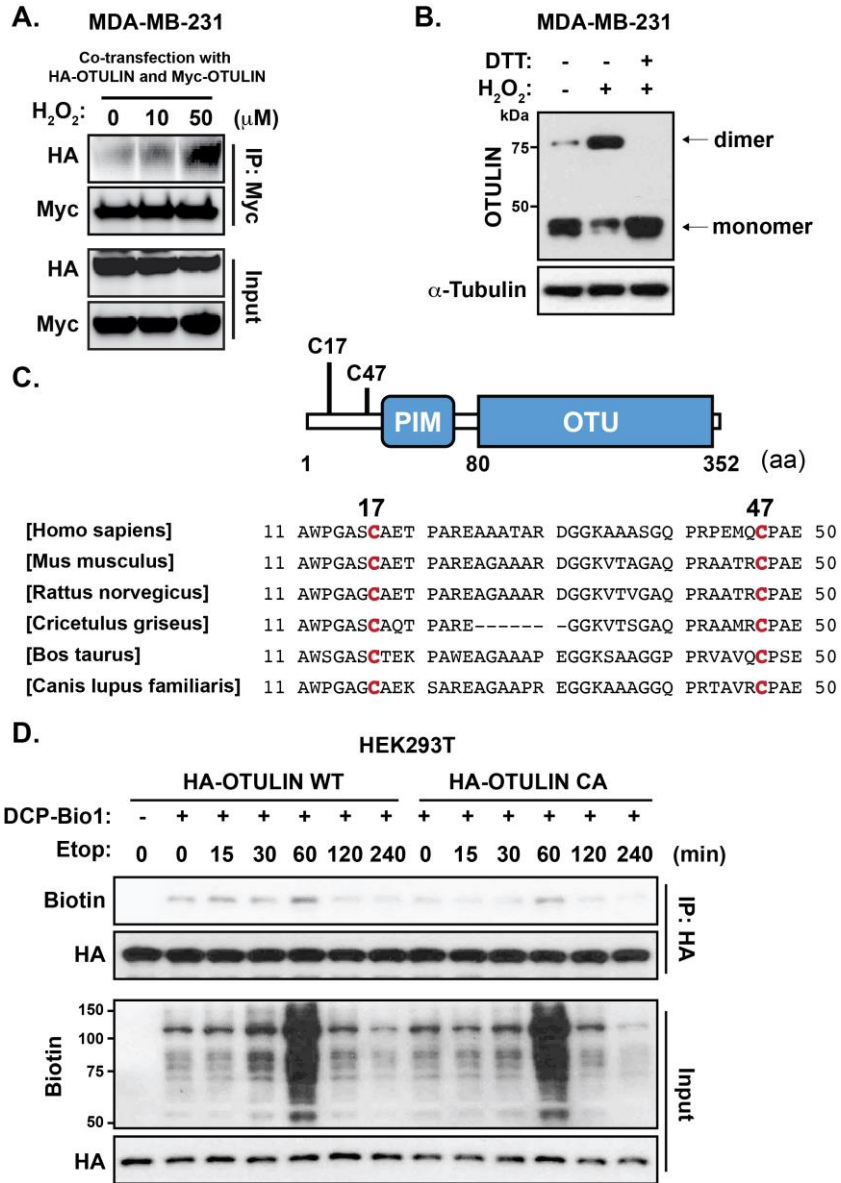


domain of OTULIN (i.e., 1-80aa), which contains the PIM motif, but not the C-terminal part, of OTULIN that interacted with GFP-OTULIN (**Figure 3-10C**). Artificially increasing Myc-tagged OTULIN (0.5-2 μ g) greatly decreased linear ubiquitinated HA-OTULIN in a dose-dependent manner (**Figure 3-10D**), which correlated with increased OTULIN self-interaction and decreased the interaction with HOIP per OTULIN (**Figure 3-10E**). When we gradually increased OTULIN levels, there were two potential events that may reason the result. Firstly, HA-OTULIN got deubiquitinated by overexpressed Myc-OTULIN, and then HA-OTULIN with lesser linear ubiquitin chains lost the interaction with HOIP. Secondly, overexpression of Myc-OTULIN competed with HA-OTULIN on HOIP interaction, and then HA-OTULIN got less linear ubiquitination. However, which event is predominant remains elusive. To test whether OTULIN self-interaction is affected by genotoxic stress, we determined the levels of OTULIN self-interaction under genotoxic conditions by Co-IP and DSS crosslinking assay; the latter is specifically used to identify protein interaction. DSS is a non-cleavable crosslinker that has an amine-reactive N-hydroxysuccinimide (NHS) ester at each end. NHS esters can stabilize the protein interaction by reacting with primary amines to form stable amide bonds. Co-IP showed that OTULIN self-interaction was enhanced by Etop and CPT in HEK293T cells (**Figure 3-10F**). Consistently, the amount of OTULIN dimer was increased by Etop treatment with DSS incubation. In addition, there was no oligomerization of OTULIN assembly detected (**Figure 3-10G**).

Nest, we investigate why genotoxic stress could cause OTULIN self-interaction. Oxidative stress is induced during chemotherapy [136], which often involves PTMs on critical cysteine residues to cause the conformational and functional change of a protein by forming disulfide bonds [137]. To test if OTULIN forms dimer through disulfide bonds, we treated MDA-MB-231 cells with hydrogen peroxide (H_2O_2), and prepared protein loading sample without dithiothreitol (DTT). We found H_2O_2 facilitated intermolecular OTULIN interaction in a dose-dependent manner (**Figure 3-11A**). Upon lysis with 10 mM DTT, all OTULIN protein was reduced to the monomeric form (**Figure 3-11B**), indicating that OTULIN dimerize through covalent disulfide bonds because of the DTT-sensitive nature. Disulfide bonds form via cysteine oxidation, hence we tried to find the available cysteine residues in the N-terminal of OTULIN. Cys17 and Cys47 of OTULIN are conserved among different species (**Figure 3-11C**). DCP-Bio1 can be used to label oxidative cysteine by effectively detecting cysteine sulfenic acid [138]. OTULIN C17/47A mutant showed less biotin labelling compared to WT OTULIN, suggesting Cys17/47 is available for protein oxidation (**Figure 3-11D**). To further demonstrate the propensity of Cys17/47 for oxidation, we designed a cysteine alkylation (by N-ethylmaleimide, NEM)-reduction (by DTT)-alkylation (by iodoacetamide, IAM) assay to determine the oxidation of OTULIN cysteines by LC-MS/MS. Reduced cysteines were first labeled by NEM, and then reversible oxidized cysteines (e.g., disulfide, S-glutathionylation) were reduced by DTT for IAM alkylation (**Figure 3-11E**). IAM-labeled C17 and C47 were called carbamidomethylation (CAM), the ratios of which were increased upon Etop treatment in HEK293T cells (**Figure 3-11F**), indicating that C17/47 of OTULIN can be oxidized and increasingly oxidized during Etop treatment. We thus investigated the impacts of mutated cysteine residues on OTULIN dimerization. Either of

Figure 3-11. OTULIN dimerization is a pre-requisite for OTULIN self-deubiquitination and the subsequent dissociation from LUBAC under genotoxic condition.

(A) Co-IP analysis of the interaction between Myc-OTULIN and HA-OTULIN in MDA-MB-231 cells treated with H₂O₂ (0, 10, or 50 μM) for 15 min. (B) Immunoblotting analysis of OTULIN dimerization in MDA-MB-231 cells. Cells were treated with H₂O₂ (50 μM, 15 min) or PBS, and subject to cell lysis with or without DTT (10 mM). (C) Amino acid sequence alignments of OTULIN N-terminus shows conservation of Cys17 and Cys47 in various species. (D) IP analysis of the biotin labeled HA-OTULIN (WT or C17/47A) in HEK293T cells treated with Etop (2 μM) for indicated time points and lysed with DCP-Bio1 as described in methods. (E) Workflow of the identification of alkylated peptides of enriched OTULIN. During cell lysis, NEM was firstly used to label reduced cysteine, then DTT was used to reduce the reversible cysteine, and then IAM was used to label the just reduced cysteines (i.e., the levels of IAM-labeled cysteines indicate the cysteine oxidation). Enriched OTULIN was used for the analysis of alkylated peptides by LC/MS/MS. (F) LC/MS/MS analysis of cysteine alkylation by NEM and IAM. HEK293T was treated with Etop (2 μM) for 2 h. The percentage of IAM-labeled cysteine was calculated by the abundances of cysteine with carbamidomethyl divided by the total abundances of corresponding cysteine (× 100%). Total cysteine = S-NEM + S-IAM. No S-O₂H (sulfinylation) or S-O₃H (sulfonylation) was identified. (G) Immunoblotting analysis of OTULIN dimerization in OTULIN-KO MDA-MB-231 cells reconstituted with OTULIN WT, C17A, C47A, or C17/47A. Cells were then treated with or without Dox (2 μg/ml, 2 h) and subject to cell lysis without DTT or β-mercaptoethanol (2-ME). (H) Linear ubiquitination of immunoprecipitated HA-tagged OTULIN in MDA-MB-231 cells transfected with HA-OTULIN WT, C17A, C47A, or C17/47A, and then treated with Dox (2 μg/ml, 2 h). (I) Co-IP analysis of the interaction between HOIP and HA-OTULIN in MDA-MB-231 cells processed as in (F). (J) Immunoblotting analysis of Tyr56-phosphorylation of OTULIN in OTULIN-KO MDA-MB-231 cells reconstituted with OTULIN WT or C17/47A, and then treated with or without Dox (2 μg/ml, 2 h). (K) Immunoblotting analysis of Tyr56-phosphorylation of OTULIN in N2a cells treated with H₂O₂ (100 μM, 24 h) with or without imatinib (500 nM).



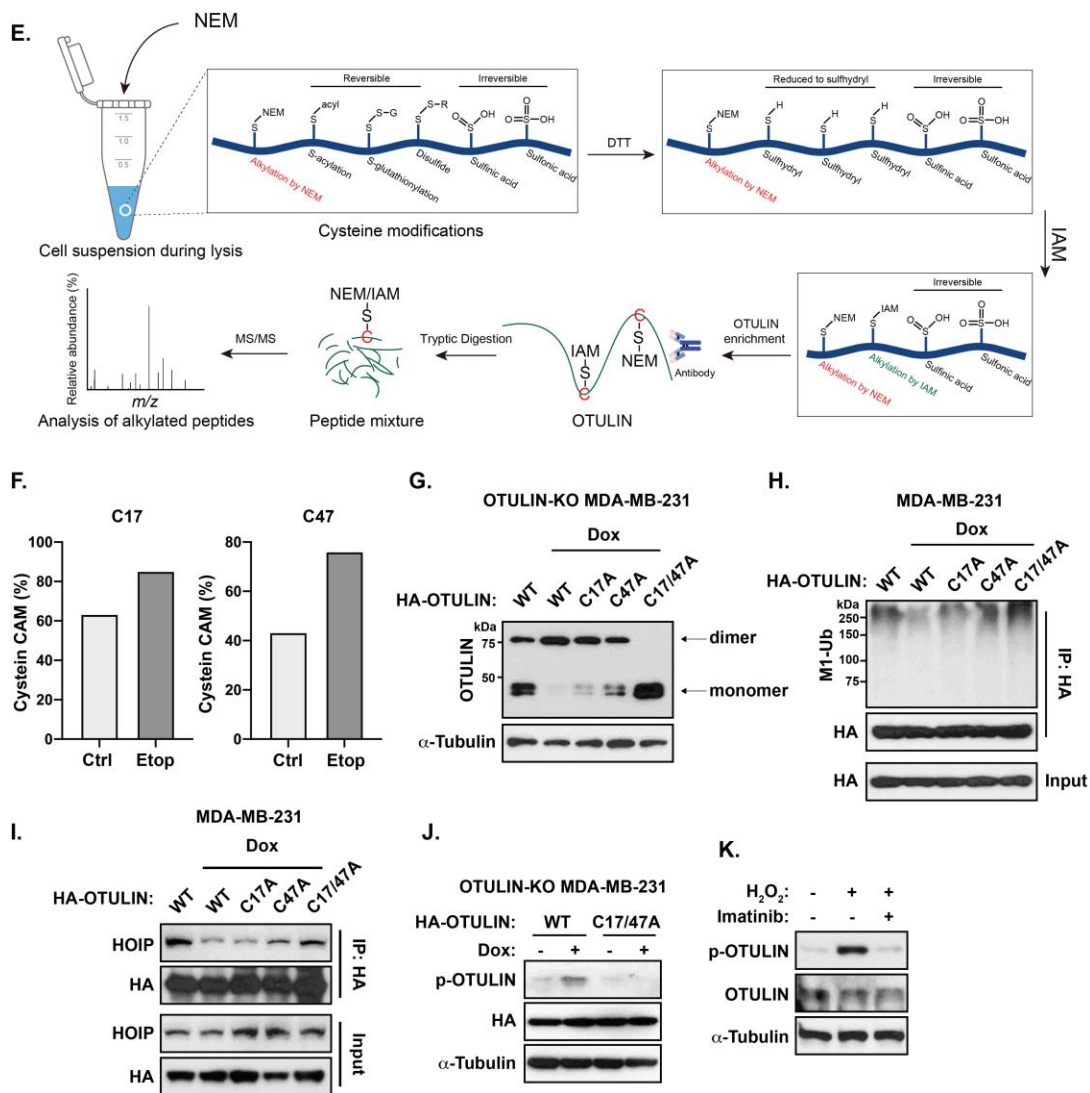


Figure 3-11. Continued.

the OTULIN cysteine mutant causes a significant reduction of the dimer formation upon Dox treatment as compared to WT group. Of note, double cysteine mutant of OTULIN completely prevented OTULIN from Dox-induced dimerization (**Figure 3-11G**). Furthermore, the linear ubiquitin levels of OTULIN and the HOIP binding to OTULIN were negatively correlated with OTULIN dimerization, affected by OTULIN cysteine mutation (**Figure 3-11H, I**). Since OTULIN C17/47A significantly affected the HOIP OTULIN interaction, it was plausible to postulate that OTULIN C17/47A mutation could influence NF- κ B activation upon genotoxic stress or TNF α treatment. Notably, OTULIN C17/47A mutation failed to inhibit NF- κ B activation after TNF α and Etop treatment (**Figure 3-7H**). Altogether, these findings display a critical residue for OTULIN dimerization which underlies the loss-of-function of OTULIN during the genotoxic and inflammatory response.

The negative regulated effect of OTULIN on NF- κ B signaling has been mostly studied in the context of inflammatory response such as TNF α stimulus [22, 27, 34, 94, 129]. We conducted some crucial assays under TNF α stimulus to determine whether genotoxic stress-mediated OTULIN linear ubiquitination and dimerization can be applied to the situation in inflammatory response. The time-course study under TNF α treatment presented similar mode showing the oxidative deficiency of OTULIN C17/47A, and OTULIN dimerization negatively correlated with OTULIN linear ubiquitination and OTULIN-HOIP interaction, suggesting that TNF α induces the same OTULIN modifications as genotoxic stress (**Figure 3-12A, B, C, and F**). In addition, TNF α induces the linear deubiquitination of OTULIN in an OTULIN-dependent manner, but not CYLD (**Figure 3-12D, E**). Furthermore, TNF α treatment did not alter the affinity between HOIP and CYLD (**Figure 3-12G**).

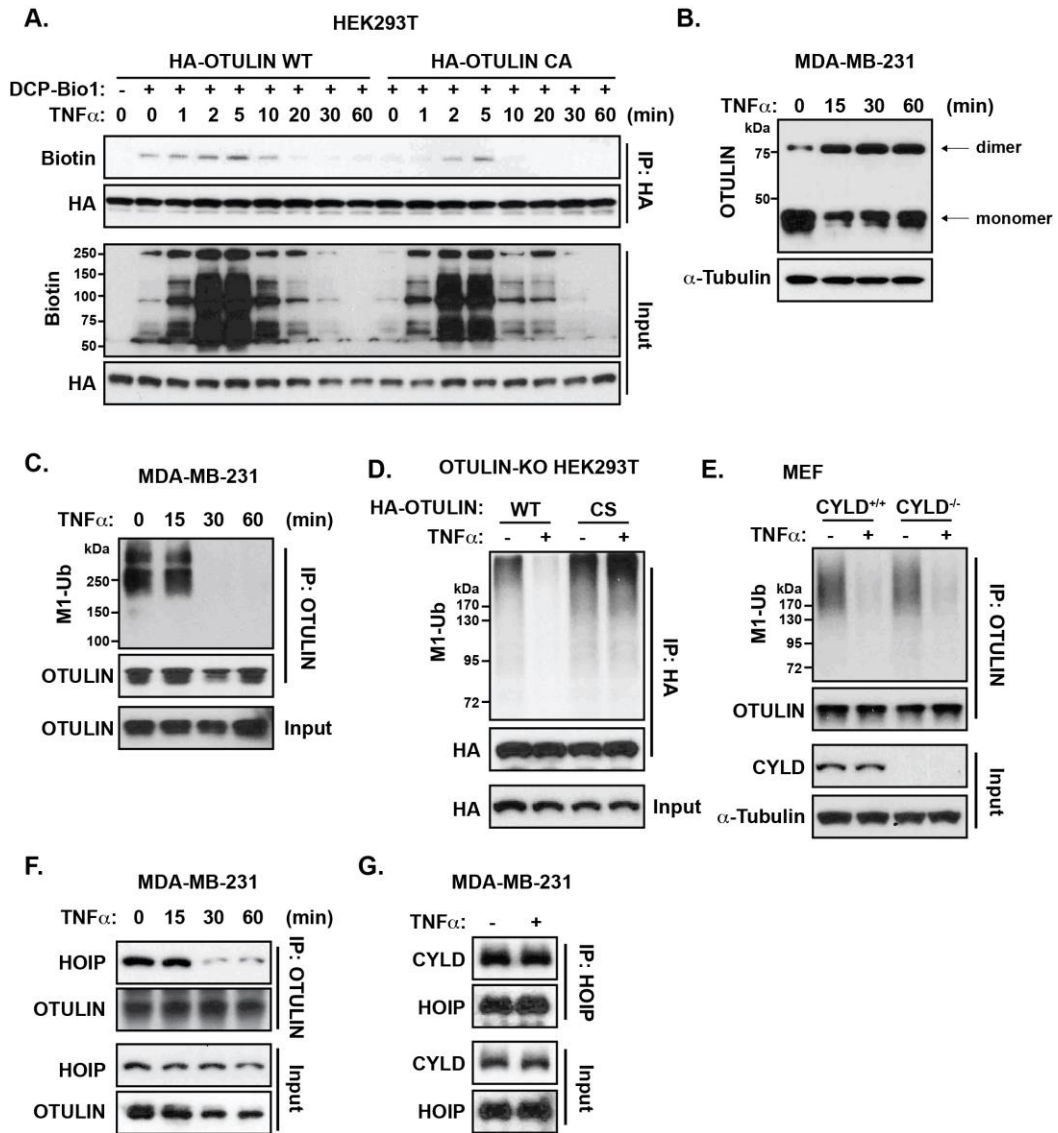
We also determine the impact of OTULIN C17/47A on the OTULIN phosphorylation. OTULIN Tyr56 within the PIM domain is critical for its interaction to HOIP, and OTULIN phosphorylation and mutation at Tyr56 directly disrupt LUBAC-OTULIN complex [22, 34]. Tyr56 is embedded in PIM pocket when OTULIN interacts with HOIP, which may prevent the phosphorylation of Try56. To test if the OTULIN mutant (C17/47A) liable to LUBAC interaction will prevent its phosphorylation, we induced the OTULIN phosphorylation by Dox [139] in OTULIN-KO MDA-MB-231 cells reconstituted with OTULIN WT or C17/47A mutant. Interestingly, OTULIN C17/47A mutant decreases phosphorylation levels on the Tyr56 residue upon Dox treatment compared to WT (**Figure 3-11J**), suggesting that the OTULIN-LUBAC interaction structurally prevents OTULIN phosphorylation. In addition to Dox, OTULIN phosphorylation could also be induced by H₂O₂ treatment, which was blocked by ABL1 inhibitor imatinib (**Figure 3-11K**).

OTULIN Loss of Function Is Detected in Clinical TNBC Samples

Our model shows that OTULIN can form dimer, which releases the OTULIN from HOIP, and leads to activation of NF- κ B pathway. To test if the model can also be applied to human specimens, we acquired 6 pairs of clinical human TNBC samples. In

Figure 3-12. Analysis of OTULIN dimers, ubiquitination, and HOIP interaction during TNF α treatment.

(A) Co-IP analysis of the biotin labeled HA-OTULIN (WT or C17/47A) in HEK293T cells treated with TNF α (10 ng/ml) for indicated time points and lysed with DCP-Bio1 as described in methods. (B) Immunoblotting analysis of OTULIN dimerization in MDA-MB-231 cells treated with TNF α (10 ng/ml) for 0, 15, 30, 60 min, and subject to cell lysis without DTT or 2-ME. (C) Linear ubiquitination of immunoprecipitated OTULIN in MDA-MB-231 cells treated with TNF α (10 ng/ml) for 0, 15, 30, 60 min. (D) Linear ubiquitination of immunoprecipitated HA-OTULIN in OTULIN-KO HEK293T cells reconstituted with HA-OTULIN WT or C129S, and then treated with or without TNF α (10 ng/ μ l, 15 min). (E) Linear ubiquitination of immunoprecipitated OTULIN in CYLD^{+/+} or CYLD^{-/-} MEFs treated with or without TNF α (10 ng/ μ l, 15 min). 2% of protein lysate was used as Input for indicated protein detection by immunoblotting. (F) Co-IP analysis of the interaction between HOIP and OTULIN in MDA-MB-231 cells treated with TNF α (10 ng/ml) for 0, 15, 30, 60 min. (G) Co-IP analysis of the interaction between HOIP and CYLD in MDA-MB-231 cells treated with or without TNF α (10 ng/ml, 15 min).



consistent with the cell experiment, OTULIN in the clinical samples also presented dimer formation, which especially increased in #1, #2, and #5 patient breast cancer tissues (**Figure 3-13A**). Unexpectedly, OTULIN expression level of OTULIN tumor tissues markedly increased in 3 out of the 6 clinical samples which correlated with the loss of interaction between OTULIN and HOIP and the loss of linear ubiquitinated OTULIN, compared to adjacent nontumor tissues (**Figure 3-13B, C**). #3, #4, and #6 patient cancer and adjacent normal tissues displayed the same HOIP-OTULIN interaction but different OTULIN phosphorylation levels, which indicates that there were other factors regulating OTULIN phosphorylation (**Figure 3-13C**). To our surprise, though with higher amounts of OTULIN, all these three samples (cancer tissues of #1, #2, #5) displayed high levels of NF- κ B activation (p-p65/Ser536) levels (**Figure 3-13C, F**). The explanation for this might be that, although OTULIN was in a high level, negative feedback from dimerization might have allowed the NF- κ B signaling to be activated through some other positive regulators in these samples. These cancer samples only had few functional OTULIN monomers that could counteract LUBAC-mediated NF- κ B activation. Chronic inflammation may cause a high OTULIN dimerization in these cancer samples. In the remaining 3 pairs of specimens (group B), the relative relationship between the OTULIN protein levels and the OTULIN-HOIP interaction is constant with no significant difference between cancer and normal tissues, associated with comparable NF- κ B activation (**Figure 3-13D through H**).

Bioinformatic analysis based on a published proteomic database using a large cohort of primary breast tumor tissues revealed protein expression levels in four breast cancer subtypes: basal-like (BL), HER2⁺, luminal A, and luminal B [140]. TNBC is often classified as a subtype of BLBC by gene expression profiling analysis. The overlap of gene expression profiles can be as high as 60-90% between TNBC and BLBC compared to an only 11.5% overlap between non-TNBC and BLBC [113]. It is interesting that both OTULIN and LUBAC protein expression levels were altered significantly in the basal-like group, while changes of CYLD was not appreciable. In particular, OTULIN protein level was elevated in 16 out of 26 cases of BLBC (> 60%) by 2-8 folds: 6 cases at 2 folds, 6 cases at 4 folds, 2 cases at 6 folds, and 2 cases at 8 folds, while the increase of OTULIN protein in the other three groups were much milder (~2 folds) among 30-36% of all cases. On the contrary, HOIP protein level is mildly reduced in most of the 26 cases of BLBC, as compared to other groups (**Table 3-1**). For OTULIN, we still observed a high heterogeneity of expression level in BLBC, which indicates the requirement of a personalized treatment strategy (**Figure 3-14A**). The significant effect of OTULIN-LUBAC interaction may supply a new approach for future personalized therapy. An interesting data showed that OTULIN translation was dramatically increased after SARS-CoV-2 infected, the reason behind this remains to be further investigated (**Figure 3-14B**).

Figure 3-13. Analysis of OTULIN dimers, ubiquitination, and HOIP interaction in breast cancer clinical samples.

(A) Immunoblotting analysis of OTULIN dimer formation in breast cancer and adjacent nontumorous tissue samples from 6 TNBC patients processed without DTT or 2-ME. (B) Co-IP analysis of the interaction between HOIP and OTULIN in clinical samples processed with IP buffer containing DTT and loading buffer with 2-ME. Immunoblotting analysis of NF- κ B activation (p-p65), OTULIN, and HOIP expression level. (C) Linear ubiquitination and phosphorylation of immunoprecipitated OTULIN in clinical samples boiled with IP buffer containing DTT at 95°C for 30 min, which subjected to immunoprecipitation by low amount of anti-OTULIN antibody (500 ng) and Dynabeads (10 μ l) to make them saturated. (D-H) Quantification graph based on densitometry of the blotting data from the panels of B and C using two-way ANOVA followed by Tukey's post-hoc test. Data are presented as mean \pm SEM. **p < 0.01; ***p < 0.001; ns, not significant. Pt: patient; N: normal tissues; BC: breast cancer tissues. Red arrows indicate the same individual samples that show loss of function of OTULIN (i.e., correlated loss of OTULIN-HOIP interaction and OTULIN deubiquitination).

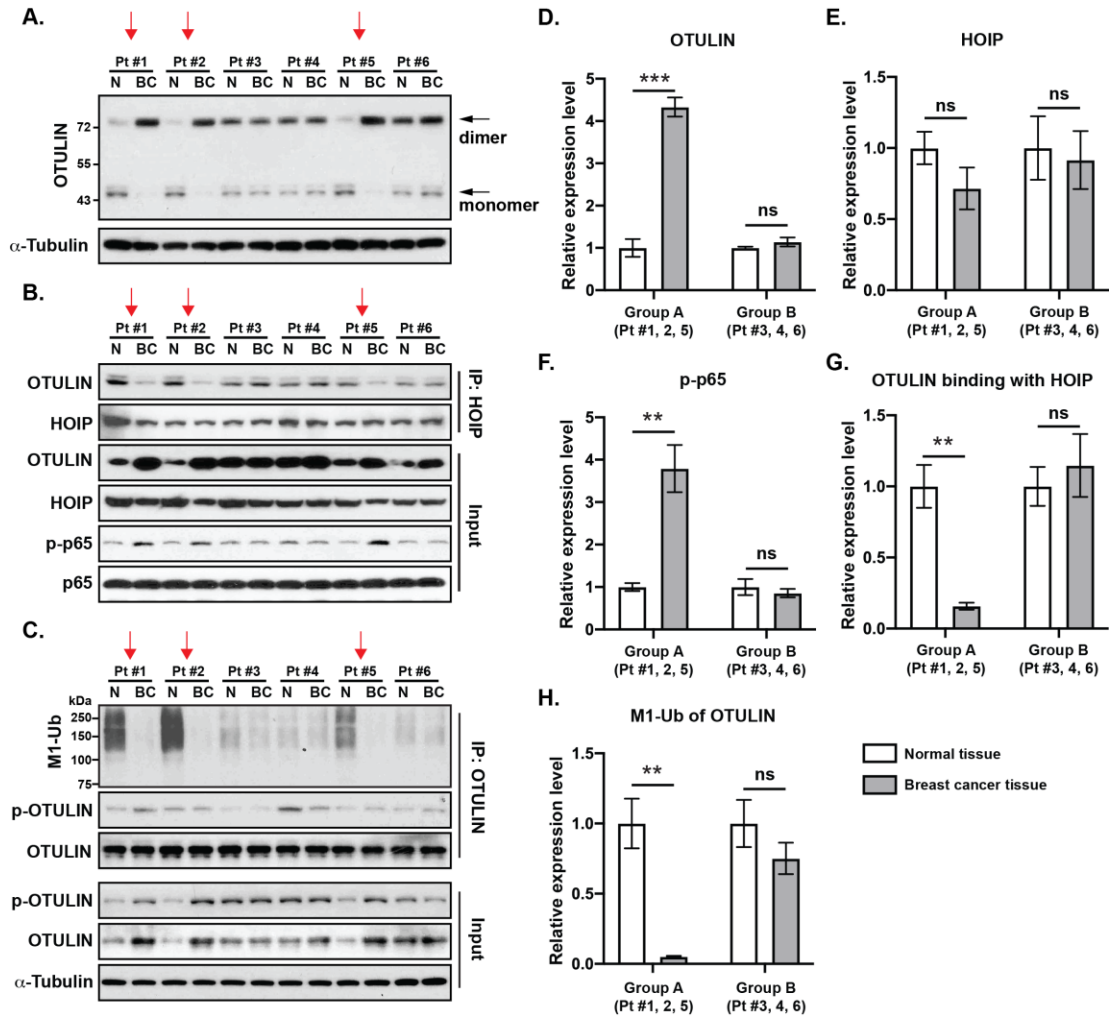


Table 3-1. Fold change of the protein expression.

BLBC vs.	OTULIN	HOIP	CYLD
Others	1.16	0.90	1.03
Control	1.41	0.86	1.18

Notes: fold change of the expression of OTULIN, HOIP, and CYLD in basal-like breast cancer vs. other breast cancers and basal-like breast cancer vs. normal breast tissue. The log₂-transformed and then Z-score-normalized quantitative data of these three proteins were used for the analysis.

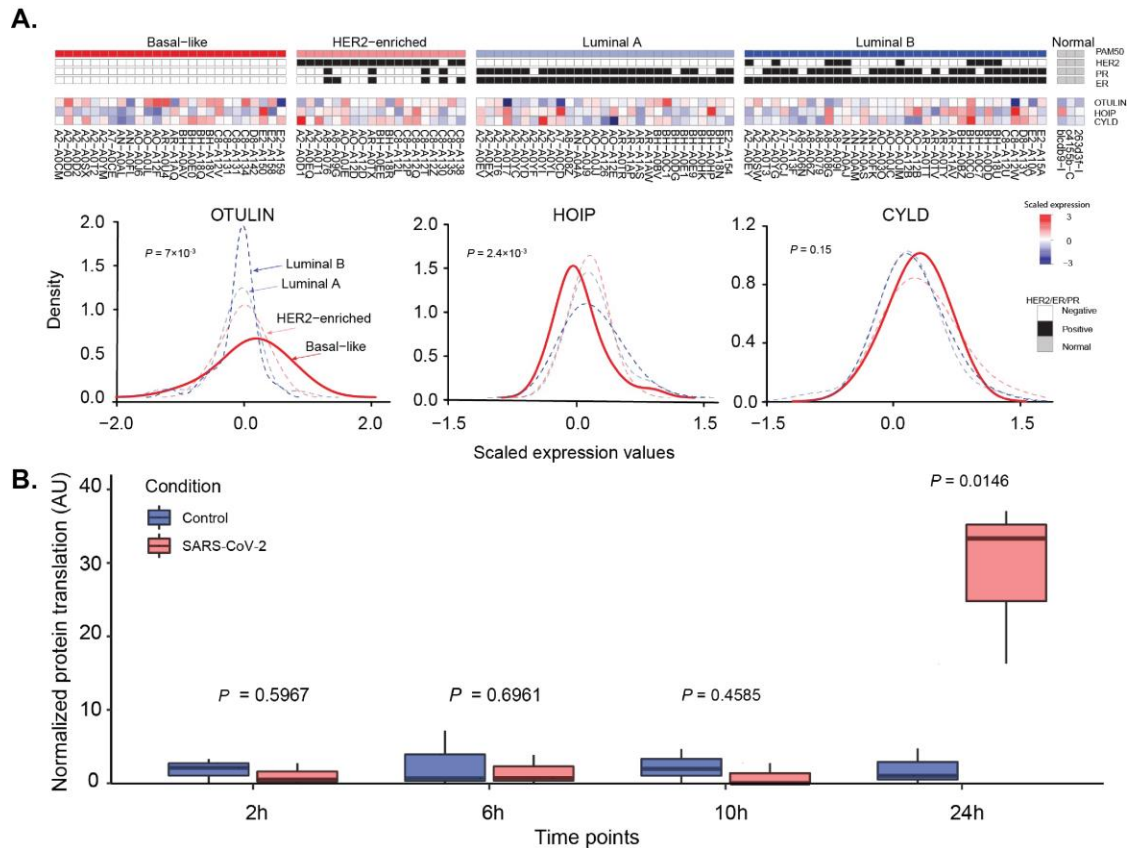


Figure 3-14. Bioinformatic analysis.

(A) Expression of OTULIN, HOIP, and CYLD proteins across 111 patient samples. Top panels present the heatmap of relative expression level of protein OTULIN, HOIP, and CYLD, respectively, across 108 breast tumor samples and 3 controls. The tumor samples were divided into four subtypes: Basal-like, red ($n = 26$); HER2-enriched, pink ($n = 19$); luminal subtype A, light blue ($n = 29$); luminal subtype B, dark blue ($n = 34$). Normalized isobaric tags for relative and absolute quantitation (iTRAQ) protein abundance ratio was shown for each protein. The expression data were downloaded from the clinical proteomic tumor analysis consortium (CPTAC) data portal (<https://cptac-data-portal.georgetown.edu/cptac/s/S029>) [140]. Lower panels present distributions of expression of OTULIN, HOIP, and CYLD proteins between the four tumor types. (B) Translation of OTULIN protein over time from Caco-2 epithelial cells after SARS-CoV2 infection [141]. Mean translation in arbitrary units (AU) was plotted for mock-infected (control) and infected samples. Translatome was measured by stable isotope labelling with amino acids in cell culture (SILAC). In the original work, a total of 2,715 proteins were quantified for translation. The OTULIN translation was extracted and plotted from the original data.

CHAPTER 4. DISCUSSION

The Ubiquitin System in NF- κ B Activation

It has been almost three decades since the discovery of ubiquitin chains to modulate NF- κ B activation, with the revelation that I κ B α is modified with K48-linked ubiquitin chains by ubiquitin ligase complex SCF ^{β TrCPs} in response to receptor activation, resulting in rapid proteasomal degradation [142]. Following that, K63-Ub chains were shown to have a non-degradative function in signal transduction and NF- κ B activation by facilitating the activation of TAK1 [143]. After the identification of linear ubiquitin for over a decade, it also has the signaling features to promote IKK β phosphorylation by TAK1 [6, 11, 61]. Together with K48- and K63-linked chains, they orchestrate the activation of NF- κ B involved in inflammation, cell survival and immune responses [144].

The Novel Mechanism of OTULIN-LUBAC Interplay

By conducting multiple experimental approaches in MDA-MB-231 and HEK293T cells, we demonstrate that linear ubiquitination of OTULIN under unstressed condition in a LUBAC-dependent manner is required for stabilizing the interaction between OTULIN and HOIP, the core catalytic unit of LUBAC. The presence of OTULIN on LUBAC enhanced by linear ubiquitin chains limits the activation of NF- κ B through deubiquitinating the substrates involved in NF- κ B signaling, such as NEMO, RIPK1. However, inflammatory/genotoxic stress could induce OTULIN dimerization which causes its intermolecular deubiquitination, afterwards, OTULIN is subsequently released from HOIP, leading to overactive NF- κ B signaling. Especially in TNBC patients, the unregulated genotoxic NF- κ B activation is correlated with increased cancer cell survival (i.e., the main feature of chemoresistance). Our work discloses for the first time that the LUBAC-mediated OTULIN linear ubiquitination is in turn required for the interaction with LUBAC and the inhibition of NF- κ B signaling. In consistent with the cellular data, clinical samples also present the similar evidence: 3 out of the 6 TNBC specimens display high levels of OTULIN dimerization in cancerous tissue compared to the adjacent normal breast tissue, which correlates with a nearly complete loss of OTULIN linear ubiquitination, significantly disrupted OTULIN-HOIP interaction (> 70%, $p < 0.01$), and increased NF- κ B activation (**Figure 3-13A, B, C**). Interestingly, these same three cancerous tissue specimens also showed significantly increased expression of OTULIN and slightly decreased expression of HOIP protein (**Figure 3-13D, E**). Remarkably, the reciprocally changed levels of OTULIN and HOIP revealed from these small sets of TNBC specimens are also reflected in large cohorts of breast cancer specimens; no significant change in CYLD protein expression was shown (**Figure 3-14A**). Together, these data indicate a prominent role of the OTULIN-LUBAC axis in regulating genotoxic NF- κ B signaling that increased OTULIN and lower LUBAC levels in TNBC patients are likely associated with poor prognosis, short survival, and increased chemoresistance.

It should be noted that our genotoxic cellular models did not recapitulate one aspect of the clinical samples on the high expression levels of OTULIN in the cancerous tissue that displayed non-functional OTULIN in NF- κ B inhibition. In our cellular models under unstressed conditions, the majority of the overexpressed OTULIN stay as monomers and in association with LUBAC, while they form dimers under acute genotoxic conditions via a mechanism of ROS-mediated Cys modification. Therefore, the inhibitory effect of OTULIN seems to depend on the functional OTULIN monomers rather than the dysfunctional OTULIN dimers. In the cancerous tissues that may undergo chronic stress over months or years, it is plausible to postulate that OTULIN is upregulated as an adaptive stress response. However, upon sustained and perhaps high levels of oxidative stress during the oncogenesis, both the ROS and the upregulated OTULIN somehow facilitate its dimerization and the subsequent loss of function. Owing to the heterogeneity of clinical cancer tissues, OTULIN and LUBAC components may be dysregulated at additional multiple levels, involving transcriptional, post-transcriptional and post-translational mechanisms. Although these full events may not be easily recapitulated by acute cellular model, the model we postulated for a chronic clinical condition does not contradict the overall findings we obtained from the cellular models and the concluded mechanisms.

Hyperphosphorylation of OTULIN at Tyr56 has been reported to prevent HOIP binding because this residue is located at the most critical position in the N-terminal domain-binding motif of OTULIN to HOIP-PUB domain [22, 34]. Although ABL1 is required for OTULIN phosphorylation under genotoxic stress [139], if other stresses like TNF α can induce OTULIN phosphorylation via ABL1 remains to be investigated. In this work, we discovered that genotoxic stress and TNF α induce OTULIN dimerization (**Figure 3-10G, 12B**) which is mediated by oxidative stress (**Figure 3-11A, B**). Collectively, both OTULIN dimerization and phosphorylation can be induced by genotoxic stress, which results in disassociation of OTULIN from the HOIP/LUBAC complex.

Intermolecular Dimerization Mediated by Disulfide Bonds

Self-association of proteins to form dimers and higher-order oligomers is a regular event that is important for the control of enzymes, receptors, ion channels, and transcription factors [145]. For instance, NEMO homodimer associated by disulfide bonds is required for TNF α -induced NF- κ B activation [146]. Unwanted protein self-association can also result in the formation of pathogenic structures [145]. OTULIN dimers initially were undetectable under regular protein isolation conditions but only appeared when processed with a DSS crosslinker (**Figure 3-10G**). The result suggests us that OTULIN is forming dimers through non-covalent bonds (ionic bonds, hydrophobic interactions, hydrogen bonds, etc.) or covalent bonds (disulfide bonds). Disulfide bonds are covalent interactions that occur upon oxidative stress [137]. Our data has shown OTULIN dimerization require its N-terminal domain, which includes two conservative cysteine residues, Cys17 and Cys47. Notably, the selective Cys-mutated OTULIN failed in both dimerization (**Figure 3-11G**) and Tyr56 phosphorylation (**Figure 3-11J**) under

Dox treatment, indicating a disulfide bond-dependent OTULIN dimerization is required for the phosphorylation of OTULIN Tyr56. This action may be explained by conformational changes. The resolved crystal structure showed OTULIN Tyr56 is located at a close position to the critical catalytic domain [22, 34], which may be inaccessible to any kinases under unstressed conditions and therefore phosphorylated level of OTULIN in normal condition is low. We further speculate that OTULIN C17/47A mutant without dimerization will bind to HOIP tightly, in that case, Try56 is embedded in the HOIP-PUB pocket. Hence, OTULIN has no chance to expose Tyr56 residue for Dox-induced phosphorylation by ABL1. ABL1 still can be activated by oxidative stress [147]. Therefore, inhibiting the oxidative stress to stabilize the interaction between OTULIN and HOIP may represents a feasible therapeutic strategy via preventing OTULIN dimerization and Try56 phosphorylation, this benefit is apparent not only for combating chemoresistance, but also for most of the human diseases.

Ubiquitination of OTULIN

Another exciting finding in this work is that OTULIN is linearly ubiquitinated on K64/66 sites by LUBAC, which is a positive feedback loop for OTULIN-LUBAC interaction. Interestingly, OTULIN was also found to be K63-ubiquitinated at the same residues (K64/66) by TRIM32 under TNF α stimulation but not studied in the genotoxic stressed condition [148], which may explain why K63-Ub is undetectable without any treatment (**Figure 3-5C**). Different with linear ubiquitin chains, K63 ubiquitin chains interfere with the interaction between OTULIN and LUBAC, leading to an overactivated NF- κ B signaling. Theoretically, both K63 and linear ubiquitination can compete for the K64/66 sites, but which one predominantly occupies this site depending on the specific upstream signals. Here, our solid data from different cellular models, including both HEK293T and MDA-MB-231 cells, revealed that OTULIN linear ubiquitination at K64/66 is assembled by LUBAC in resting cells. This modification is counteracted by OTULIN self-association, which can be induced by genotoxic stress and TNF α treatment.

OTULIN's Differential Functions in NF- κ B and Wnt/ β -catenin Pathway

Our recently published work depicted a differential role of OTULIN in positively regulating Wnt/ β -catenin pathway, which is another crucial signaling mechanism underlying chemoresistance upon overactivation [139]. Unlike the NF- κ B signaling, in which OTULIN-HOIP interaction is necessary for OTULIN recruitment to NEMO, the phosphorylated state of OTULIN (Tyr56) but not the OTULIN-HOIP interaction is required for OTULIN recruitment to β -catenin. Interestingly, genotoxic stress induces OTULIN phosphorylation on Tyr56 by tyrosine-protein kinase ABL1, leading to OTULIN disassociation from the HOIP/LUBAC complex. The released phosphorylated form of OTULIN is recruited to β -catenin for linear chain deubiquitination. Subsequently, p-OTULIN- β -catenin complex also reduces the K48-Ub chains in an unknown way, thereby stabilizing β -catenin complex from proteasomal degradation.

According to these studies, we have delineated the roles of OTULIN involved these two signaling pathways under genotoxic response. Further research of OTULIN on the relative interplay between these two pathways in terms of their contributions and balance is needed.

The Regulation of OTULIN Expression

Although various roles of OTULIN in regulating cellular processes have been revealed, how the upstream signaling and the regulatory events on OTULIN expression is regulated, if OTULIN expresses in a cell-specific manner, is there any other PTMs critical for its function, are still unknown. Previous data have shown the levels of OTULIN are higher under certain conditions: Breast tumor tissues ($n = 65$) revealed significantly higher levels of OTULIN mRNA compared to normal breast tissues ($n = 25$) by qPCR analysis [139]. TCGA-BRCA genomic dataset showed significantly higher transcription levels of OTULIN in the BL subtype of breast cancer than that in other molecular subtypes (i.e., HER2⁺, luminal A, luminal B, and normal subtypes) [139]. On the other hand, cerebral ischemia/reperfusion injury increases OTULIN expression in transient middle cerebral artery occlusion (tMCAO) rats, and OTULIN expression is upregulated in activated microglial cells [149]. Electroacupuncture (EA) treatment significantly increases OTULIN expression in tMCAO rats [150].

Mechanistic Importance of Our Study

Given the paramount importance of the NF- κ B signaling in regulating various pathophysiological processes, including cancer development and chemoresistance, and ligand-mediated innate and adaptive immune and inflammatory responses (e.g., TNF α , IL-1, and interferons), our mechanistic findings based on genotoxic response will likely be applied to canonical NF- κ B signaling. Indeed, we reproduced all key experiments under TNF α -induced condition (**Figure 3-12**). Negative regulators by PTM are crucial to limit and fine-tune overactivated NF- κ B signaling [45], in which DUBs have emerged as a significant part. Our findings fill a piece of gap in our understanding of ubiquitin assembly and disassembly regarding the LUBAC-OTULIN interplay.

The Overall Significance of Our Study

OTULIN in COVID-19 patients

Given that TNF α -induced NF- κ B overactivation is an important signaling pathway underlying a myriad of autoinflammatory and autoimmune conditions, including the current SAR-CoV2 pandemic (i.e., cytokine storms) [151], we tried an in-depth bioinformatic analysis for evidence of a potential role of OTULIN. Caco-2 cells were commonly used for SARS-CoV infection study, and therefore can be used for SARS-

CoV-2 infection. OTULIN expression was significantly increased in cultured human colon epithelial carcinoma cell line, Caco-2, after being challenged with SAR-CoV2 viruses 24 h (**Figure 3-14B**) [141]. Although immune cells of the myeloid lineage (e.g., monocytes and macrophages) are believed to take primary responsible for pathological inflammation in COVID-19 patients [152], OTULIN expression in these cell types after the infection with SAR-CoV2 viruses is temporarily unknown. Interestingly, some reports showed that increased protein level of OTULIN correlates with the severity of the COVID-19 patients [153, 154]. All of the evidence showed that OTULIN is increased in response to the stress signal, which might be a negative feedback of host prepared for the inflammatory response. Furthermore, it has been reported that OTULIN-LUBAC axis can regulate the host defense against other pathogens by affecting NF- κ B activation [155, 156]. Taken together, a growing amount of evidence suggests targeting the NF- κ B pathway can be a possible therapeutic strategy for COVID-19 patients in the critical stage [157].

OTULIN in neurodegenerative diseases

Accumulation of misfolded protein aggregates in the brain is a common feature of neurodegenerative diseases (NDDs), such as Alzheimer's disease (AD), Parkinson's disease (PD), Huntington's disease (HD), and amyotrophic lateral sclerosis (ALS) [158]. The pathogenesis of NDDs is highly associated with failure of cellular protein homeostasis, which is mediated by protein quality control system [159]. The ubiquitin-proteasome system (UPS) and autophagy are two major quality control systems responsible for degradation of proteins and organelles in eukaryotic cells [160]. Ubiquitination of misfolded proteins, like K-48 ubiquitination, is predicted to facilitate their proteasomal degradation, such as mutant Huntingtin, TDP-43, and SOD1. A study showed a decrease of proteotoxicity with silencing of OTULIN, showing the neuroprotective role of linear ubiquitination independent of NF- κ B activation in neurodegenerative disease [161]. On the other hand, OTULIN's classic role is in anti-inflammation (e.g., inhibiting NF- κ B activation). Therefore, OTULIN can still play a role against neuroinflammation via antagonizing NF- κ B pathway. Neuroinflammation is another invariant feature of NDDs, commonly associated with NF- κ B activation [162, 163]. So far, there is one study reporting that OTULIN plays a NF- κ B-dependent neuroprotective role following acute ischemic stroke [149]. Particularly, silencing of OTULIN expression reverses the inhibitory effect of electroacupuncture on the transformation of microglia and astrocytes from resting states to activated states and the secretion of TNF α , IL-1 β , and IL-6. For OTULIN cellular localization, OTULIN protein primarily resides in the cytoplasm of microglia and neurons, but only a small amount of OTULIN was in the nuclei. In addition, OTULIN was undetectable in astrocytes. EA induces OTULIN expression increased and redistribution in the ischemic penumbra of the cerebral cortex [150].

AD is featured by senile plaques of amyloid beta (A β) and neurofibrillary tangles (NFTs) of phosphorylated tau aggregates as well as neuroinflammation [164]. A β toxicity leads to synaptic loss and cognitive impairment, which can be ameliorated by Tau

reduction [165]. Of note, it has been reported that NFTs, not amyloid plaques are best related to the severity of dementia [166]. Furthermore, neuroinflammation contributes as much or more to the pathogenesis of AD as the A β and NFTs do [164]. Given the well-defined role of OTULIN in anti-NF- κ B inflammation and its emerging role in protein degradation [130], OTULIN can exert seemingly opposing and contradictory roles in NDDs such as AD. We have performed preliminary work in exploring potential roles of OTULIN in these two aspects: 1) in anti-inflammatory response induced by lipopolysaccharide (LPS) and 2) in facilitating tau protein degradation. Our data suggest that OTULIN can play different roles at different disease conditions which will be further discussed in the next Chapter.

CHAPTER 5. CONCLUSIONS AND FUTURE DIRECTIONS

Conclusions

Our study has deepened the understanding of the relationship between OTULIN and LUBAC under genotoxic or inflammatory conditions.

The following findings are the highlights of our study (**Figure 5-1**). (1) OTULIN counteracts LUBAC-mediated NF- κ B activation upon genotoxic stress. (2) The presence of OTULIN on LUBAC is required for inhibiting genotoxic NF- κ B activation. (3) Linear ubiquitination of OTULIN is dependent on LUBAC. (4) Linear ubiquitination of OTULIN enhances its binding to LUBAC. (5) Genotoxic stress- or TNF α -induced OTULIN dimerization facilitates its self-deubiquitination. (6) OTULIN protein levels are upregulated in TNBC tissues and SAR-CoV2 infected Caco-2 cells.

Taken together, these findings facilitate our understanding of the negative role of OTULIN via the regulation of the linear ubiquitination and provide a new perspective about future drug development strategy for inflammatory disease and TNBC therapy.

The Roles of OTULIN in Neuroinflammation and Tau Accumulation

People over 65 years old gradually suffer from AD which is the most common cause of dementia, leading to a decline in thinking and independence in personal daily activities. AD is pathologically characterized by the presence of β -amyloid-containing plaques and tau-containing NFTs (i.e., tauopathy) [167]. On the other hand, the early and substantial contribution of inflammation in the pathogenesis of AD is supported by the analysis of clinical manifestations prior to AD, such as mild cognitive impairment. Neuroinflammation is a pathophysiological process which is featured by increased secretion of pro-inflammatory cytokines (IL-1 β , IL-6, TNF α), chemokines (CCL2, CCL5, CXCL1), reactive oxygen species, and secondary messengers (NO and prostaglandins) in the central nervous system (CNS) [164]. There are currently only two types of approved medications to treat Alzheimer's disease: inhibitors of the cholinesterase enzyme and antagonists of N-methyl-D-aspartate (NMDA), both of which can only relieve the symptoms of AD but are not applicable to the cure or prevention of AD [168]. Targeting tau's degradation is a promising therapeutic concept to ameliorate AD, which can be divided into autophagy-lysosomal or ubiquitin-proteasomal degradation [169]. The function and fate of tau are closely regulated by various PTMs, including phosphorylation, acetylation, SUMOylation, nitration, glycation, O-glycosylation, and ubiquitination [170]. Recently, it has been found that LUBAC-conjugated linear ubiquitination of Huntingtin facilitates its proteasomal degradation, which is corroborated by the data that silencing HOIP exacerbates the proteotoxicity of Huntingtin aggregates, whereas silencing of OTULIN has the opposite effect [161]. Based on our current knowledge, it is plausible to investigate if LUBAC-OTULIN axis can regulate the accumulation/clearance of tau and the neuroinflammation in AD.

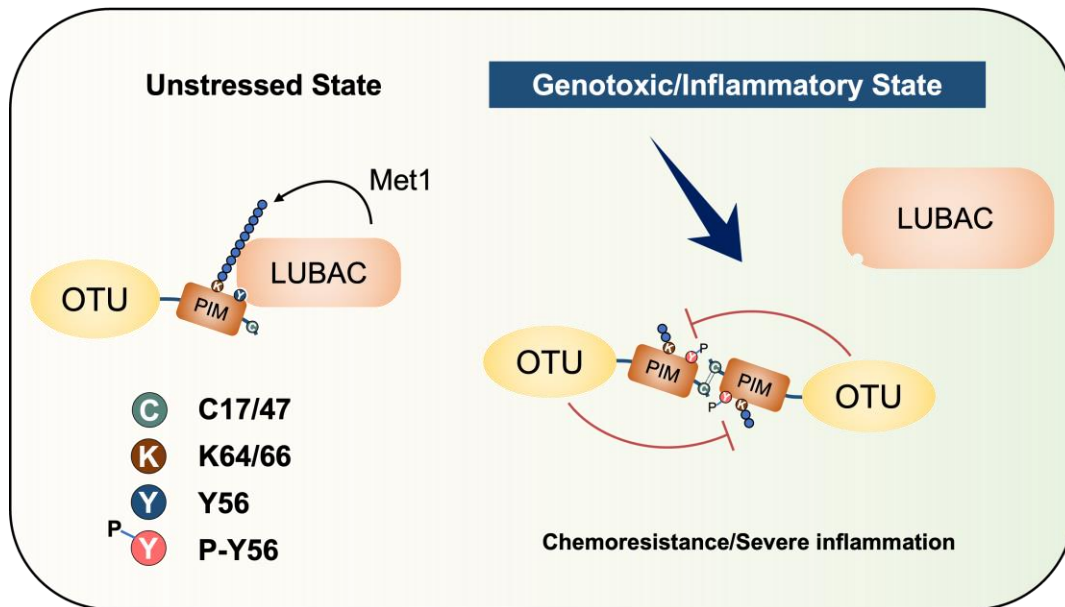


Figure 5-1. Graphical abstract regarding the crucial roles of OTULIN in NF- κ B-mediated chemoresistance and inflammation.

Under unstressed condition, OTULIN binds to HOIP which limits the linear ubiquitination of the substrate molecules such as NEMO, governing a normal NF- κ B activation. Under genotoxic or inflammatory condition, OTULIN molecules dimerize, promoting Tyr56 phosphorylation and its self-deubiquitination, resulting in its dissociation from HOIP. Ultimately, OTULIN loss of function leads to an aberrant NF- κ B activation and subsequent chemoresistance or inflammatory symptoms.

OTULN inhibitor promotes the mRNA levels of pro-inflammatory cytokines

Microglia, the resident phagocytes of the CNS, constantly patrol the brain for pathogens and cellular debris; it is arguably one of the major sources of pro-inflammatory cytokines (i.e., IL-1 β , IL-6, TNF α) in AD. Hence, microglia are the central players for any discussion of neuroinflammation. We used BV2 microglial cells to investigate the role of OTULIN in neuroinflammation. Our lab previously identified a druggable compound UC495 which selectively inhibits OTULIN's catalytic activity (**Figure 5-2A**). LPS induced the upregulation of pro-inflammatory cytokines (IL-1 β , IL-6, TNF α) of BV2 cells, which is promoted by OTULIN inhibitor UC495 pretreatment (**Figure 5-2B through D**). This acute cellular model suggests that OTULIN may inhibit neuroinflammatory response.

Linear ubiquitination of tau by LUBAC associates with its degradation

Tauopathy indicates a accumulation of tau aggregates in the brain, which is highly correlated with the failure of cellular protein homeostasis. By immunoprecipitation of tau in two pairs of mouse model, we have found that tau was modified by a less linear ubiquitination correlated with an increased tau proteotoxicity in the tauopathy PS19 (tau P301S) mouse models than that in the normal mouse brain cortex. (**Figure 5-3A**). To test if the linear ubiquitination of tau is facilitated by LUBAC, we transfected LUBAC (Myc-HOIP and HA-HOIL-1) into neuroblastoma N2a cells and compared linear ubiquitinated levels of Flag-tau. We found overexpression of LUBAC greatly promoted tau's linear ubiquitination, which also correlated with the decreased level of tau. Oxidative stress is a calamitous factor implicated in the progression of AD, PD, and other neurodegenerative diseases, contributing to protein misfolding, glia cell activation, mitochondrial dysfunction and subsequent cellular apoptosis [171]. Consistently, H₂O₂-induced oxidative stress prevented tau from ubiquitination and degradation and increased OTULIN phosphorylation (**Figure 5-3B**). Further studies are required to test how oxidative stress affects tau's linear ubiquitination and degradation and if OTULIN phosphorylation is involved in tau modification. Moreover, the interaction of LUBAC-Tau was observed by co-IP assay, supporting our data that LUBAC can conjugate linear ubiquitin chains on tau (**Figure 5-3C**). Tau mutants P301L are the human tau gene causing frontotemporal dementia and parkinsonism [172]. Interestingly, tau P301L mutant didn't bind to LUBAC, which consistently had a higher basal level, even when transfected with LUBAC (**Figure 5-3C**). The deficiency of LUBAC-Tau P301L interaction might be due to some conformational change of tau. Furthermore, tau P301L mutant presented higher proteotoxicity than tau WT. In consistent with the tau basal level change, the proteotoxicity of tau WT significantly increased in HOIP-KO HEK293T cells, whereas HOIP deficiency didn't change the proteotoxicity of tau P301L, suggesting that LUBAC cannot affect the degradation of tau P301L due to its inability to bind with LUBAC (**Figure 5-3D**). These data suggest that the tau can be conjugated with linear ubiquitin chains by LUBAC, which reduces the tau proteotoxicity by promoting its degradation.

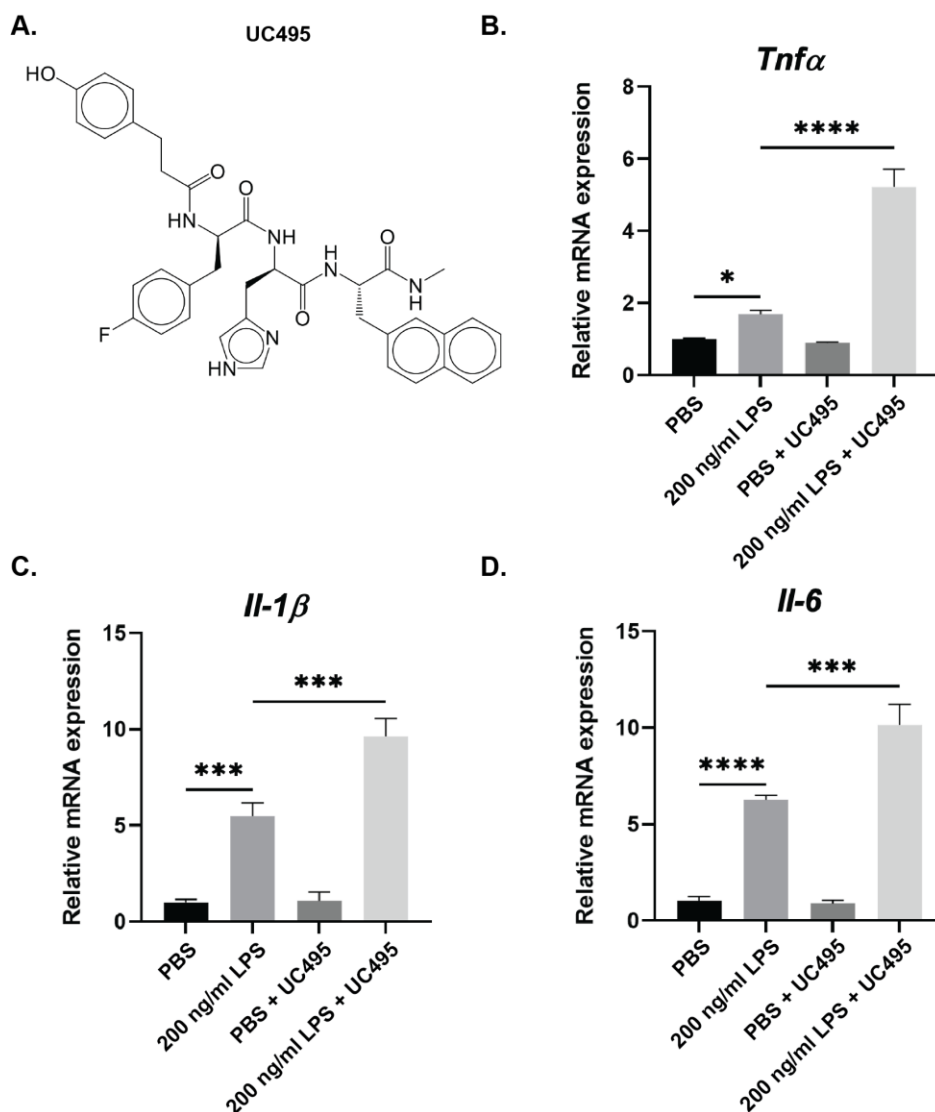


Figure 5-2. LPS-induced neuroinflammation is promoted by UC495. (A) Chemical structural formula of compound UC495. (B-C) QPCR analysis of mRNA expression levels of *Tnf- α* , *Il-1 β* , and *Il-6*. BV2 cells were treated with or without PBS, LPS (200 ng/ml, 24 h), and UC495 (10 μ M, 24h) ($n = 3$). Two-way ANOVA followed by Tukey's post-hoc test was used to determine statistical significance for multiple comparisons. Data are presented as mean \pm SEM. *** $p < 0.001$; **** $p < 0.001$; ns, not significant.

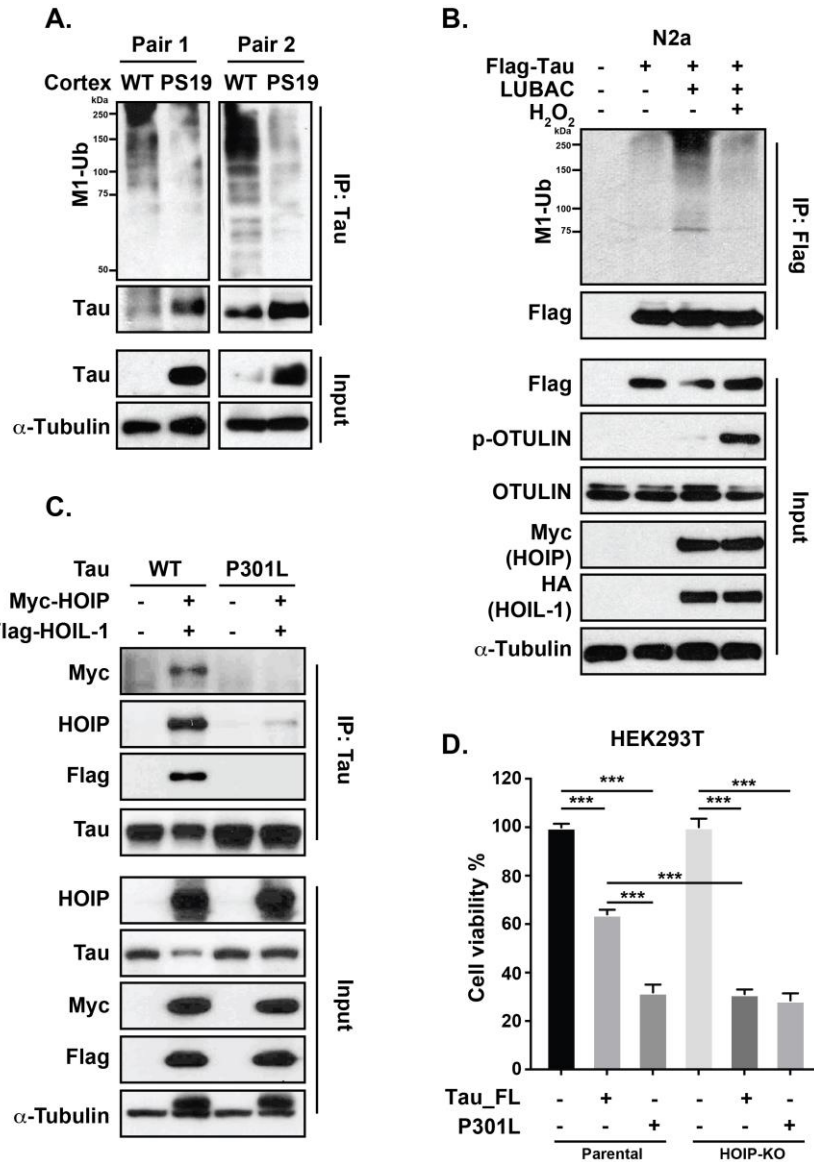


Figure 5-3. LUBAC ubiquitinates tau with linear ubiquitin chains and promotes its degradation.

(A) Linear ubiquitination of immunoprecipitated tau of cortex lysates from non-transgenic (WT tau) or PS19 mice. Protein expression was determined by immunoblotting with indicated antibodies. (B) Linear ubiquitination of immunoprecipitated tau in N2a cell transfected with Flag-tau and LUBAC (Myc-HOIP and HA-HOIL-1). H_2O_2 (100 μ M, 24 h) was applied for inducing oxidative stress after transfection. (C) Co-IP analysis of the interaction between LUBAC and tau in HEK293T cells transfected with tau (WT or P301L), Myc-HOIP, and Flag-HOIL-1. Protein expression was determined by immunoblotting with indicated antibodies. (D) CCK-8 analysis of cell viability in Parental and HOIP-KO HEK293T cells transfected with tau WT or P301L mutant for 72 h ($n = 3$). Two-way ANOVA followed by Tukey's post-hoc test was used to determine statistical significance for multiple comparisons. Data are presented as mean \pm SEM. *** $p < 0.001$.

OTULIN reduces tau linear ubiquitination and increases tau proteotoxicity by enhancing its protein stability

Linear ubiquitination is reversible PTM which is usually orchestrated by LUBAC-OTULIN axis. It would be interesting to see if OTULIN also cleaves the linear ubiquitination of tau, and subsequently aggravates its accumulation. We found the linear ubiquitination level significantly increased, along with a decreased tau basal level, in OTULIN-KO HEK293T cells compared to parental cells (**Figure 5-4A**). In contrast to HOIP-KO cells, OTULIN deficiency attenuated the proteotoxicity of tau WT, but had no effect on tau P301L mutant (**Figure 5-4B**). Collectively, these data show that OTULIN can disassemble tau linear ubiquitination and promote its stability, resulting in tau accumulation and increased proteotoxicity. However, tau P301L mutant likely cannot be modified by linear ubiquitin chains which makes tau P301L mutant more stable than WT tau, partly explaining why tau P301L mutant has a higher proteotoxicity which is more liable to neurodegenerative disease.

Our preliminary data has indicated that linear ubiquitination may play a role in the proteotoxicity of tau, which can be regulated by E3 ligase LUBAC and DUB OTULIN. To fully understand those mechanisms, we will verify our hypothesis through these approaches. (1) It remains to be tested if tau is ubiquitinated with linear chains in a LUBAC-dependent manner. We will determine the tau linear ubiquitination in HOIP-KO HEK293T cells. If HOIP-KO abolishes tau linear ubiquitination, we will complement HOIP WT or catalytic inactive HOIP C885S in HOIP-KO cells to validate the critical role of HOIP in regulating tau linear ubiquitination. The inhibitor of LUBAC still can be used for this purpose, such as gliotoxin [128]. The ubiquitination residues of tau can be investigated by LC-MS/MS and linear ubiquitination residues of tau can be verified by tau KR mutations, such as Lys254, Lys257, Lys311, Lys353. In addition, it is interesting to test if tau could be ubiquitinated by other types of chains, such as K48, K11, and K63. (2) We will further confirm the interaction between tau and LUBAC. Although the exogenous LUBAC binds to tau, the interaction between endogenous tau and LUBAC still need to be validated by co-IP assay. In vitro pulldown assay is required to test the direct binding between tau and LUBAC. (3) Linear ubiquitination of tau is positively associated with its degradation. Hence, we hypothesize linear ubiquitination can promote the degradation of Tau. OTULIN still has some ubiquitin-independent functions, which may also affect tau degradation. To investigate the mechanism, we will test if catalytic inactive OTULIN C129S/HOIP C885S mutant reconstitution in respective KO cells can affect the degradation of tau. Moreover, cycloheximide will be applied to block *de novo* protein synthesis when the stability of tau proteins is monitored at different time points in the above settings. Taken together, our future work may provide a promising strategy to ameliorate the cognitive decline and relieve neurodegenerative symptoms of patients with AD and other tauopathies by promoting tau clearance.

Consider the different effects of OTULIN on CNS, patients with different AD progression would react differently to OTULIN targeting treatment. For example, patients before/in the early stage (mild) may benefit more from the overexpression of OTULIN for limiting the proinflammatory cytokines, which causes the neural injury. As

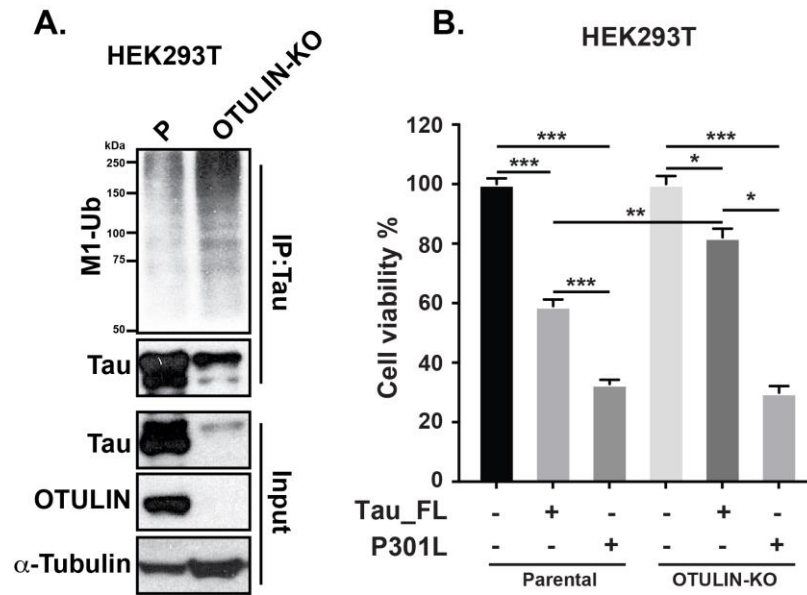


Figure 5-4. OTULIN is required for tau deubiquitination and aggravates tau proteotoxicity.

(A) Linear ubiquitination of immunoprecipitated tau in parental and OTULIN-KO HEK293T cells. Protein expression was determined by immunoblotting assay with indicated antibodies. (B) CCK-8 analysis of cell viability in Parental and OTULIN-KO HEK293T cells transfected with tau WT or P301L mutant for 72 h ($n = 3$). Two-way ANOVA followed by Tukey's post-hoc test was used to determine statistical significance for multiple comparisons. Data are presented as mean \pm SEM. * $p < 0.05$; ** $p < 0.01$; *** $p < 0.001$.

the AD progresses and comes into the middle stage (moderate) or late stage (severe), when a mass of aggregated proteins accumulated in the brain, silencing of OTULIN might be a better strategy for eliminating the misfolded and aggregated proteins. Notably, we have identified an OTULIN inhibitor (UC495) which might be helpful for AD patient treatment. Hence, the spatial-temporal effects of OTULIN on AD regulation need to be further clarified.

LIST OF REFERENCES

1. Goldstein, G., et al., *Isolation of a polypeptide that has lymphocyte-differentiating properties and is probably represented universally in living cells*. Proc Natl Acad Sci U S A, 1975. **72**(1): p. 11-5. <https://doi.org/10.1073/pnas.72.1.11>.
2. Vijay-Kumar, S., C.E. Bugg, and W.J. Cook, *Structure of ubiquitin refined at 1.8 Å resolution*. J Mol Biol, 1987. **194**(3): p. 531-44. [https://doi.org/10.1016/0022-2836\(87\)90679-6](https://doi.org/10.1016/0022-2836(87)90679-6).
3. Hershko, A. and A. Ciechanover, *The ubiquitin system*. Annu Rev Biochem, 1998. **67**: p. 425-79. <https://doi.org/10.1146/annurev.biochem.67.1.425>.
4. Scheffner, M., U. Nuber, and J.M. Huibregtse, *Protein ubiquitination involving an E1-E2-E3 enzyme ubiquitin thioester cascade*. Nature, 1995. **373**(6509): p. 81-3. <https://doi.org/10.1038/373081a0>.
5. Komander, D. and M. Rape, *The Ubiquitin Code*. Annual Review of Biochemistry, 2012. **81**(1): p. 203-229. <https://doi.org/10.1146/annurev-biochem-060310-170328>.
6. Kirisako, T., et al., *A ubiquitin ligase complex assembles linear polyubiquitin chains*. EMBO J, 2006. **25**(20): p. 4877-87. <https://doi.org/10.1038/sj.emboj.7601360>.
7. Oikawa, D., et al., *Linear Ubiquitin Code: Its Writer, Erasers, Decoders, Inhibitors, and Implications in Disorders*. Int J Mol Sci, 2020. **21**(9). <https://doi.org/10.3390/ijms21093381>.
8. Jahan, A.S., C.R. Elbaek, and R.B. Damgaard, *Met1-linked ubiquitin signalling in health and disease: inflammation, immunity, cancer, and beyond*. Cell Death Differ, 2021. **28**(2): p. 473-492. <https://doi.org/10.1038/s41418-020-00676-w>.
9. Tokunaga, F., et al., *SHARPIN is a component of the NF-kappaB-activating linear ubiquitin chain assembly complex*. Nature, 2011. **471**(7340): p. 633-6. <https://doi.org/10.1038/nature09815>.
10. Iwai, K., H. Fujita, and Y. Sasaki, *Linear ubiquitin chains: NF-kappaB signalling, cell death and beyond*. Nat Rev Mol Cell Biol, 2014. **15**(8): p. 503-8. <https://doi.org/10.1038/nrm3836>.
11. Niu, J., et al., *LUBAC regulates NF-kappaB activation upon genotoxic stress by promoting linear ubiquitination of NEMO*. EMBO J, 2011. **30**(18): p. 3741-53. <https://doi.org/10.1038/emboj.2011.264>.
12. Sasaki, Y., et al., *Defective immune responses in mice lacking LUBAC-mediated linear ubiquitination in B cells*. EMBO J, 2013. **32**(18): p. 2463-76. <https://doi.org/10.1038/emboj.2013.184>.
13. Boisson, B., et al., *Immunodeficiency, autoinflammation and amylopectinosis in humans with inherited HOIL-1 and LUBAC deficiency*. Nat Immunol, 2012. **13**(12): p. 1178-86. <https://doi.org/10.1038/ni.2457>.
14. Boisson, B., et al., *Human HOIP and LUBAC deficiency underlies autoinflammation, immunodeficiency, amylopectinosis, and lymphangiectasia*. J Exp Med, 2015. **212**(6): p. 939-51. <https://doi.org/10.1084/jem.20141130>.
15. Eisenhaber, B., et al., *The ring between ring fingers (RBR) protein family*. Genome Biol, 2007. **8**(3): p. 209. <https://doi.org/10.1186/gb-2007-8-3-209>.

16. Smit, J.J., et al., *The E3 ligase HOIP specifies linear ubiquitin chain assembly through its RING-IBR-RING domain and the unique LDD extension*. EMBO J, 2012. **31**(19): p. 3833-44. <https://doi.org/10.1038/emboj.2012.217>.
17. Lechtenberg, B.C., et al., *Structure of a HOIP/E2~ubiquitin complex reveals RBR E3 ligase mechanism and regulation*. Nature, 2016. **529**(7587): p. 546-50. <https://doi.org/10.1038/nature16511>.
18. Fujita, H., et al., *Cooperative Domain Formation by Homologous Motifs in HOIL-1L and SHARPIN Plays A Crucial Role in LUBAC Stabilization*. Cell Rep, 2018. **23**(4): p. 1192-1204. <https://doi.org/10.1016/j.celrep.2018.03.112>.
19. Shimizu, S., et al., *Differential Involvement of the Npl4 Zinc Finger Domains of SHARPIN and HOIL-1L in Linear Ubiquitin Chain Assembly Complex-Mediated Cell Death Protection*. Mol Cell Biol, 2016. **36**(10): p. 1569-83. <https://doi.org/10.1128/MCB.01049-15>.
20. Sato, Y., et al., *Specific recognition of linear ubiquitin chains by the Npl4 zinc finger (NZF) domain of the HOIL-1L subunit of the linear ubiquitin chain assembly complex*. Proc Natl Acad Sci U S A, 2011. **108**(51): p. 20520-5. <https://doi.org/10.1073/pnas.1109088108>.
21. Fujita, H., et al., *Mechanism underlying IkappaB kinase activation mediated by the linear ubiquitin chain assembly complex*. Mol Cell Biol, 2014. **34**(7): p. 1322-35. <https://doi.org/10.1128/MCB.01538-13>.
22. Schaeffer, V., et al., *Binding of OTULIN to the PUB domain of HOIP controls NF-kappaB signaling*. Mol Cell, 2014. **54**(3): p. 349-61. <https://doi.org/10.1016/j.molcel.2014.03.016>.
23. Elliott, P.R., et al., *SPATA2 Links CYLD to LUBAC, Activates CYLD, and Controls LUBAC Signaling*. Mol Cell, 2016. **63**(6): p. 990-1005. <https://doi.org/10.1016/j.molcel.2016.08.001>.
24. Allen, M.D., A. Buchberger, and M. Bycroft, *The PUB domain functions as a p97 binding module in human peptide N-glycanase*. J Biol Chem, 2006. **281**(35): p. 25502-8. <https://doi.org/10.1074/jbc.M601173200>.
25. Aksentijevich, I. and Q. Zhou, *NF-kappaB Pathway in Autoinflammatory Diseases: Dysregulation of Protein Modifications by Ubiquitin Defines a New Category of Autoinflammatory Diseases*. Front Immunol, 2017. **8**: p. 399. <https://doi.org/10.3389/fimmu.2017.00399>.
26. Keusekotten, K., et al., *OTULIN antagonizes LUBAC signaling by specifically hydrolyzing Met1-linked polyubiquitin*. Cell, 2013. **153**(6): p. 1312-26. <https://doi.org/10.1016/j.cell.2013.05.014>.
27. Damgaard, R.B., et al., *The Deubiquitinase OTULIN Is an Essential Negative Regulator of Inflammation and Autoimmunity*. Cell, 2016. **166**(5): p. 1215-1230 e20. <https://doi.org/10.1016/j.cell.2016.07.019>.
28. Rivkin, E., et al., *The linear ubiquitin-specific deubiquitinase gumby regulates angiogenesis*. Nature, 2013. **498**(7454): p. 318-24. <https://doi.org/10.1038/nature12296>.
29. Zhou, Q., et al., *Biallelic hypomorphic mutations in a linear deubiquitinase define otulipenia, an early-onset autoinflammatory disease*. Proc Natl Acad Sci U S A, 2016. **113**(36): p. 10127-32. <https://doi.org/10.1073/pnas.1612594113>.

30. Fiil, B.K., et al., *OTULIN restricts Met1-linked ubiquitination to control innate immune signaling*. Mol Cell, 2013. **50**(6): p. 818-830.
<https://doi.org/10.1016/j.molcel.2013.06.004>.
31. Rodgers, M.A., et al., *The linear ubiquitin assembly complex (LUBAC) is essential for NLRP3 inflammasome activation*. J Exp Med, 2014. **211**(7): p. 1333-47. <https://doi.org/10.1084/jem.20132486>.
32. Wertz, I.E., et al., *Phosphorylation and linear ubiquitin direct A20 inhibition of inflammation*. Nature, 2015. **528**(7582): p. 370-5.
<https://doi.org/10.1038/nature16165>.
33. Hrdinka, M. and M. Gyrd-Hansen, *The Met1-Linked Ubiquitin Machinery: Emerging Themes of (De)regulation*. Mol Cell, 2017. **68**(2): p. 265-280.
<https://doi.org/10.1016/j.molcel.2017.09.001>.
34. Elliott, P.R., et al., *Molecular basis and regulation of OTULIN-LUBAC interaction*. Mol Cell, 2014. **54**(3): p. 335-48.
<https://doi.org/10.1016/j.molcel.2014.03.018>.
35. Sen, R. and D. Baltimore, *Multiple nuclear factors interact with the immunoglobulin enhancer sequences*. Cell, 1986. **46**(5): p. 705-16.
[https://doi.org/10.1016/0092-8674\(86\)90346-6](https://doi.org/10.1016/0092-8674(86)90346-6).
36. Baltimore, D., *NF-kappaB is 25*. Nat Immunol, 2011. **12**(8): p. 683-5.
<https://doi.org/10.1038/ni.2072>.
37. Liu, T., et al., *NF-kappaB signaling in inflammation*. Signal Transduct Target Ther, 2017. **2**. <https://doi.org/10.1038/sigtrans.2017.23>.
38. Dolcet, X., et al., *NF-kB in development and progression of human cancer*. Virchows Arch, 2005. **446**(5): p. 475-82. <https://doi.org/10.1007/s00428-005-1264-9>.
39. Smale, S.T., *Dimer-specific regulatory mechanisms within the NF-kappaB family of transcription factors*. Immunol Rev, 2012. **246**(1): p. 193-204.
<https://doi.org/10.1111/j.1600-065X.2011.01091.x>.
40. Hayden, M.S. and S. Ghosh, *NF-kappaB, the first quarter-century: remarkable progress and outstanding questions*. Genes Dev, 2012. **26**(3): p. 203-34.
<https://doi.org/10.1101/gad.183434.111>.
41. Zhang, Q., M.J. Lenardo, and D. Baltimore, *30 Years of NF-kappaB: A Blossoming of Relevance to Human Pathobiology*. Cell, 2017. **168**(1-2): p. 37-57.
<https://doi.org/10.1016/j.cell.2016.12.012>.
42. Hayden, M.S. and S. Ghosh, *Shared principles in NF-kappaB signaling*. Cell, 2008. **132**(3): p. 344-62. <https://doi.org/10.1016/j.cell.2008.01.020>.
43. Wang, W., A.M. Mani, and Z.H. Wu, *DNA damage-induced nuclear factor-kappa B activation and its roles in cancer progression*. J Cancer Metastasis Treat, 2017. **3**: p. 45-59. <https://doi.org/10.20517/2394-4722.2017.03>.
44. Dondelinger, Y., et al., *Poly-ubiquitination in TNFR1-mediated necroptosis*. Cell Mol Life Sci, 2016. **73**(11-12): p. 2165-76. <https://doi.org/10.1007/s00018-016-2191-4>.
45. Huang, B., et al., *Posttranslational modifications of NF-kappaB: another layer of regulation for NF-kappaB signaling pathway*. Cell Signal, 2010. **22**(9): p. 1282-90. <https://doi.org/10.1016/j.cellsig.2010.03.017>.

46. Smale, S.T., *Hierarchies of NF-kappaB target-gene regulation*. Nat Immunol, 2011. **12**(8): p. 689-94. <https://doi.org/10.1038/ni.2070>.
47. Lee, E.G., et al., *Failure to regulate TNF-induced NF-kappaB and cell death responses in A20-deficient mice*. Science, 2000. **289**(5488): p. 2350-4. <https://doi.org/10.1126/science.289.5488.2350>.
48. Boldin, M.P., et al., *miR-146a is a significant brake on autoimmunity, myeloproliferation, and cancer in mice*. J Exp Med, 2011. **208**(6): p. 1189-201. <https://doi.org/10.1084/jem.20101823>.
49. Sun, S.C., *Non-canonical NF-kappaB signaling pathway*. Cell Res, 2011. **21**(1): p. 71-85. <https://doi.org/10.1038/cr.2010.177>.
50. McCool, K.W. and S. Miyamoto, *DNA damage-dependent NF-kappaB activation: NEMO turns nuclear signaling inside out*. Immunol Rev, 2012. **246**(1): p. 311-26. <https://doi.org/10.1111/j.1600-065X.2012.01101.x>.
51. Wu, Z.H. and S. Miyamoto, *Many faces of NF-kappaB signaling induced by genotoxic stress*. J Mol Med (Berl), 2007. **85**(11): p. 1187-202. <https://doi.org/10.1007/s00109-007-0227-9>.
52. Huang, T.T., et al., *Sequential modification of NEMO/IKKgamma by SUMO-1 and ubiquitin mediates NF-kappaB activation by genotoxic stress*. Cell, 2003. **115**(5): p. 565-76. [https://doi.org/10.1016/s0092-8674\(03\)00895-x](https://doi.org/10.1016/s0092-8674(03)00895-x).
53. Mabb, A.M., S.M. Wuerzberger-Davis, and S. Miyamoto, *PIASy mediates NEMO sumoylation and NF-kappaB activation in response to genotoxic stress*. Nat Cell Biol, 2006. **8**(9): p. 986-93. <https://doi.org/10.1038/ncb1458>.
54. Janssens, S., et al., *PIDD mediates NF-kappaB activation in response to DNA damage*. Cell, 2005. **123**(6): p. 1079-92. <https://doi.org/10.1016/j.cell.2005.09.036>.
55. Stilmann, M., et al., *A nuclear poly(ADP-ribose)-dependent signalosome confers DNA damage-induced IkappaB kinase activation*. Mol Cell, 2009. **36**(3): p. 365-78. <https://doi.org/10.1016/j.molcel.2009.09.032>.
56. Fu, K., et al., *Sam68/KHDRBS1 is critical for colon tumorigenesis by regulating genotoxic stress-induced NF-kappaB activation*. Elife, 2016. **5**. <https://doi.org/10.7554/eLife.15018>.
57. Lee, S.J., et al., *A novel ionizing radiation-induced signaling pathway that activates the transcription factor NF-kappaB*. Oncogene, 1998. **17**(14): p. 1821-6. <https://doi.org/10.1038/sj.onc.1202088>.
58. Piret, B., S. Schoonbroodt, and J. Piette, *The ATM protein is required for sustained activation of NF-kappaB following DNA damage*. Oncogene, 1999. **18**(13): p. 2261-71. <https://doi.org/10.1038/sj.onc.1202541>.
59. Wu, Z.H., et al., *Molecular linkage between the kinase ATM and NF-kappaB signaling in response to genotoxic stimuli*. Science, 2006. **311**(5764): p. 1141-6. <https://doi.org/10.1126/science.1121513>.
60. Jin, H.S., et al., *cIAP1, cIAP2, and XIAP act cooperatively via nonredundant pathways to regulate genotoxic stress-induced nuclear factor-kappaB activation*. Cancer Res, 2009. **69**(5): p. 1782-91. <https://doi.org/10.1158/0008-5472.CAN-08-2256>.

61. Wu, Z.H., et al., *ATM- and NEMO-dependent ELKS ubiquitination coordinates TAK1-mediated IKK activation in response to genotoxic stress*. Mol Cell, 2010. **40**(1): p. 75-86. <https://doi.org/10.1016/j.molcel.2010.09.010>.
62. Hinz, M., et al., *A cytoplasmic ATM-TRAF6-cIAP1 module links nuclear DNA damage signaling to ubiquitin-mediated NF-kappaB activation*. Mol Cell, 2010. **40**(1): p. 63-74. <https://doi.org/10.1016/j.molcel.2010.09.008>.
63. Jossion, S., et al., *RelB regulates manganese superoxide dismutase gene and resistance to ionizing radiation of prostate cancer cells*. Oncogene, 2006. **25**(10): p. 1554-9. <https://doi.org/10.1038/sj.onc.1209186>.
64. Xu, Y., et al., *SN52, a novel nuclear factor-kappaB inhibitor, blocks nuclear import of RelB:p52 dimer and sensitizes prostate cancer cells to ionizing radiation*. Mol Cancer Ther, 2008. **7**(8): p. 2367-76. <https://doi.org/10.1158/1535-7163.MCT-08-0238>.
65. Lessard, L., et al., *Nuclear localisation of nuclear factor-kappaB transcription factors in prostate cancer: an immunohistochemical study*. Br J Cancer, 2005. **93**(9): p. 1019-23. <https://doi.org/10.1038/sj.bjc.6602796>.
66. Hanahan, D. and R.A. Weinberg, *The hallmarks of cancer*. Cell, 2000. **100**(1): p. 57-70. [https://doi.org/10.1016/s0092-8674\(00\)81683-9](https://doi.org/10.1016/s0092-8674(00)81683-9).
67. Ben-Neriah, Y. and M. Karin, *Inflammation meets cancer, with NF-kappaB as the matchmaker*. Nat Immunol, 2011. **12**(8): p. 715-23. <https://doi.org/10.1038/ni.2060>.
68. Li, Q. and I.M. Verma, *NF-kappaB regulation in the immune system*. Nat Rev Immunol, 2002. **2**(10): p. 725-34. <https://doi.org/10.1038/nri910>.
69. Gelfo, V., et al., *Roles of IL-1 in Cancer: From Tumor Progression to Resistance to Targeted Therapies*. Int J Mol Sci, 2020. **21**(17). <https://doi.org/10.3390/ijms21176009>.
70. El-Omar, E.M., et al., *Interleukin-1 polymorphisms associated with increased risk of gastric cancer*. Nature, 2000. **404**(6776): p. 398-402. <https://doi.org/10.1038/35006081>.
71. Wajant, H., *The role of TNF in cancer*. Results Probl Cell Differ, 2009. **49**: p. 1-15. https://doi.org/10.1007/400_2008_26.
72. Kim, H.J., N. Hawke, and A.S. Baldwin, *NF-kappaB and IKK as therapeutic targets in cancer*. Cell Death Differ, 2006. **13**(5): p. 738-47. <https://doi.org/10.1038/sj.cdd.4401877>.
73. Perkins, N.D., *The diverse and complex roles of NF-kappaB subunits in cancer*. Nat Rev Cancer, 2012. **12**(2): p. 121-32. <https://doi.org/10.1038/nrc3204>.
74. Mina, R., et al., *New pharmacotherapy options for multiple myeloma*. Expert Opin Pharmacother, 2016. **17**(2): p. 181-92. <https://doi.org/10.1517/14656566.2016.1115016>.
75. Couzin-Frankel, J., *Breakthrough of the year 2013. Cancer immunotherapy*. Science, 2013. **342**(6165): p. 1432-3. <https://doi.org/10.1126/science.342.6165.1432>.
76. Orłowski, R.Z. and A.S. Baldwin, Jr., *NF-kappaB as a therapeutic target in cancer*. Trends Mol Med, 2002. **8**(8): p. 385-9. [https://doi.org/10.1016/s1471-4914\(02\)02375-4](https://doi.org/10.1016/s1471-4914(02)02375-4).

77. Baumann, P., et al., *Alkylating agents induce activation of NFkappaB in multiple myeloma cells*. *Leuk Res*, 2008. **32**(7): p. 1144-7.
<https://doi.org/10.1016/j.leukres.2007.11.015>.
78. Bednarski, B.K., et al., *Active roles for inhibitory kappaB kinases alpha and beta in nuclear factor-kappaB-mediated chemoresistance to doxorubicin*. *Mol Cancer Ther*, 2008. **7**(7): p. 1827-35. <https://doi.org/10.1158/1535-7163.MCT-08-0321>.
79. Baldwin, A.S., *Control of oncogenesis and cancer therapy resistance by the transcription factor NF-kappaB*. *J Clin Invest*, 2001. **107**(3): p. 241-6.
<https://doi.org/10.1172/JCI11991>.
80. Tamatani, M., et al., *Tumor necrosis factor induces Bcl-2 and Bcl-x expression through NFkappaB activation in primary hippocampal neurons*. *J Biol Chem*, 1999. **274**(13): p. 8531-8. <https://doi.org/10.1074/jbc.274.13.8531>.
81. Guttridge, D.C., et al., *NF-kappaB controls cell growth and differentiation through transcriptional regulation of cyclin D1*. *Mol Cell Biol*, 1999. **19**(8): p. 5785-99. <https://doi.org/10.1128/MCB.19.8.5785>.
82. Stehlik, C., et al., *Nuclear factor (NF)-kappaB-regulated X-chromosome-linked iap gene expression protects endothelial cells from tumor necrosis factor alpha-induced apoptosis*. *J Exp Med*, 1998. **188**(1): p. 211-6.
<https://doi.org/10.1084/jem.188.1.211>.
83. Naugler, W.E. and M. Karin, *The wolf in sheep's clothing: the role of interleukin-6 in immunity, inflammation and cancer*. *Trends Mol Med*, 2008. **14**(3): p. 109-19. <https://doi.org/10.1016/j.molmed.2007.12.007>.
84. Grivennikov, S.I., F.R. Greten, and M. Karin, *Immunity, inflammation, and cancer*. *Cell*, 2010. **140**(6): p. 883-99. <https://doi.org/10.1016/j.cell.2010.01.025>.
85. Niu, J., et al., *Induction of miRNA-181a by genotoxic treatments promotes chemotherapeutic resistance and metastasis in breast cancer*. *Oncogene*, 2016. **35**(10): p. 1302-1313. <https://doi.org/10.1038/onc.2015.189>.
86. Shimizu, Y., L. Taraborrelli, and H. Walczak, *Linear ubiquitination in immunity*. *Immunol Rev*, 2015. **266**(1): p. 190-207. <https://doi.org/10.1111/imr.12309>.
87. Haas, T.L., et al., *Recruitment of the linear ubiquitin chain assembly complex stabilizes the TNF-R1 signaling complex and is required for TNF-mediated gene induction*. *Mol Cell*, 2009. **36**(5): p. 831-44.
<https://doi.org/10.1016/j.molcel.2009.10.013>.
88. Tokunaga, F., et al., *Involvement of linear polyubiquitylation of NEMO in NF-kappaB activation*. *Nat Cell Biol*, 2009. **11**(2): p. 123-32.
<https://doi.org/10.1038/ncb1821>.
89. Hostager, B.S., et al., *HOIL-1L interacting protein (HOIP) as an NF-kappaB regulating component of the CD40 signaling complex*. *PLoS One*, 2010. **5**(6): p. e11380. <https://doi.org/10.1371/journal.pone.0011380>.
90. Gerlach, B., et al., *Linear ubiquitination prevents inflammation and regulates immune signalling*. *Nature*, 2011. **471**(7340): p. 591-6.
<https://doi.org/10.1038/nature09816>.
91. Ikeda, F., et al., *SHARPIN forms a linear ubiquitin ligase complex regulating NF-kappaB activity and apoptosis*. *Nature*, 2011. **471**(7340): p. 637-41.
<https://doi.org/10.1038/nature09814>.

92. Zak, D.E., et al., *Systems analysis identifies an essential role for SHANK-associated RH domain-interacting protein (SHARPIN) in macrophage Toll-like receptor 2 (TLR2) responses*. Proc Natl Acad Sci U S A, 2011. **108**(28): p. 11536-41. <https://doi.org/10.1073/pnas.1107577108>.
93. Draber, P., et al., *LUBAC-Recruited CYLD and A20 Regulate Gene Activation and Cell Death by Exerting Opposing Effects on Linear Ubiquitin in Signaling Complexes*. Cell Rep, 2015. **13**(10): p. 2258-72. <https://doi.org/10.1016/j.celrep.2015.11.009>.
94. Heger, K., et al., *OTULIN limits cell death and inflammation by deubiquitinating LUBAC*. Nature, 2018. **559**(7712): p. 120-124. <https://doi.org/10.1038/s41586-018-0256-2>.
95. Mercogliano, M.F., et al., *Tumor Necrosis Factor alpha Blockade: An Opportunity to Tackle Breast Cancer*. Front Oncol, 2020. **10**: p. 584. <https://doi.org/10.3389/fonc.2020.00584>.
96. Jemal, A., et al., *Global cancer statistics*. CA Cancer J Clin, 2011. **61**(2): p. 69-90. <https://doi.org/10.3322/caac.20107>.
97. Medina, M.A., et al., *Triple-Negative Breast Cancer: A Review of Conventional and Advanced Therapeutic Strategies*. Int J Environ Res Public Health, 2020. **17**(6). <https://doi.org/10.3390/ijerph17062078>.
98. Muneer, I., et al., *Discovery of Novel Inhibitors From Medicinal Plants for V-Domain Ig Suppressor of T-Cell Activation*. Front Mol Biosci, 2021. **8**: p. 716735. <https://doi.org/10.3389/fmolb.2021.716735>.
99. Wolff, A.C., et al., *Recommendations for human epidermal growth factor receptor 2 testing in breast cancer: American Society of Clinical Oncology/College of American Pathologists clinical practice guideline update*. Arch Pathol Lab Med, 2014. **138**(2): p. 241-56. <https://doi.org/10.5858/arpa.2013-0953-SA>.
100. Shiovitz, S. and L.A. Korde, *Genetics of breast cancer: a topic in evolution*. Ann Oncol, 2015. **26**(7): p. 1291-9. <https://doi.org/10.1093/annonc/mdv022>.
101. Corso, G., et al., *Prognosis and outcome in CDH1-mutant lobular breast cancer*. Eur J Cancer Prev, 2018. **27**(3): p. 237-238. <https://doi.org/10.1097/CEJ.0000000000000405>.
102. Shahbandi, A., H.D. Nguyen, and J.G. Jackson, *TP53 Mutations and Outcomes in Breast Cancer: Reading beyond the Headlines*. Trends Cancer, 2020. **6**(2): p. 98-110. <https://doi.org/10.1016/j.trecan.2020.01.007>.
103. Vitug, A.F. and L.A. Newman, *Complications in breast surgery*. Surg Clin North Am, 2007. **87**(2): p. 431-51, x. <https://doi.org/10.1016/j.suc.2007.01.005>.
104. Segaloff, A., *Hormonal therapy of breast cancer*. Cancer Treat Rev, 1975. **2**(2): p. 129-35. [https://doi.org/10.1016/s0305-7372\(75\)80006-5](https://doi.org/10.1016/s0305-7372(75)80006-5).
105. Newman, L.A. and S.E. Singletary, *Overview of adjuvant systemic therapy in early stage breast cancer*. Surg Clin North Am, 2007. **87**(2): p. 499-509, xi. <https://doi.org/10.1016/j.suc.2007.01.002>.
106. Gazelle, G.S., et al., *Tumor ablation with radio-frequency energy*. Radiology, 2000. **217**(3): p. 633-46. <https://doi.org/10.1148/radiology.217.3.r00dc26633>.

107. Li, Y., et al., *Recent Progress on Immunotherapy for Breast Cancer: Tumor Microenvironment, Nanotechnology and More*. Front Bioeng Biotechnol, 2021. **9**: p. 680315. <https://doi.org/10.3389/fbioe.2021.680315>.
108. Kumar, P. and R. Aggarwal, *An overview of triple-negative breast cancer*. Arch Gynecol Obstet, 2016. **293**(2): p. 247-69. <https://doi.org/10.1007/s00404-015-3859-y>.
109. Kim, C., et al., *Chemoresistance Evolution in Triple-Negative Breast Cancer Delineated by Single-Cell Sequencing*. Cell, 2018. **173**(4): p. 879-893 e13. <https://doi.org/10.1016/j.cell.2018.03.041>.
110. Foulkes, W.D., I.E. Smith, and J.S. Reis-Filho, *Triple-negative breast cancer*. N Engl J Med, 2010. **363**(20): p. 1938-48. <https://doi.org/10.1056/NEJMra1001389>.
111. Dent, R., et al., *Triple-negative breast cancer: clinical features and patterns of recurrence*. Clin Cancer Res, 2007. **13**(15 Pt 1): p. 4429-34. <https://doi.org/10.1158/1078-0432.CCR-06-3045>.
112. Isakoff, S.J., *Triple-negative breast cancer: role of specific chemotherapy agents*. Cancer J, 2010. **16**(1): p. 53-61. <https://doi.org/10.1097/PPO.0b013e3181d24ff7>.
113. Yin, L., et al., *Triple-negative breast cancer molecular subtyping and treatment progress*. Breast Cancer Res, 2020. **22**(1): p. 61. <https://doi.org/10.1186/s13058-020-01296-5>.
114. Lee, A., et al., *Chemotherapy response assay test and prognosis for breast cancer patients who have undergone anthracycline- and taxane-based chemotherapy*. J Breast Cancer, 2011. **14**(4): p. 283-8. <https://doi.org/10.4048/jbc.2011.14.4.283>.
115. Dickey, J.S. and V.A. Rao, *Current and proposed biomarkers of anthracycline cardiotoxicity in cancer: emerging opportunities in oxidative damage and autophagy*. Curr Mol Med, 2012. **12**(6): p. 763-71. <https://doi.org/10.2174/156652412800792561>.
116. Nedeljkovic, M. and A. Damjanovic, *Mechanisms of Chemotherapy Resistance in Triple-Negative Breast Cancer-How We Can Rise to the Challenge*. Cells, 2019. **8**(9). <https://doi.org/10.3390/cells8090957>.
117. Zheng, H.C., *The molecular mechanisms of chemoresistance in cancers*. Oncotarget, 2017. **8**(35): p. 59950-59964. <https://doi.org/10.18632/oncotarget.19048>.
118. Gewirtz, D.A., M.L. Bristol, and J.C. Yalowich, *Toxicity issues in cancer drug development*. Curr Opin Investig Drugs, 2010. **11**(6): p. 612-4.
119. Hasan, S., R. Taha, and H.E. Omri, *Current Opinions on Chemoresistance: An Overview*. Bioinformation, 2018. **14**(2): p. 80-85. <https://doi.org/10.6026/97320630014080>.
120. Brasseur, K., N. Gevry, and E. Asselin, *Chemoresistance and targeted therapies in ovarian and endometrial cancers*. Oncotarget, 2017. **8**(3): p. 4008-4042. <https://doi.org/10.18632/oncotarget.14021>.
121. Lu, C. and A. Shervington, *Chemoresistance in gliomas*. Mol Cell Biochem, 2008. **312**(1-2): p. 71-80. <https://doi.org/10.1007/s11010-008-9722-8>.
122. Hoesel, B. and J.A. Schmid, *The complexity of NF-kappaB signaling in inflammation and cancer*. Mol Cancer, 2013. **12**: p. 86. <https://doi.org/10.1186/1476-4598-12-86>.

123. Godwin, P., et al., *Targeting nuclear factor-kappa B to overcome resistance to chemotherapy*. *Front Oncol*, 2013. **3**: p. 120.
<https://doi.org/10.3389/fonc.2013.00120>.
124. Sanjana, N.E., O. Shalem, and F. Zhang, *Improved vectors and genome-wide libraries for CRISPR screening*. *Nat Methods*, 2014. **11**(8): p. 783-784.
<https://doi.org/10.1038/nmeth.3047>.
125. Miyamoto, S., B.J. Seufzer, and S.D. Shumway, *Novel IkappaB alpha proteolytic pathway in WEHI231 immature B cells*. *Mol Cell Biol*, 1998. **18**(1): p. 19-29.
<https://doi.org/10.1128/MCB.18.1.19>.
126. Bisen, S., et al., *Proteomic Analysis of Baboon Cerebral Artery Reveals Potential Pathways of Damage by Prenatal Alcohol Exposure*. *Mol Cell Proteomics*, 2019. **18**(2): p. 294-307. <https://doi.org/10.1074/mcp.RA118.001047>.
127. Li, M., et al., *Reciprocal interplay between OTULIN-LUBAC determines genotoxic and inflammatory NF-kB signal responses*. *Proc Natl Acad Sci U S A*, in press.
128. Sakamoto, H., et al., *Gliotoxin suppresses NF-kappaB activation by selectively inhibiting linear ubiquitin chain assembly complex (LUBAC)*. *ACS Chem Biol*, 2015. **10**(3): p. 675-81. <https://doi.org/10.1021/cb500653y>.
129. Damgaard, R.B., et al., *OTULIN deficiency in ORAS causes cell type-specific LUBAC degradation, dysregulated TNF signalling and cell death*. *EMBO Mol Med*, 2019. **11**(3). <https://doi.org/10.15252/emmm.201809324>.
130. Weinelt, N. and S.J.L. van Wijk, *Ubiquitin-dependent and -independent functions of OTULIN in cell fate control and beyond*. *Cell Death Differ*, 2020.
<https://doi.org/10.1038/s41418-020-00675-x>.
131. Suzuki, T., et al., *The PUB domain: a putative protein-protein interaction domain implicated in the ubiquitin-proteasome pathway*. *Biochem Biophys Res Commun*, 2001. **287**(5): p. 1083-7. <https://doi.org/10.1006/bbrc.2001.5688>.
132. Kamiya, Y., et al., *NMR characterization of the interaction between the PUB domain of peptide:N-glycanase and ubiquitin-like domain of HR23*. *FEBS Lett*, 2012. **586**(8): p. 1141-6. <https://doi.org/10.1016/j.febslet.2012.03.027>.
133. Spratt, D.E., H. Walden, and G.S. Shaw, *RBR E3 ubiquitin ligases: new structures, new insights, new questions*. *Biochem J*, 2014. **458**(3): p. 421-37.
<https://doi.org/10.1042/BJ20140006>.
134. Yamamoto, Y. and R.B. Gaynor, *Therapeutic potential of inhibition of the NF-kappaB pathway in the treatment of inflammation and cancer*. *J Clin Invest*, 2001. **107**(2): p. 135-42. <https://doi.org/10.1172/JCI11914>.
135. Takiuchi, T., et al., *Suppression of LUBAC-mediated linear ubiquitination by a specific interaction between LUBAC and the deubiquitinases CYLD and OTULIN*. *Genes Cells*, 2014. **19**(3): p. 254-72. <https://doi.org/10.1111/gtc.12128>.
136. Conklin, K.A., *Chemotherapy-associated oxidative stress: impact on chemotherapeutic effectiveness*. *Integr Cancer Ther*, 2004. **3**(4): p. 294-300.
<https://doi.org/10.1177/1534735404270335>.
137. Robinson, P.J. and N.J. Bulleid, *Mechanisms of Disulfide Bond Formation in Nascent Polypeptides Entering the Secretory Pathway*. *Cells*, 2020. **9**(9).
<https://doi.org/10.3390/cells9091994>.

138. Nelson, K.J., et al., *Use of dimedone-based chemical probes for sulfenic acid detection methods to visualize and identify labeled proteins*. *Methods Enzymol*, 2010. **473**: p. 95-115. [https://doi.org/10.1016/S0076-6879\(10\)73004-4](https://doi.org/10.1016/S0076-6879(10)73004-4).
139. Wang, W., et al., *ABL1-dependent OTULIN phosphorylation promotes genotoxic Wnt/beta-catenin activation to enhance drug resistance in breast cancers*. *Nat Commun*, 2020. **11**(1): p. 3965. <https://doi.org/10.1038/s41467-020-17770-9>.
140. Mertins, P., et al., *Proteogenomics connects somatic mutations to signalling in breast cancer*. *Nature*, 2016. **534**(7605): p. 55-62. <https://doi.org/10.1038/nature18003>.
141. Bojkova, D., et al., *Proteomics of SARS-CoV-2-infected host cells reveals therapy targets*. *Nature*, 2020. **583**(7816): p. 469-472. <https://doi.org/10.1038/s41586-020-2332-7>.
142. Palombella, V.J., et al., *The ubiquitin-proteasome pathway is required for processing the NF-kappa B1 precursor protein and the activation of NF-kappa B*. *Cell*, 1994. **78**(5): p. 773-85. [https://doi.org/10.1016/s0092-8674\(94\)90482-0](https://doi.org/10.1016/s0092-8674(94)90482-0).
143. Wang, C., et al., *TAK1 is a ubiquitin-dependent kinase of MKK and IKK*. *Nature*, 2001. **412**(6844): p. 346-51. <https://doi.org/10.1038/35085597>.
144. Iwai, K., *Diverse roles of the ubiquitin system in NF-kappaB activation*. *Biochim Biophys Acta*, 2014. **1843**(1): p. 129-36. <https://doi.org/10.1016/j.bbamcr.2013.03.011>.
145. Marianayagam, N.J., M. Sunde, and J.M. Matthews, *The power of two: protein dimerization in biology*. *Trends Biochem Sci*, 2004. **29**(11): p. 618-25. <https://doi.org/10.1016/j.tibs.2004.09.006>.
146. Herscovitch, M., et al., *Intermolecular disulfide bond formation in the NEMO dimer requires Cys54 and Cys347*. *Biochem Biophys Res Commun*, 2008. **367**(1): p. 103-8. <https://doi.org/10.1016/j.bbrc.2007.12.123>.
147. Warsch, W., et al., *STAT5 triggers BCR-ABL1 mutation by mediating ROS production in chronic myeloid leukaemia*. *Oncotarget*, 2012. **3**(12): p. 1669-87. <https://doi.org/10.18632/oncotarget.806>.
148. Zhao, M., et al., *Non-proteolytic ubiquitination of OTULIN regulates NF-kappaB signaling pathway*. *J Mol Cell Biol*, 2019. <https://doi.org/10.1093/jmcb/mjz081>.
149. Xu, H., et al., *Lentivirus-mediated overexpression of OTULIN ameliorates microglia activation and neuroinflammation by depressing the activation of the NF-kappaB signaling pathway in cerebral ischemia/reperfusion rats*. *J Neuroinflammation*, 2018. **15**(1): p. 83. <https://doi.org/10.1186/s12974-018-1117-5>.
150. Xu, H., Y. Wang, and Y. Luo, *OTULIN is a new target of EA treatment in the alleviation of brain injury and glial cell activation via suppression of the NF-kappaB signalling pathway in acute ischaemic stroke rats*. *Mol Med*, 2021. **27**(1): p. 37. <https://doi.org/10.1186/s10020-021-00297-0>.
151. Girija, A.S.S., E.M. Shankar, and M. Larsson, *Could SARS-CoV-2-Induced Hyperinflammation Magnify the Severity of Coronavirus Disease (CoViD-19) Leading to Acute Respiratory Distress Syndrome?* *Front Immunol*, 2020. **11**: p. 1206. <https://doi.org/10.3389/fimmu.2020.01206>.

152. Merad, M. and J.C. Martin, *Pathological inflammation in patients with COVID-19: a key role for monocytes and macrophages*. Nat Rev Immunol, 2020. **20**(6): p. 355-362. <https://doi.org/10.1038/s41577-020-0331-4>.
153. Chen, Y.M., et al., *Blood molecular markers associated with COVID-19 immunopathology and multi-organ damage*. EMBO J, 2020. **39**(24): p. e105896. <https://doi.org/10.15252/emj.2020105896>.
154. Overmyer, K.A., et al., *Large-Scale Multi-omic Analysis of COVID-19 Severity*. Cell Syst, 2021. **12**(1): p. 23-40 e7. <https://doi.org/10.1016/j.cels.2020.10.003>.
155. Noad, J., et al., *LUBAC-synthesized linear ubiquitin chains restrict cytosol-invading bacteria by activating autophagy and NF-kappaB*. Nat Microbiol, 2017. **2**: p. 17063. <https://doi.org/10.1038/nmicrobiol.2017.63>.
156. van Wijk, S.J.L., et al., *Linear ubiquitination of cytosolic Salmonella Typhimurium activates NF-kappaB and restricts bacterial proliferation*. Nat Microbiol, 2017. **2**: p. 17066. <https://doi.org/10.1038/nmicrobiol.2017.66>.
157. Kircheis, R., et al., *NF-kappaB Pathway as a Potential Target for Treatment of Critical Stage COVID-19 Patients*. Front Immunol, 2020. **11**: p. 598444. <https://doi.org/10.3389/fimmu.2020.598444>.
158. Ross, C.A. and M.A. Poirier, *Protein aggregation and neurodegenerative disease*. Nat Med, 2004. **10 Suppl**: p. S10-7. <https://doi.org/10.1038/nm1066>.
159. Jellinger, K.A., *Basic mechanisms of neurodegeneration: a critical update*. J Cell Mol Med, 2010. **14**(3): p. 457-87. <https://doi.org/10.1111/j.1582-4934.2010.01010.x>.
160. Pohl, C. and I. Dikic, *Cellular quality control by the ubiquitin-proteasome system and autophagy*. Science, 2019. **366**(6467): p. 818-822. <https://doi.org/10.1126/science.aax3769>.
161. van Well, E.M., et al., *A protein quality control pathway regulated by linear ubiquitination*. EMBO J, 2019. **38**(9). <https://doi.org/10.15252/emj.2018100730>.
162. Yang, Q.Q. and J.W. Zhou, *Neuroinflammation in the central nervous system: Symphony of glial cells*. Glia, 2019. **67**(6): p. 1017-1035. <https://doi.org/10.1002/glia.23571>.
163. Shih, R.H., C.Y. Wang, and C.M. Yang, *NF-kappaB Signaling Pathways in Neurological Inflammation: A Mini Review*. Front Mol Neurosci, 2015. **8**: p. 77. <https://doi.org/10.3389/fnmol.2015.00077>.
164. Heneka, M.T., et al., *Neuroinflammation in Alzheimer's disease*. Lancet Neurol, 2015. **14**(4): p. 388-405. [https://doi.org/10.1016/S1474-4422\(15\)70016-5](https://doi.org/10.1016/S1474-4422(15)70016-5).
165. Roberson, E.D., et al., *Reducing endogenous tau ameliorates amyloid beta-induced deficits in an Alzheimer's disease mouse model*. Science, 2007. **316**(5825): p. 750-4. <https://doi.org/10.1126/science.1141736>.
166. Nelson, P.T., et al., *Correlation of Alzheimer disease neuropathologic changes with cognitive status: a review of the literature*. J Neuropathol Exp Neurol, 2012. **71**(5): p. 362-81. <https://doi.org/10.1097/NEN.0b013e31825018f7>.
167. Long, J.M. and D.M. Holtzman, *Alzheimer Disease: An Update on Pathobiology and Treatment Strategies*. Cell, 2019. **179**(2): p. 312-339. <https://doi.org/10.1016/j.cell.2019.09.001>.

168. Breijyeh, Z. and R. Karaman, *Comprehensive Review on Alzheimer's Disease: Causes and Treatment*. *Molecules*, 2020. **25**(24). <https://doi.org/10.3390/molecules25245789>.
169. Jiang, S. and K. Bhaskar, *Degradation and Transmission of Tau by Autophagic-Endolysosomal Networks and Potential Therapeutic Targets for Tauopathy*. *Front Mol Neurosci*, 2020. **13**: p. 586731. <https://doi.org/10.3389/fnmol.2020.586731>.
170. Alquezar, C., S. Arya, and A.W. Kao, *Tau Post-translational Modifications: Dynamic Transformers of Tau Function, Degradation, and Aggregation*. *Front Neurol*, 2020. **11**: p. 595532. <https://doi.org/10.3389/fneur.2020.595532>.
171. Chen, X., C. Guo, and J. Kong, *Oxidative stress in neurodegenerative diseases*. *Neural Regen Res*, 2012. **7**(5): p. 376-85. <https://doi.org/10.3969/j.issn.1673-5374.2012.05.009>.
172. Kim, E., K. Sakata, and F.F. Liao, *Bidirectional interplay of HSF1 degradation and UPR activation promotes tau hyperphosphorylation*. *PLoS Genet*, 2017. **13**(7): p. e1006849. <https://doi.org/10.1371/journal.pgen.1006849>.

VITA

Mingqi Li was born in northeast of China in 1992. He completed his master's degree at Harbin University of Basic Medicine (7-year program) in 2018. He continued to study in the University of Tennessee Health Science Center (UTHSC) as a Ph.D. student in the Integrated Biomedical Sciences program, majoring in Cancer and Developmental Biology. Mingqi Li expects to complete his Ph.D. in July 2022.